COMPREHENSIVE ASSESSMENT OF DIFFERENT BIPV TYPOLOGIES IN ADDRESSING THE DUCK CURVE PROBLEMS

by

Hamideh Hossei

A dissertation submitted to the faculty of
The University of North Carolina at Charlotte
in partial fulfillment of the requirements
for the degree of Doctor of Philosophy in
Infrastructure and Environmental Systems

Charlotte

2024

Approved by:

_____
Dr. Kyoung Hee Kim

_____
Dr. Jaewon Oh

_____
Dr. Chengde Wu

_____
Dr. Suzanne A. Boyd

ABSTRACT

HAMIDEH HOSSEI. Comprehensive assessment of different BIPV typologies in addressing the duck curve problems. (Under the direction of DR. KYOUNG HEE KIM).

The need to supply electricity to the building sector is growing worldwide. Currently, integrating photovoltaic (PV) panels into building rooftops is the primary method for harnessing solar energy. However, this practice, along with the use of solar farms, contributes to power grid fluctuation issues, known as the duck curve. Two main issues associated with the duck curve are PV power curtailment at midday and a sudden increase in utility operation during late afternoon hours. These problems are more significant in regions with higher PV power penetration into the grid, raising concerns that the current power grid infrastructure may not be able to accommodate the operation of conventional utilities alongside PV power generators.

Since the building sector is a major electricity consumer, supplying this sector's demand with an optimized PV system that not only meets building electricity needs and reduces energy consumption but also mitigates duck curve issues can significantly contribute to energy sustainability. This thesis investigates the impact of Building-Integrated Photovoltaic (BIPV) systems in mitigating power grid fluctuations through a comprehensive analysis. The findings of this study are presented in four research papers, each addressing a specific aspect of the main research objective. A brief summary of the findings is as follows:

Paper One: "Circuit Connection Reconfiguration of Partially Shaded BIPV Systems: A Solution for Power Loss Reduction" explores solutions to tackle power drops in BIPV façades due to partial shading conditions. The paper presents a novel circuit connection that significantly reduces power output reduction in BIPV façade systems.

Paper Two: "Comprehensive Analysis of Energy and Visual Performance of Building-Integrated Photovoltaics in All ASHRAE Climate Zones" examines various BIPV typologies, including PV-south louvers and PV-mounted roofs, in terms of building energy consumption, PV power output, and occupants' visual comfort. Results indicate that PV-south louvers significantly reduce building energy consumption in very hot, hot, and warm climates. In colder climates with significant heating demands, roof-mounted systems provide a better balance between power generation and solar heat gain. PV-south louvers effectively reduce glare on office working surfaces while providing the desired illuminance levels for occupants. However, PV-mounted roofs can cause excessive illuminance, leading to disturbing glare over large portions of the floor area.

Paper Three: "Assessing the PV-Integrated South Façade in Mitigating the BIPV System Oversupply" evaluates the effectiveness of PV-south louvers in reducing BIPV power curtailment at midday. The results show that these typologies effectively reduce power curtailment in very hot, hot, and warm climates, except in warm-marine sub-climate zone (3C). In mixed climates, the performance of these typologies varies across different months.

Paper Four: "Assessing the Impact of PV-Integrated West Façade in Alleviating the Duck Curve Steep Ramp in All ASHRAE Climate Zones" investigates the impact of PV-west fins on alleviating the duck curve's steep ramp in the late afternoon. The impact is limited in very hot and hot climates but shows more potential in warm, mixed, and cool climates. Cold, very cold, and Arctic climates exhibit higher effectiveness during warmer months.

This thesis provides a comprehensive analysis of the impact of BIPV systems in mitigating the duck curve issue. By optimizing BIPV configurations and understanding their performance across different climate zones, the findings of this thesis offer valuable insights into improving

building energy and BIPV power production efficiency as well as addressing grid stability issues associated with the fast-growing integration of PV systems into the built environment.

ACKNOWLEDGEMENTS

I would like to express my sincere gratitude to my advisor Dr. Kyoung Hee Kim for her invaluable support and guidance throughout my doctoral journey. Dr. Kim's expertise in architecture, engineering and building science proved instrumental in shaping the direction of this research. Her willingness to offer insightful feedback, encourage critical thinking, and dedicate significant time to my progress was instrumental to the completion of this thesis. I'm grateful for the opportunities that she provided for me to explore and find my passion in professional life.

I would also thank my dissertation committee members, Dr. Chengde Wu, Dr. Jaewon Oh, and Dr. Suzanne Boyd, for their valuable insights and contributions to my research to ensure the quality of this work. I would also like to thank Department of INES and School of Architecture at UNC Charlotte for their support, resources, and opportunities that have contributed to my academic growth. My deepest gratitude goes to my beloved husband and my parents for their unwavering encouragement, understanding, and love throughout this academic journey. Your support has been my anchor.

This work would not have been possible without the collective support and encouragement of all these individuals and institutions. I am truly fortunate to have had such a strong support network. Thank you all for being part of my academic journey.

DEDICATION

To Amin, who celebrated every breakthrough and helped me weather every setback. Your unwavering support allowed me to finally conquer this challenge and present this thesis, a testament to our journey together. With all my love and gratitude.

TABLE OF CONTENTS

LIST OF TABLES

LIST OF FIGURES

CHAPTER 1: INTRODUCTION

1.1 Overview

In 2021, the US set a greenhouse gas reduction goal of 40% by 2030 [1], and 80% by 2050 [2]. To meet the power sector decarbonization goal, the US needs to increase its yearly total new solar electric capacity added to the grid by an average of 30 GW per year until 2025 and ramp up the annual addition to 60 GW from 2025 to 2030, which is four times higher than the current development rate. To meet the decarbonization target of 2050, the US needs at least 0.5% of the contiguous surface area to install ground-mounted solar technologies [3]. This means approximately 15,600 mi^2 of the land area must be dedicated exclusively to ground-mounted solar energy systems. While one might consider this is a small portion of the contiguous surface of the U.S., they overlook the land topography, Terrain morphology, indigenous ecology, and other environmental factors for implementing such systems. According to the energy zones mapping tool [4], there are limited land suitable for the U.S. to install ground-mounted PV systems (Figure 1.1), and of that area, much less will be available due to extensive human occupancy.

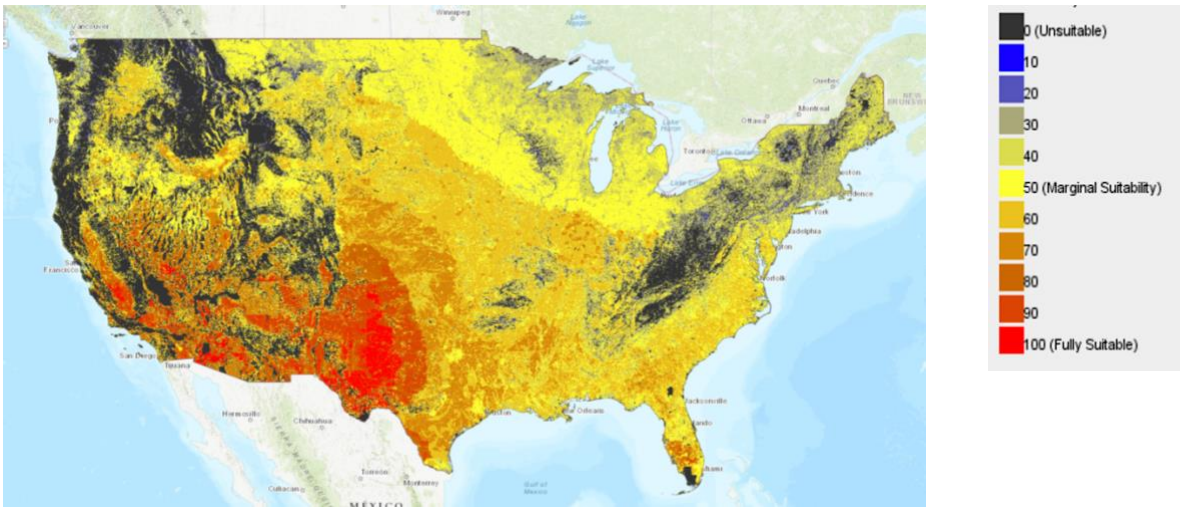

Figure 1.1 Regions that are suitable for utility scale PV systems.

Not only preparing that amount of land area proper for installing ground-mounted solar panels is extremely costly due to high costs of land, but also it requires cutting a large number of trees, flattening topography, and destroying ecological systems which are contradictory to the main goal of solar energy as being a source of clean and eco-friendly energy.

Additionally, in terms of energy infrastructure, due to the high penetration of distributed PV systems like rooftop PV and small ground-mounted PV systems, the fluctuations in PV power generation are on the rise. This situation poses a potential strain on the regulation of distribution voltage. Consequently, there is a risk of accelerated deterioration of electromechanical utility equipment and increased complexity in the setup of circuit-breakers and other protection systems. These challenges could lead to increased costs, hinder further PV deployment, or both [5]. Furthermore, oversupply or power curtailment is another significant issue. This occurs when PV power generation exceeds electricity demand, and the surplus power is fed back into the grid. Notably, this becomes more problematic during noon hours in spring and summer.

In regions with high solar penetration, such as California, a phenomenon known as the "duck curve" has been identified by the California Independent System Operator (CAISO) [6]. The curve depicts two key challenges: first, a significant decrease in net electricity load during mid-day, leading to oversupply and potential curtailment of PV systems; second, a sharp increase in grid electricity demand during late hours of the day, causing a steep ramp in the curve. This steep ramp raises concerns that traditional energy generators may not be able to adjust quickly enough, particularly on days characterized by the duck curve [10]. Additionally, as solar power curtailment increases with higher solar penetration into the grid, the return on investment (ROI) becomes prolonged. The ultimate consequence of those failures would be increased costs and reduced environmental and economic benefits of PV systems.

1.2 Research gaps

The installation of rooftop solar systems has been the predominant method for on-site solar energy generation, and this approach is expected to account for 10%-20% of total solar deployment by 2050 [11]. Since rooftop PV panels will perform similarly to solar farms and exacerbate the duck curve, it is crucial to ensure that BIPV systems do not intensify this effect while maintaining high efficiency, given the anticipated growth of PV systems.

While roof-mounted PV systems are capable of offsetting low-rise buildings' energy consumption, with more urban areas expansion and population growth, the availability of rooftop space on high-rise buildings will become increasingly limited to meet the entire building's electricity demand loads [12] [13]. Consequently, to optimize power production and enhance energy efficiency in high-rise buildings, their façade surfaces offer more promising potential for achieving decarbonization goals. The taller the building, the greater the opportunity to install PV material and generate on-site electricity. With more than 6 million commercial buildings in the U.S. [14], the total area of the exterior envelopes of those buildings has a great potential to integrate solar panels to offset electricity usage of the buildings' energy load demand.

A commonly explored solution to address the duck curve involves solar farms and battery storage systems. However, this study takes a different approach by focusing on buildings as a solution to mitigate duck curve issues. It establishes scoring methods for both south-facing PV-louver systems and west-facing PV-fin systems, quantifying the effectiveness of each BIPV system in addressing the challenges associated with the duck curve. Additionally, existing research on BIPV systems primarily focuses on a limited number of climate zones. This research aims to close this gap by investigating the performance of BIPV systems in all ASHRAE climate zones. Each

chapter of this thesis addresses one of the existing research gaps, as explained in the following sections:

1.2.1 Panels self-shading in BIPV systems

The main challenge in integrating PV into the façade is that the PV materials with higher efficiency are not transparent, limiting the penetration of sunlight into the building. Attaining significant levels of transparency in BIPV glass without compromising efficiency and incurring additional costs remains challenging. While BIPV facades that specifically customized to requirements of a project are extremely expensive, many designers and engineers opt for thin film PV materials, trading electricity production efficiency for receiving indoor daylight inside of the building. Horizontally installed PV modules on the south facing facade (PV-louvers) or vertical PV-fins installed on the west façade allow sunlight penetration into the building. However, those BIPV façade systems are often subject to partial shadows from panels' self-shading. Currently, the tools and methods suggested by researchers to tackle PV array's partial shading problems are not applicable to BIPV façade systems as they are designed to be integrated into large-scale PV systems.

1.2.2 Investigation of different BIPV typologies' performance in all ASHRAE climate zones

As Figure 1.2 illustrates, BIPV systems consist of various components with different characteristics that interact to create an advanced system. Site condition, analysis period, PV system architecture design are only a few factors affecting BIPV systems. Simply supplying buildings with electricity from PV systems without optimizing building energy consumption is inefficient. Although many cities and states, such as New York and California, are mandating the implementation of PV systems in both new and existing constructions, there are currently no requirements for installing BIPV systems. A comprehensive assessment of the impact of different

BIPV typologies on power generation and building energy consumption across all ASHRAE climate zones has been lacking.

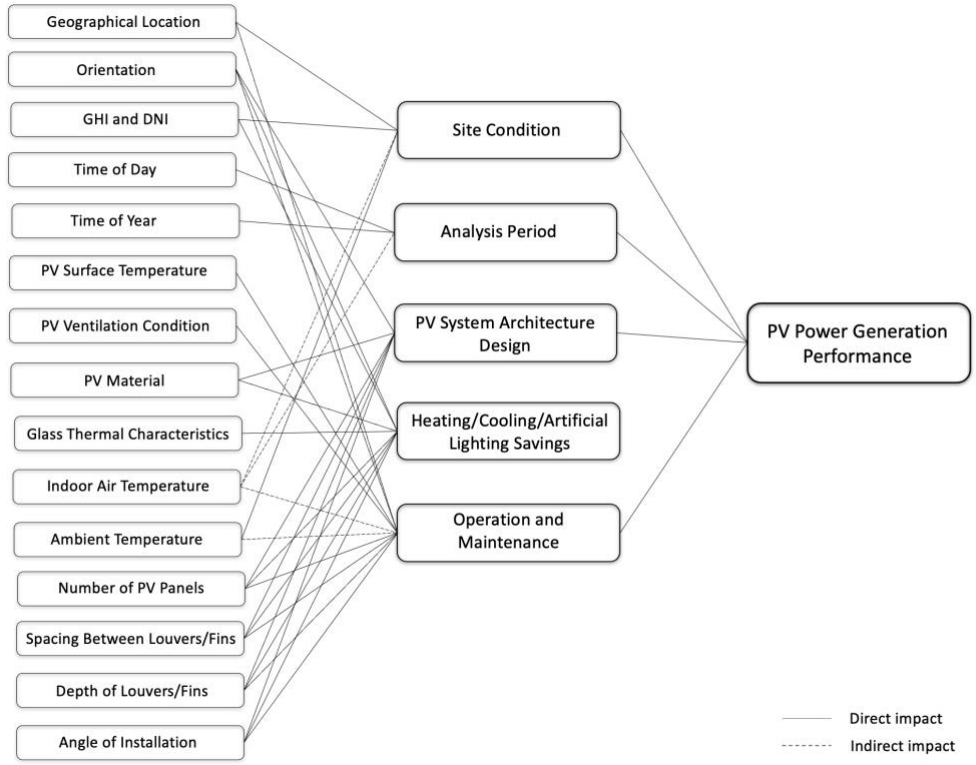

Figure 1.2 Variables affecting BIPV system performance.

1.2.3 PV system oversupply and power curtailment

Energy consumption and PV power production vary significantly depending on climate, and they do not follow the same pattern. Therefore, a more granular study is needed to investigate the performance of different BIPV typologies in various climate zones and their impact on building energy consumption, including heating, cooling, and lighting. Since PV system oversupply or power curtailment is a significant issue in regions with high solar power penetration, it is crucial to understand consumers' trade-off decisions involving grid electricity consumption, BIPV system efficiency, and associated costs as early in the design process as possible. From a utility standpoint,

preventing PV power oversupply ensures reliable and sustainable energy systems in regions with high solar penetration.

1.2.4 responding to the building electricity demand in late hours of the day

There is a growing need for small-scale PV systems that can be integrated into buildings to offset their electricity consumption during late hours of the day while addressing the challenges associated with the steep ramp of the duck curve. This study aims to bridge the gap by investigating the hypothesis that integrating PV panels into the west facades of commercial buildings will provide utilities with a buffer to gradually ramp up their production in the later hours of the day.

1.3 Research questions

The duck curve presents two significant challenges: steep ramps in building net energy consumption and PV systems' electricity overgeneration. This study focuses on exploring the impact of BIPV facade systems on addressing these issues. To achieve this goal, several key questions are addressed:

1. How different BIPV typologies impact the alleviation of the duck curve and mitigating the problems associated with it?
2. How different BIPV typologies contribute to the building energy consumption across different climate zones?
    a) What trade-offs exist between different BIPV typologies' power production and building energy consumption in different climate zones?
    b) In which climate zones can BIPVs reduce the PV system overgeneration and shift the deep valley of the duck curve during midday?

3. How to minimize the power output drops caused by PV modules' self-shading in different BIPV systems?

This thesis investigates those key research questions through a comprehensive analysis of building energy consumption. The analysis includes heating, cooling, lighting, equipment usage, and PV system power production performance. The goal is to close the knowledge gap and provide insights relevant to the research questions (Figure 1.3). This thesis adheres to the 3-paper dissertation format used at the University of the North Carolina at Charlotte. Each chapter corresponds to a specific research objective, as follows:

Chapter 2: This chapter constitutes the first paper of this thesis. It investigates building energy consumption and the potential power production of PV-louvers on the south façade. Additionally, it examines the occupants' visual comfort. As mentioned in section 1.2, there is a gap in the existing literature regarding the performance of BIPV systems across all ASHRAE climate zones. This research aimed to address this gap by testing three hypotheses:

- PV-south louvers will enhance the energy performance of buildings located in cooling-dominant regions.
- PV-mounted roofs will improve the energy performance of buildings in heating-dominant regions.
- BIPV facades will provide better visual comfort compared to PV-mounted roofs.

To test these hypotheses, Rhino and GH were used to create the 3D model, LB to simulate the irradiance levels on the PV surface, and CS to simulate building energy consumption.

Chapters 3 and 4 constitute the second and third papers of this thesis, respectively. They focus on two critical gaps: responding to building electricity demand without exacerbating the

duck curve issues and understanding building-specific strategies to mitigate these issues. The hypotheses and research methods are explained as follows.

Chapter 3: This chapter tests the hypothesis that PV-louvers on the south façade will not only meet building electricity needs but also reduce oversupply compared to traditional roof-mounted PV systems. The software and tools used to validate this hypothesis were consistent with those in Chapter 2.

Chapter 4: The hypothesis in this chapter is that integrating PV-fins on the west façade will offset the building's electricity consumption, reducing reliance on utilities in the late hours of the day. Additionally, injecting surplus electricity into the grid will alleviate the steep ramp of the duck curve. To test these hypotheses, Rhino and GH were used to create the 3D model, LB to simulate the irradiance levels on the PV surface, and HB to simulate building energy consumption.

Chapter 5: This chapter reviews existing methods and tools to address partial shadows and highlights a crucial gap: the available tools to mitigate power drops due to partial shadows are not applicable to BIPV systems. In BIPV façade systems, irradiance non-uniformity occurs at the PV cell level, unlike large-scale PV systems where shadows affect the PV modules or arrays of modules. To close this gap, it was hypothesized that a circuit connection based on uniform irradiance levels would prevent power drops due to panels' self-shading in BIPV façade systems. To test this hypothesis, I used Rhino and GH to create the 3D model, LB to simulate irradiance levels on the PV surface, and PV Lighthouse to calculate the potential current and voltage output.

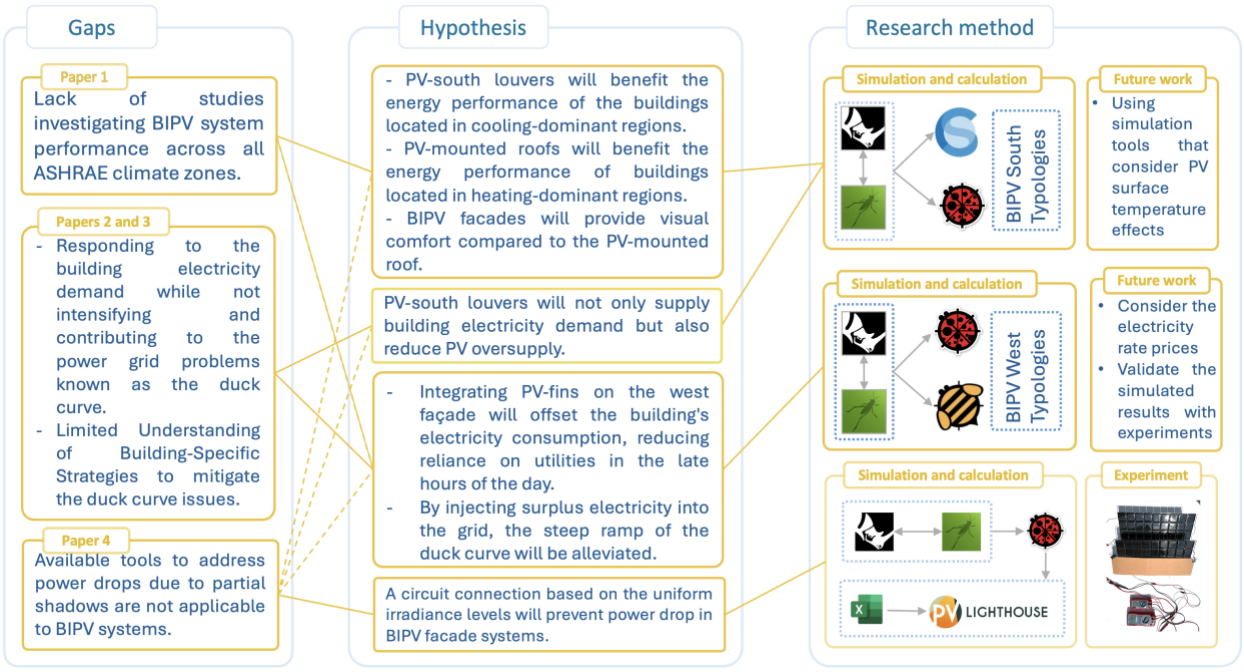

Figure 1.3 Research steps.

CHAPTER 2 (PAPER 1)

COMPREHENSIVE ANALYSIS OF ENERGY AND VISUAL PERFORMANCE OF BUILDING-INTEGRATED PHOTOVOLTAICS IN ALL ASHRAE CLIMATE ZONES

Hamideh Hossei[1], Kyoung-Hee Kim[2]
[1] Department of Infrastructure and Environmental System, UNC Charlotte, USA – 9201 University City Blvd, Charlotte, NC 28223
[2] School of Architecture, UNC Charlotte, USA – 9201 University City Blvd, Charlotte, NC 28223

Graphic abstract

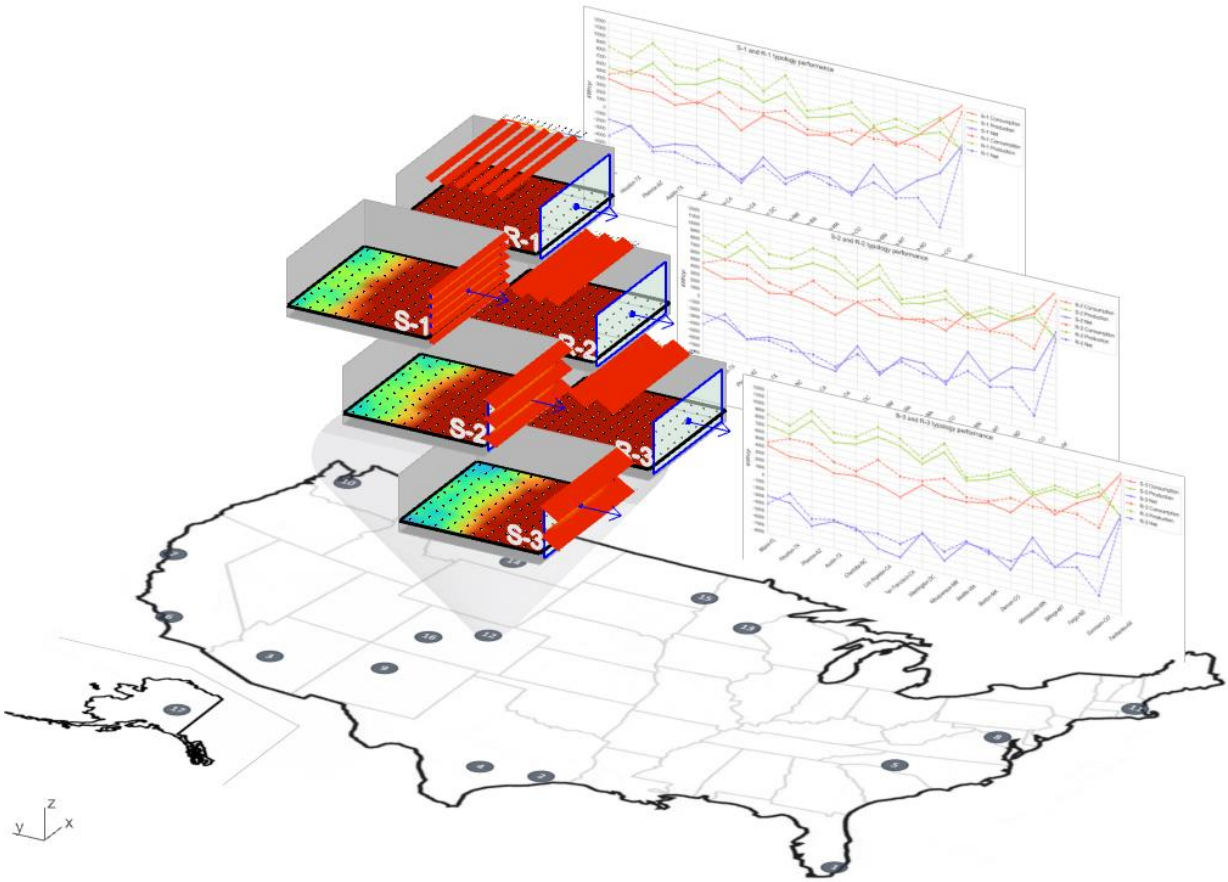

Abstract

Integrating PV panels into building facades (BIPV) necessitates a comprehensive understanding of the PV system's impact on building energy consumption within the site's climate zone. Maximizing PV power output depends on factors such as location, climate type, and latitude. However, minimizing total electricity consumption, which includes cooling, heating, and lighting loads, is significantly influenced by the design of the PV system and the climate region. This study conducted a thorough evaluation of the impact of south-facing PV-integrated louvers on both PV power generation and building energy performance, as well as occupants' visual comfort, across 17 ASHRAE climate regions in the U.S. The results indicated that south-facing PV-integrated louvers significantly reduced building energy consumption in climate zones 1 to 3, as well as 4B and 5B. Wider louvers with longer spacing (S-3 typology) were particularly effective in zones with moderate cooling needs (4A, 4B, 4C). However, in colder climates (6-8) with significant heating demands, roof-mounted systems provided a better balance between power generation and solar heat gain for the building. The PV-louver designs effectively reduced sunlight penetration and maintained illuminance levels within the desired range across most of the floor area. Conversely, roof typologies exhibited lower lighting loads but resulted in significantly high mean illuminance levels on the working surface, leading to disturbing glare for occupants across a large portion of the floor area. The findings of this research offer practical implications for architects, engineers, and policymakers seeking sustainable building solutions.

Nomenclature

Symbols	
U Value	Heat transfer coefficient or thermal transmittance
α	Latitude of the location
E	irradiance on PV surface
η_{PV}	PV panels efficiency
LF	Loss factor of the PV system
η_{inv}	nominal rated DC-to-AC conversion efficiency of the inverter
E_v	Vertical illuminance
L_s	Solar disc
ω_s	solid angle of the sun
P	Position index
Abbreviations	
UDI	Useful daylight illuminance
NZE	Net-zero energy
ASHRAE	American Society of Heating, Refrigerating and Air-Conditioning Engineers
IGU	insulated glass unit
PV	Photovoltaic panel
BIPV	Building integrated photovoltaic panels
WWR	Window-to-wall ratio
LED	Light emitting diode
sDA	Spatial daylight autonomy
MWh	Megawatt hour
kWh	Kilowatt hour
3D	Three dimensions
SHGC	Solar heat gain coefficient
EPW	EnergyPlus weather file
GH	Grasshopper, a plugin for Rhino software
LB	Ladybug, an environmental analysis plugin for Grasshopper for Rhino software
cd/m^2	Candela per cubic meter
W/m	Watt per meter
DC	Direct current
AC	Alternating current
PVPP	PV power production
TMY	Typical meteorological year
NSRDB	National Solar Radiation Database
CS	ClimateStudio
W/m^2K	watts per square meter per kelvin
c-Si	Crystalline silicon
CZ	Climate zone
Tvis	Visible light transmittance
DGP	Probability of the disturbing glare
sDG	Spatial disturbing glare
PVPP	PV power production

1. Introduction

Residential and commercial buildings consumed 22% and 18% of the total energy in the U.S. in 2022 [1]. Integrating PV panels into building roofs is the most common method to offset grid electricity consumption in residential and small to medium commercial buildings. While roof installation is more benefitial for buildings up to 6 story height [2], in case of buildings with a significant facade-to-roof ratio, facades offer larger active surfaces for PV panel integration [3]. In addition to maximizing PV system power production, reducing building energy consumption plays a vital role in addressing the building sector's reliance on fossil fuel-based electricity. To achieve net-zero (NZE) and net-positive BIPVs, the PV system should not only generate on-site electricity but also decrease the building's overall energy consumption while ensuring visual comfort for occupants.

While the building facade offers an excellent opportunity for harnessing solar energy and installing PV panels, understanding the impact of BIPV facade systems on overall building performance is crucial. The overall energy consumption of a building is influenced by three performance metrics: cooling, heating, and lighting loads (Figure 2.1). Vertical PV system design parameters, including the distance, number, length, and width of the PV panels, PV modules tilt angle as well as site condition such as the building's geographical location, latitude, weather condition and facade orientation, affects these performance metrics differently. Consequently, achieving a balance among all performance metrics and the PVPP will result in the optimal BIPV component combination.

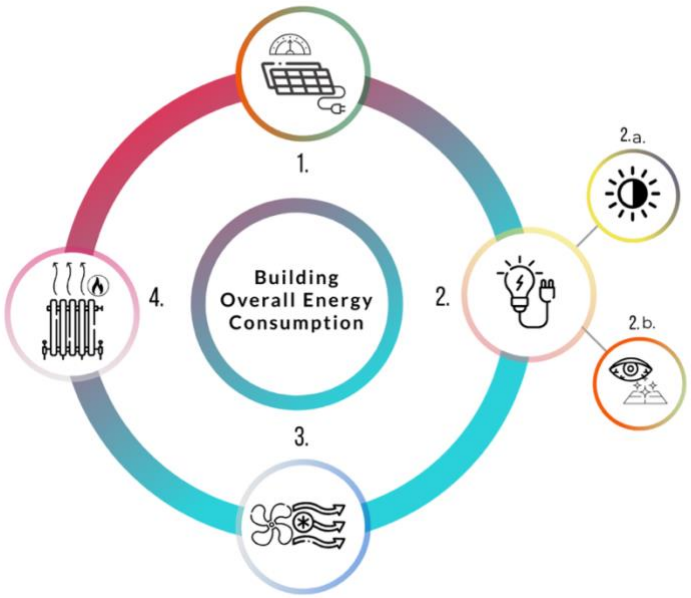

Figure 2.1 Four systems' performances that affect the building's overall energy consumption: 1- PV power production, 2- lighting such as 2.a- artificial lights energy consumption and 2.b) glare, 3- cooling loads, and 4- heating loads.

1.1. PV system design variables: to date, numerous studies have examined the impacts of these variables on PVPP performance and one or more of the building energy performance metrics. For instance, Azami et al. explored the influence of building form and facade orientation on PVPP performance [4]. Similarly, Hwang et al. delved into BIPV system design variables, such as module length, distance, and installation angle, affecting PV power production [5].

The orientation and tilt angle of PV modules significantly impact BIPV energy output. When PVs are installed flat on the building facade, there is an increased cosine loss compared to roof or ground-mounted PVs. Yang's research demonstrated that vertically placing PV panels on the facade reduces power output by approximately 50% compared to the optimal angle [6]. Therefore, optimizing the panel tilt angle is crucial for achieving higher energy yield. While it has been shown that 98.6% of the PV system's optimum performance can be achieved using a tilt angle equal to the location's latitude [7], previous studies indicate that installing PV panels flat on the

building façade generate more electricity during winter months [8] [9]. Kim et al proposed a unique shape for instegrating PV into the façade of the building which had a parametric curvature to maximize the PV cells power production during the entire year [10].

To determine the effects of site conditions, many researchers have considered various climates. For instance, Mesloub et al. investigated the overall energy consumption of a BIPV facade, including artificial lighting, heating, and cooling, in semi-arid climates [11]. Similarly, another study took into account seasonal temperatures and orientation to analyze the power production performance of different ventilated PV cladding facades in hot climate regions. The researchers concluded that regardless of the PV technology, a south-facing facade is the optimal orientation for maximizing power production. Moreover, the west and east facades generated up to 40% more electricity from April to August. They suggested that combining the south and west facades is an effective approach to achieving nearly zero-energy buildings [12].

Alrashidi et al. demonstrated that the orientation of the PV cells affects the diurnal temrature changes of the PV cells and as a result the building cooling loads. In their experimental setup, the lower transparent PV cells caused the most reduction in the building solar heat gain [13]. Liu et al. explained that the solar irradiance levels will affect the PV panels temprature. They investigated the BIPV power performance considering PV modules material, orientation, and tilt angle [14]. Sun et al. tested application of semi-transparent window in different window-to-wall ratio (WWR) in five typical climatic zones in China. They concluded that in order to get sufficient daylight inside of the building, WWR should be 45% or more, i.e. WWR of 75% with 80% transparent PV [15]. A similar study has been done by Cheng et al., assessing the performance of different WWRs in a double-glazed BIPV window. They validate the daylight simulations by experimental test. The result indicated that in order to get sufficient daylight inside of the building

while reducing the building energy loads, the optimum semi-transparent PV area must be 30% or 40% of a south-facing window with WWR 40% [16].

1.2. BIPV power performance: To maximize the BIPV system power output various methods have been proposed in the literature. For instance, placing the PV-louvers in a double-skin façade and ventilating the PV panels to prevent power efficiency drop due to the temperature build-up on PV surface [17], integrating concentrated systems into the BIPV façade [18] and BIPV sun tracking systems using an irradiance model [19] to maximize the irradiance levels reaching on the PV surface. However, in BIPVs reducing the building energy consumption is as important as increasing the PVPP. This importance is particularly amplified in BIPV facades. Therefore, architectures and designers should be well informed of consequences of each design decisions and their impact on energy performance of the building [20].

BIPV façade systems power performance has been evaluated in the literature in conjunction with either daylight performance or building energy consumption loads or both. Huang et al. simulated the performance of a PV integrated insulated glass unit (IGU) to evaluate thermal efficiency, lighting loads and PV power production for different scenarios. The results indicate that the PV IGU effectively reduced building heat gain up to 81.63% and heat loss up to 32.03% [21].

Shi et al. examined how various designs of PV-louvers affect cooling, heating, and lighting energy consumption across five climate types. Their findings indicate that different PV-louver designs lead to varied outcomes in building energy savings, ranging from 2.76% to 105.74% [22]. Kim et al. conducted experimental tests on the power production of three BIPV façades of PV-louver at a fixed angle, PV-louver installed flat on the façade, and different tilt angles of PV-blinds

maximize monthly power production. They concluded that the fixed louver outperform other scenarios [23].

1.3. Impact of BIPV façade systems on building energy performance: BIPV facades attenuate solar heat and daylight penetration into the building and depending on those systems' designed components and site location, leading to varying impacts on building energy consumption. To examin their impact on heating and cooling loads, Nagy et al. suggested to integrate PV panels with overhangs to reduce unnecessary solar heat gain through windows and at the same time generating a great amount of electricity [24]. Freitas et al. compared different design arrangements of PV modules integrated in different exterior surfaces of four buildings in Brazil. Their simulations results indicate that among all of the façade application alternatives, installing PV modules as sun shading elements on the entire façade surface generates higher electricity with energy balance of up to 8.05% of totla energy demand [2]. Cannavale et al. studied a real application of semi-transparent perovskite-based PV glazing in a building located in southern Italy. The building passive energy consumption decreased by 4%. Net energy consumption was diminished by 15% influenced by 27.9 MWh during a year. Comparing the BIPV façade and shading with regular clear glass windows, the result highlighted 18% reduction in the overall annual electricity use of the building [25].

Olivieri et al. introduced an "energy balance index" matrix to evaluate the heating, cooling, and lighting loads, along with the annual energy performance of a single-glazed BIPV window in Madrid, Spain. Their experimentation and simulation results demonstrated that their model could achieve energy savings of at least 18% and up to 50% annually compared to traditional glazing windows [26]. Similarly, a study integrating PV into window blinds, considering variables such as

WWR, PV material, and orientation, found that the south facade was the most advantageous for reducing net energy consumption [27].

In addition to heating and cooling performances, a number of studies also took the lighting performance into consideration. For instance, investigating energy performance of a PV vacuum glazing showed that it effectively reduced cooling loads in the climate regions with hot summer and cold winter, hot summer and warm winters, as well as heating loads in severe cold, cold and hot summer and cold winter. The energy savings potential varied based on the geographical location while it was within the range of 29.4-66.2%. To achieve occupants' preference for illumination it was suggested to use the PV vacuum glazing in combination with the clear vacuum glass. However, for the lower latitude regions, vacuum PV glazing alone is sufficient to allow daylight penetration into the building [28].

One of the challenges of BIPV façade systems is adequate light penetration through the façade into the building. The low daylight factor inside the building will increase electricity demand to meet the indoor light requirements and occupants' optical comfort. This challenge grows in importance in monocrystalline solar cells compared to thin PV film materials. Therefore, it is essential to ensure that the BIPV monocrystalline façade systems allow sufficient light dissemination into the building.

Riaz et al. studied the impact of a semi-transparent BIPV facade on indoor daylighting. Their experimental tests revealed an annual electricity generation of 6070 kWh alongside daylight levels in the building measuring 500 lx, and an average of 300 - 500 lx until 1 pm and 2:30 pm respectively during a typical day [29]. Similarly, another study examined the use of 77% transparent PV cells on an office building facade. The results indicated that, for an office space measuring 76 m2, a combination of 8 52 W LEDs provided 676 lux. It was observed that energy

consumption in the office significantly increased on cloudy days, although the researchers did not provide specific information related to the reduction factor [30].

Roberts et al investigated the effect of a semi-transparent PV-integrated double-skin facade on indoor lights. The results of the study demonstrated that the lux levels were significantly dropped in the work surface level at the center of the office room and they concluded that this type of window is not suitable for geographic locations or climate conditions similar to London, UK [31]. Compared to PV-integrated glass typologies, the BIPV blinds allow more flexibility to balance the visual effects of the façade design (Yu et al. 2021). The spacing between louvers has a greater effect on indoor light penetration in comparison to the tilt angle [32].

Assessing the potential increase in the demand for artificial lighting in occupants' working areas during daylight hours helps balance BIPV facade power production and grid electricity consumption. Various comfort lighting thresholds have been presented in the literature, including a minimum of 500 lux [28], 300 lux [33] [34], and 450-600 lux for tasks such as reading, writing and typing [30]. According to the American Society of Heating, Refrigerating and Air-Conditioning Engineers (ASHRAE) indoor lighting standard, the minimum lux levels range from 30-50 foot-candles for open offices which is equal to approximately 300-500 lux [35]. The European Committee for Standardization suggests three baseline including 300, 500 and 750 lux for indoor illumination levels [36].

According to ASHRAE standards, spatial daylight autonomy (sDA) indicates the percentage of daylight in an occupied space during the portion of the year when the building is operating according to schedules [35]. The sDA index does not account for potential glare. Nabil et al. introduced useful daylight illuminance (UDI), which is a modified index based on sDA. Their research demonstrated that the minimum lux level required for office tasks is 500 lx, while daylight

illuminance exceeding 2000 lx may cause glare [37]. Both sDA and UDI are established considering the use of indoor shutters or adjustable blinds, allowing occupants to adjust them based on the amount of daylight passing through the windows. However, achieving optimal lighting performance with BIPV facades requires considering the fixed position of the PV system on the glazing facade.

A new index for evaluating the PV-integrated windows' louvers daylighting was proposed in previous research. That means the indoor area ratio where the indoor illuminance meets 450 - 2000 lx and the natural light time surpasses 50% during a month [32]. Evaluating the possibility of increasing the need for artificial lighting in occupants' working areas during daylight hours helps to balance out BIPV facades' power production and grid electricity consumption.

1.4. BIPV implementation costs: The convergence of declining PV costs and favorable energy market conditions is creating a compelling economic case for solar installations [38]. The costs of c-Si curtainwall BIPV systems fell within the range of regular façade systems [39], making BIPV façade systems more cost friendly and affordable for many building owners. Field observation of the BIPV systems revealed that enhanced integration between PV material and the building system such as building enclosures further reduced the costs of the BIPV systems [40]. While PV modules take 43% to 77% of the entire system cost, with more technology advancement in PV materials efficiency and price reduction [41], the BIPV systems become more affordable for building owners.

1.5. Gap and problem statement: With the advancements in solar energy and the increasing demand to supply the building sector with renewable energies, the importance of optimizing BIPV

systems to meet design requirements and occupants' comfort is becoming more significant. BIPV system implementation is on the rise due to several factors. The affordability of PV materials, which are comparable in cost to building materials, along with high land expenses for ground-mounted PV systems and power loss through transmission lines from remote solar farms, combined with rising building sale prices and the desire to enhance business image and branding, are motivating building owners and the construction industry to integrate PV systems directly into buildings rather than depending on solar farms.

Integrating PV systems into new construction is growing globally. The European Parliament has passed legislation mandating member states to install solar panels on buildings and undertake renovations to enhance energy efficiency [42] [43]. Germany is leading solar implementation in Europe, with cities like Berlin, Hamburg, Rhineland-Palatinate, Bavaria, Schleswig-Holstein, and Lower Saxony having laws mandating PV system integration into buildings [44]. Similarly, in the U.S., California made rooftop solar PV a requirement on newly built homes, with some cities extending this rule to major renovations [45]. Although energy and building codes require PV integration into buildings, maximizing environmental and financial benefits of these systems requires careful planning. Solely supplying buildings with electricity from PV systems without optimizing building energy consumption is inefficient. In many cases individuals that are involved in the decision making process are uncertain whether rooftop application or facade integration will maximize power production cost savings [46]. Balancing PV power production with building energy consumption is another challenge in the design process of BIPVs, compounded by building location climate type and design constraints, which add complexity to the decision-making process. In addition to that, with urban area development and population growth, many high-rise buildings will be unable to supply the entire building with

rooftop solar electricity, deterring the construction of high-rise NZE buildings. Therefore, understanding how the building's location and choosing the right BIPV components, like PV panel size, design, and installation orientation on the building's exterior, impact BIPV power production and building energy consumption is essential.

Although a review of net zero energy buildings in hot and humid climates revealed that not all the NZE buildings have blinds or shades to control glare [47], integrating PV panels into the buildings is a great way to offset grid electricity consumption specially for tall buildings [48]. Several researchers have focused on integrating PV panels into building facades as shading devices [49] such as PV-blinds [50] [19] and PV-louvers [51] [52] aiming to reduce the building energy consumption while generating on-site electricity. However, studies have also investigated BIPV system performance in various climates, including hot [13], cold [53], tropical [54] and subtropical regions [55]. Nevertheless, these investigations often lacked coverage across different climate zones. For instance, studies like that of Sun et al. [15], which examined BIPV facade performance in five climate regions—severe cold, cold, temperate, hot summer cold winter, and hot summer warm winter—did not consider shading components such as louvers and blinds, as their BIPV system was flat on the facade surface.

Previous research on the impact of BIPV systems on energy savings and power generation has primarily focused on individual climate zones. This study, however, utilizes a more granular breakdown of 17 locations across 16 ASHRAE climate zones [56], as defined by ASHRAE 90.1. This finer-grained approach reflects the reality that building energy code requirements for calculating energy consumption vary significantly depending on climate. By simulating energy use patterns and power production potential with this level of detail, the study allows for a more precise cross-comparison of BIPV performance across diverse climatic conditions. This approach

addresses a critical gap in the existing research, where a comprehensive assessment of PV-louvers' impact on power generation and building energy consumption across all ASHRAE climate zones has been absent. To fill this gap, the study investigates the power performance and energy consumption of south-facing PV-louvers in 17 locations, utilizing three different south facade design typologies.

The outcomes of this research will provide valuable insights for homeowners, business owners, building developers, and construction professionals, enabling them to better understand how their BIPV building will perform in the real world. Additionally, this study will provide information on whether south PV-louvers will have adverse effects on building energy consumption in specific climate regions, thus assisting in informed decision-making. The results of the building energy consumption simulations and potential PVPP of this study were strongly agreed with the data from previous work done by Goia et. al [57] and PVWatts [58], respectively.

2. Materials and methods

2.1. Geometry: To conduct the simulations, a single room with dimensions of 10m x 10m x 4m (length, depth and height) was model in Rhino a 3D modeling software [59]. Each typology included a south-facing window with a window-to-wall ratio (WWR) of 80%. Rooms with a high fenestration ratio often experience overheating, resulting in discomfort or increased energy consumption, even in colder climates [60]. However, to isolate the impact of BIPV systems on building performance and highlight the differences, the rooftop typologies were considered without any shading on the south window, excluding the influence of non-BIPV parameters.

The overall simulation workflow included six BIPV typologies, three typologies of PV-louvers on the south glass facade and three roof-mounted PV (Figure 2.2). While maintaining a

consistent total surface area of 30m² for the PV system, the depth and number of PV-louvers differed across various typologies: in S-1 and R-1, there were 6 louvers at a depth of 0.5m; in S-2 and R-2, there were 3 louvers at a depth of 1m; and in S-3 and R-3, there were 2 louvers at a depth of 1.5m.

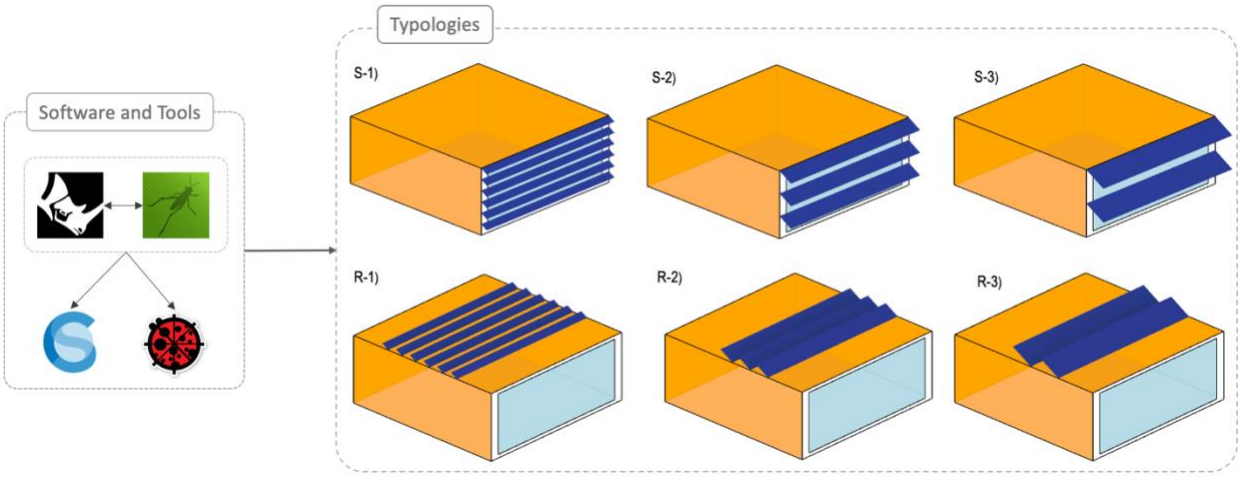

Figure 2.2 Rhino and plugins including GH, CS and LB were used to simulate performances of the three PV-louvers integrated south façade and PV-mounted roof typologies.

2.2. Site condition and building zone setup: To analyze the performance of this model in various locations, a combination of seamlessly integrated software tools was utilized. Grasshopper (GH), a visual programming environment tightly integrated with Rhino, provided a streamlined workflow for defining and running the simulations [59]. Ladybug (LB version 1.7.0) tools act as a bridge, connecting Rhino's 3D modeling capabilities to a range of validated simulation engines [61]. In this study, LB utilized EnergyPlus engine [62] along with EnergyPlus Weather (EPW) data [63] for simulating irradiance levels on the PV panels. Finally, ClimateStudio [64] (CS version 1.9.8), a plugin for Rhino that built on Radiance and EnergyPlus engines, was used to simulate the building's lighting, heating, and cooling loads.

The building energy performance analysis was conducted in 17 different locations in the U.S., across various climate regions (Table 2.1). Building program was set to an open medium office. ASHRAE 90.1 were used as the building standards in all the energy simulation settings. In all simulation runs, the building program was configured for a medium open-space office, and occupancy schedules were adjusted to match typical office operations. Weekdays began at 6 am and gradually ramped up until fully occupied by 9 am, then started decreasing at 3 pm until reaching vacancy at 9 pm. On the first day of the weekend, operations began at 6 am, increased to half occupancy by midday, and then decreased starting at 2 pm until fully vacant by 5 pm. The second day of the weekend had no occupancy scheduled.

Table 2.1, locations visualization map, PV tilt angles, and climate zones list

	City, State	Climate type	Climate zone	Latitude	PV optimum tilt angle
1	Miami, FL	Tropical	1A	25.82	24.17
2	Houston, TX	Hot-humid	2A	29.65	26.42
3	Phoenix, AZ	Hot-dry	2B	33.45	28.44
4	Austin, TX	Warm-humid	3A	30.29	26.78
5	Charlotte, NC	Warm-humid	3A	35.22	29.33
6	Los Angeles, CA	Warm-dry	3B	33.92	28.74
7	San Francisco, CA	Marine	3C	37.80	30.46
8	Washington DC	Mixed-humid	4A	38.85	31.02
9	Albuquerque, NM	Mixed-dry	4B	35.04	29.24
10	Seattle, WA	Mixed (marine)	4C	47.53	34.57
11	Boston, MA	Cold-humid	5A	42.37	32.53
12	Denver, CO	Cold-dry	5B	39.83	31.45
13	Minneapolis, MN	Cold	6A	45.07	31.45
14	Billings, MT	Very cold	6B	45.80	33.90
15	Fargo, ND	Subarctic	7A	46.93	34.34
16	Gunnison, CO	Polar	7B	38.53	30.87
17	Fairbanks, AK	Other	8	64.82	40.64

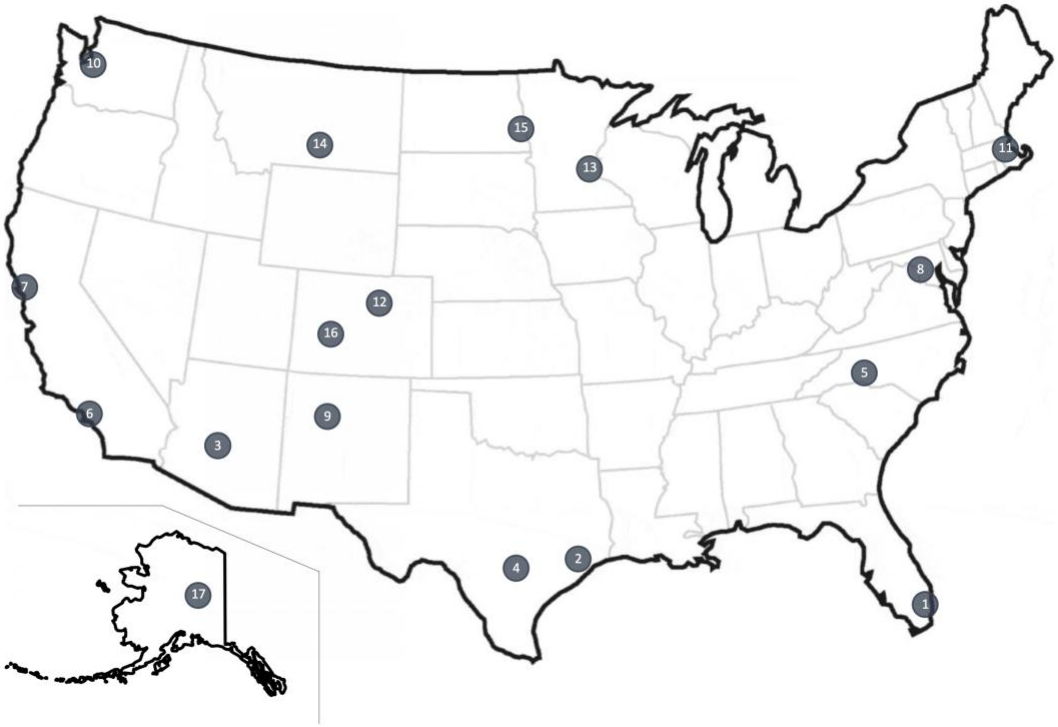

$$1.3793 + \alpha \times \left(1.2011 + \alpha \times \left(-0.014404 + \alpha \times (0.000080509)\right)\right) \quad (1)$$

where α is the latitude of the location.

3.3. BIPV system potential power production: the optimum tilt angle of the PV modules in both PV-louvers and roof-mounted PV typologies were calculated using equation 1 from Jacobson et al. research [65].

The LB plug-in utilizes the EnergyPlus code to define sky matrix attributes based on the analysis period and the location weather data. In this part of the analysis workflow, the Cumulative Sky Matrix component was used to create a matrix of both direct normal radiation and diffuse horizontal radiation values from each path of sky dome. The analysis period was set to one month to calculate the average daily irradiance levels (kWh/m2/day) on the PV surface for each month. Nonuniform irradiance levels are a common issue in PV-louver systems due to self-shading of

panels. This leads to a significant voltage drop, resulting in a dramatic reduction in PVPP performance. Previous research [48] proposed a new circuit connection for partially shaded BIPV systems. According to their study, a hybrid connection of series and parallel connections between the cells mitigated the voltage drop from 98% to 21%. Since LB simulates the irradiance levels falling on the PV surface, incorporating this hybrid circuit connection approach could potentially convert a majority of the received irradiance into power. Therefore, the calculation of potential power production for the PV system in this study relies on the irradiance levels, demonstrated in equation 2.

$$PVPP = E \times \eta_{PV} \times (1 - \mathrm{LF}) \times \eta_{inv} \quad (2)$$

Where

PVPP is potential power production,

E is irradiance on PV surface,

η_{PV} is PV panels efficiency,

LF is loss factor

η_{inv} is nominal rated DC-to-AC conversion efficiency of the inverter

Mono crystalline silicon (c-Si) PV cells were considered for the PV material in all typologies. While in the laboratory conditions c-Si PVs have an efficiency range of 25%-27%, their real-world efficiency varies from 16% to 22% [66]. In this study, η_{PV} considered to be 19% which is the median of the real-world c-Si PV efficiency range. For LF factor, losses due to soiling, shading, snow, mismatch, wiring, connector, light-induced degradation, nameplate rating, age, and availability, were accounted for 14.08% [67]. The η_{inv} factor established by the National Renewable Energy Lab (NREL), is considered to be 96% [67].

The simulated potential rooftop typologies' PVPP were validated by PVWatts (version 8) [58] which is an online simulation tool used for modeling and predicting the performance of grid-connected PV systems, including rooftop installations. It relies on an hourly typical meteorological year (TMY) database from the National Solar Radiation Database (NSRDB) and considers factors like location, system size, tilt angle, azimuth, and solar radiation data. Given that PVWatts has been shown to underestimate PV system potential power generation by up to 38% [68], our study reveals that the simulated power outputs of various roof typologies exhibited deviations ranging from 4% to 28% compared to the PVWatts calculator. Despite these variances, there was a clear alignment in the trend of PV potential power production between our simulations and the PVWatts data. After verifying the accuracy of the simulation script with the PVWatts data output, the PV array was repositioned from the horizontal roof surface to the vertical south facade surface for simulating the PV-louvers potential PVPP (Figure 2.3).

3.3.1. Building energy consumption: In this simulation workflow, the PV-louvers were defined as shading devices while the roof-mounted PV typologies had no shades on the south façade glazing area. A double-glazing system with 6 mm glass, 6 mm air gap was considered in all typologies and locations. U-value (W/m^2K), SHGC and Tvis of the window were set to 2.67, 0.703 and 0.781, respectively. Thermal properties of the opaque walls, roof and floor surfaces of the building were set to align with current standards requirements and contemporary recommendations in each locations' climate zone (see Table 2.2). The heating (E_H), cooling (E_C) and lighting (E_L) loads of the room were simulated in all building typologies using CS.

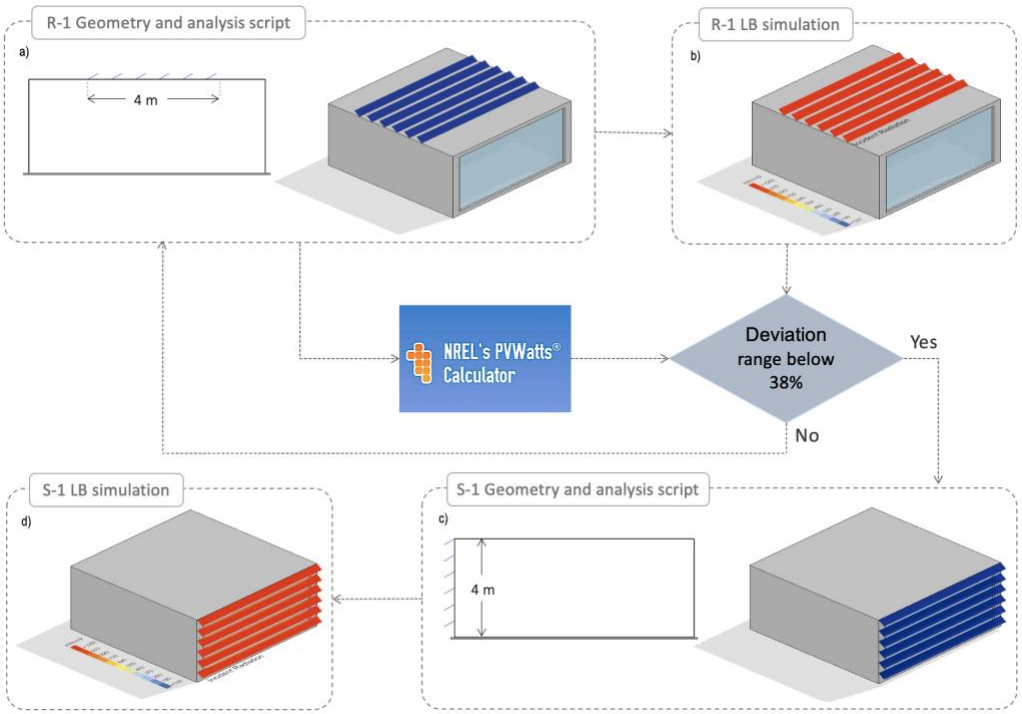

Figure 2.3 Validation process. a) PV-mounted roof, b) simulating irradiance levels on the PV-mounted roof surface, c) PV-louvers geometry, and d) simulating irradiance levels on the PV-louvers surface.

The accuracy of the energy consumption simulation script for an 80% WWR was validated by comparing the energy consumption of the roof typologies with data from previous research [57]. Afterwards, energy performance of the PV-louvers on the south-facing facade was analyzed and compared to their respective roof designs, assuming a grid connection without energy storage. The net energy use was calculated by subtracting power generated by PV system (E_{PV}) from sum of the loads using the equation below:

$$E_{net} = E_H + E_C + E_L - E_{PV} \quad (3)$$

Lighting availability schedules were set to the office schedule with the power density of 6.5 W/m. The working surface height for daylight and glare analysis was set at 0.75m above the floor. An array of 400 sensory grid points on the working surface calculated the daylight and glare simulations among all typologies. The assigned material to each geometry surfaces had a diffuse factor of 70%, 50% and 20% for ceiling, walls and floor, respectively. The acceptable illuminance levels range were defined 300lux to 1000lux, according to IES Lighting Standards [69].

3.3.2. Occupants visual comfort: Occupants visual comfort was assessed by simulating the probability of the disturbing glare (DGP) and mean illuminance levels on the working surface.

Table 2.2, Thermal properties of the opaque walls, ground floor and exterior walls in different climate zone

Parameters	**Climate Zones**							
	1	2	3	4	5	6	7	8
Roof								
U-value (W/m^2K)	0.263	0.215	0.215	0.177	0.177	0.177	0.156	0.156
Thermal Capacity ($kJ/K/m^2$)	469.7	471.13	471.13	472.78	544.17	0.422	474.09	474.47
Exterior walls								
U-value (W/m^2K)	2.11	0.748	0.624	0.537	0.47	545.93	0.377	0.26
Thermal Capacity ($kJ/K/m^2$)	532.3	538.50	540.40	542.28	544.17	545.93	547.93	556.47
Ground								
U-value (W/m^2K)	0.806	0.729	0.703	0.692	0.584	0. 584	0.571	0.571
Thermal Capacity ($kJ/K/m^2$)	471.6	471.91	472.00	472.0	472.48	472.48	472.54	472.54

The CS uses the Radiance ray tracer to calculate the distribution of illuminance, determining the probability of disruptive glare when light levels exceed 320 lux across eight distinct viewing angles.

$$DGP = c_1 \times E_v + c_2 \times log\left(1 + \sum_i \frac{L_{s,i}^2 \times \omega_{s,i}}{E_v^{a_1} \times P_i^2}\right) + c_3 \quad (4)$$

where

E_v is vertical illuminance (lux),

L_s is solar disc (cd/m²),

ω_s is solid angle of the sun,

P is position index

Based on simulation results, the CS classifies DGP into four ranges: DGP ≤ 34% as imperceptible glare, 34% < DGP ≤ 38% as perceptible glare, 38% < DGP ≤ 45% as disturbing glare, and DGP > 45% as intolerable glare. This study focuses on spatial disturbing glare (sDG) to assess visual comfort in BIPV typologies. sDG values signify views across the occupied floor area experiencing disturbing or intolerable Glare (DGP > 38%) for at least 5% of occupied hours.

3. Results

The heating, cooling and lighting energy consumption of 6 different BIPV systems were simulated in 17 different U.S. locations across all ASHRAE climate zones. Figure 2.4 depicts the results of thermal and lighting loads. The impact of adding PV-louvers to the south glass facade varied across different climate zones in terms of the building's annual cooling and heating loads. Interestingly, in tropical climates, the effect on reducing cooling loads was minimal. However, in hot-humid, hot-dry, warm-humid, warm-dry, and marine climates, the reduction in heating loads increased, with the most significant reduction observed in San Francisco, CA, which falls under the marine climate zone. In mixed-humid, mixed-dry, and mixed (marine) climate zones, PV-louvers decreased cooling loads but led to an increase in heating loads. Nevertheless, the total

thermal electricity loads for the buildings remained relatively consistent after integrating the PV-louvers on the south window. Although PV-louvers resulted in a reduction of cooling loads in cold-humid, cold-dry, cold, and very cold climate regions, they significantly increased heating loads, especially from cold-humid to very cold climates. The decrease in cooling loads in subarctic, polar, and "other" climate regions was minor, while the increase in heating loads was dramatic.

Roof typologies allowed more daylight through the south window, however as shown in Figure 2.4, BIPV façade typologies consumed more electricity to meet standard lighting levels for offices. Nevertheless, the mean illuminance levels on the office work surface exceeded standard thresholds in roof typologies, leading to excessive glare for at least half of the floor area. Table 2.2 presents visualized mean illuminance levels and evidence of disturbing glare in three locations: Austin, TX; Denver, CO; and Fargo, ND. The frequency of this distracting glare increased with the location's latitude, from Austin (30.29° N) to Fargo, ND (46.93° N). As Figure 2.4 depicts, the mean illuminance levels of the roof typologies exceed the standard threshold of 2000lux across all the locations. Figure 2.5 shows the DGP for other locations. On average, roof typologies had a DGP of 20% across different locations. Seattle, WA had the lowest DGP at 17%, while Billings, MT had the highest at 23%. Façade typologies significantly reduced DGP compared to roof typologies. The average DGP for S-1, S-2, and S-3 typologies was 3.0%, 3.6%, and 1.9%, respectively.

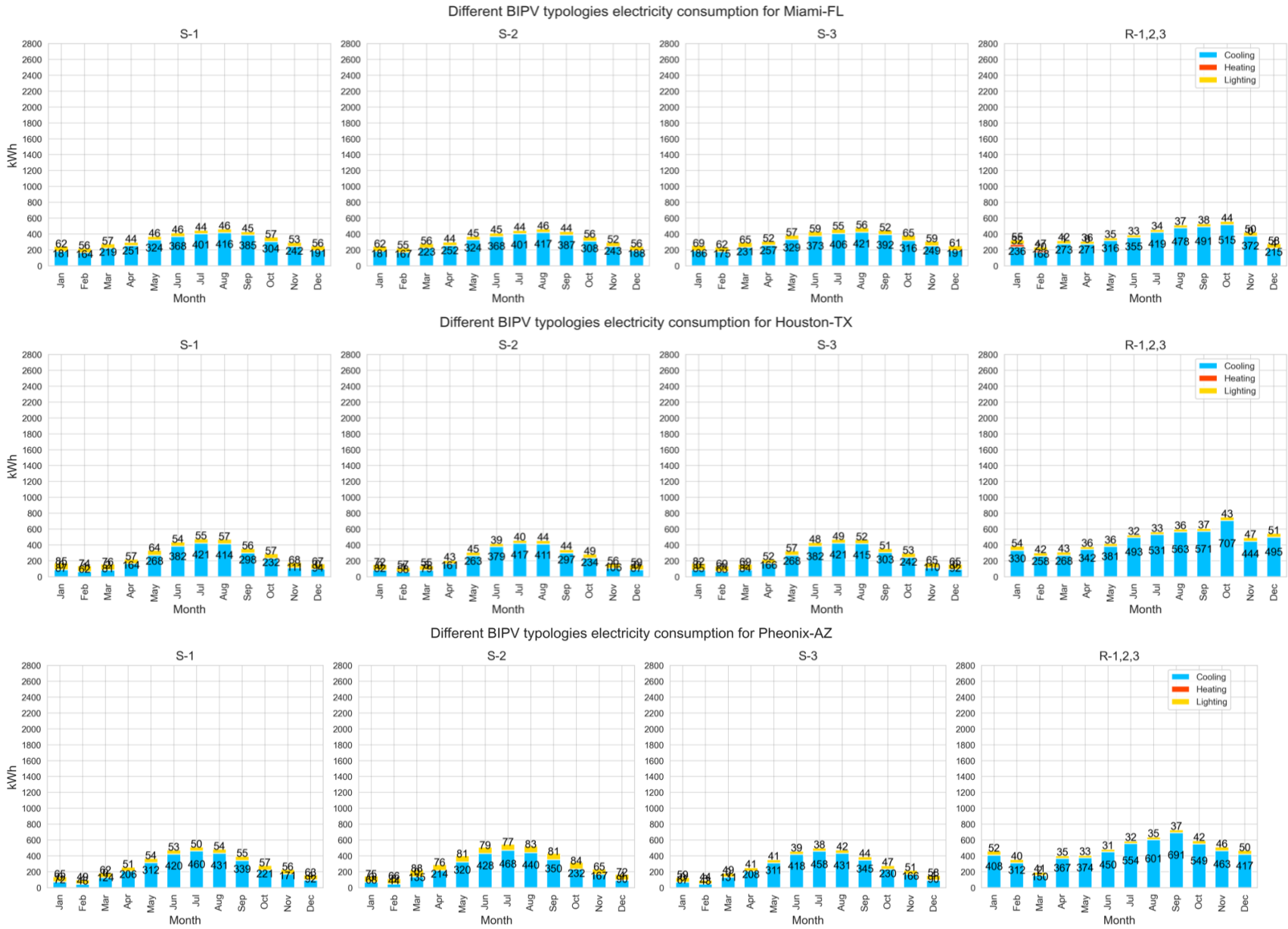
Different BIPV typologies electricity consumption for Miami-FL
S-1
S-2
S-3
R-1,2,3
Cooling
Heating
Lighting
kWh
Month
Jan
Feb
Mar
Apr
May
Jun
Jul
Aug
Sep
Oct
Nov
Dec
Different BIPV typologies electricity consumption for Houston-TX
S-1
S-2
S-3
R-1,2,3
Cooling
Heating
Lighting
kWh
Month
Different BIPV typologies electricity consumption for Pheonix-AZ
S-1
S-2
S-3
R-1,2,3
Cooling
Heating
Lighting
kWh
Month

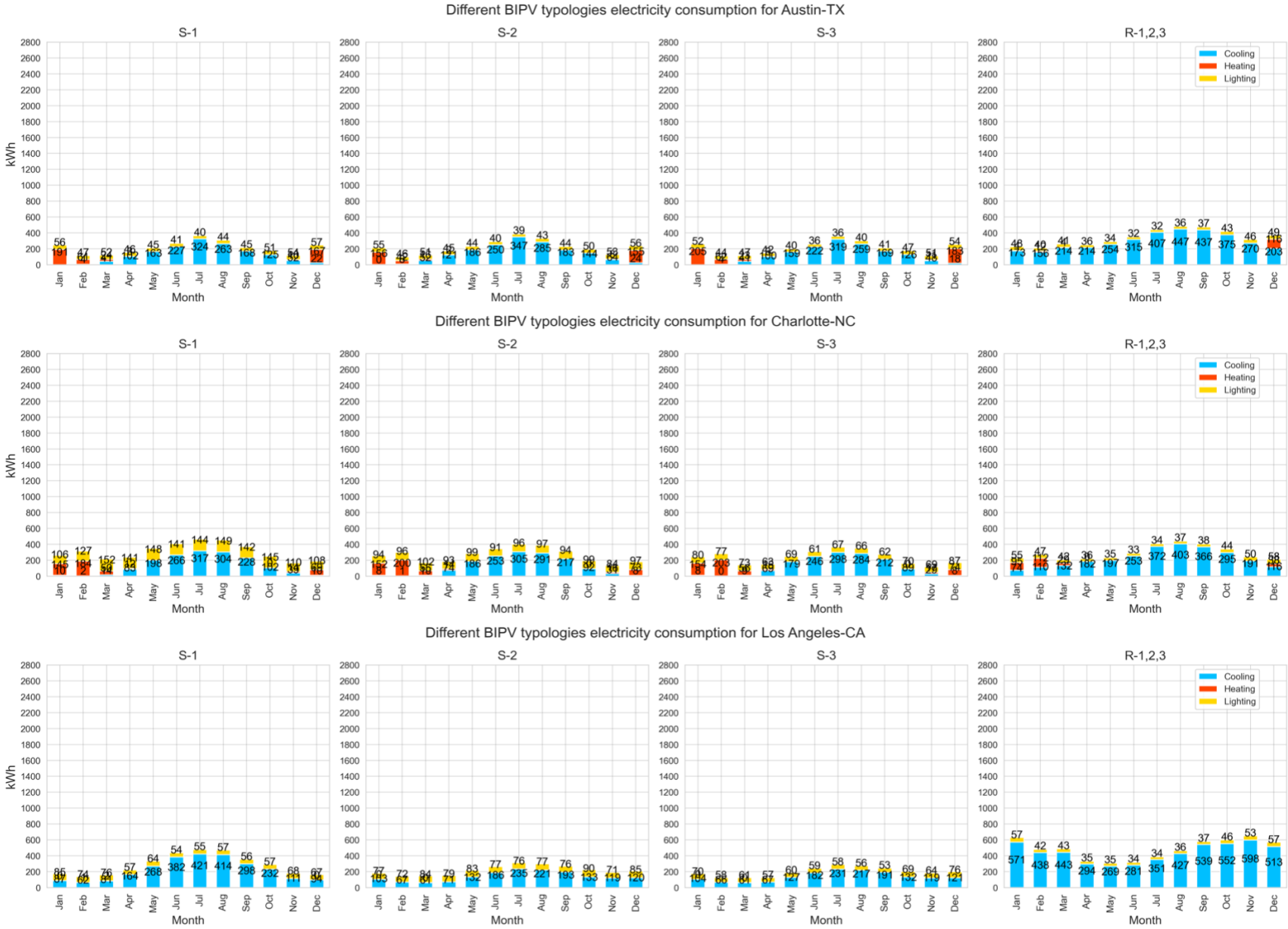
Different BIPV typologies electricity consumption for Austin-TX
S-1
S-2
S-3
R-1,2,3
Cooling
Heating
Lighting
kWh
Month
Different BIPV typologies electricity consumption for Charlotte-NC
S-1
S-2
S-3
R-1,2,3
Cooling
Heating
Lighting
kWh
Month
Different BIPV typologies electricity consumption for Los Angeles-CA
S-1
S-2
S-3
R-1,2,3
Cooling
Heating
Lighting
kWh
Month

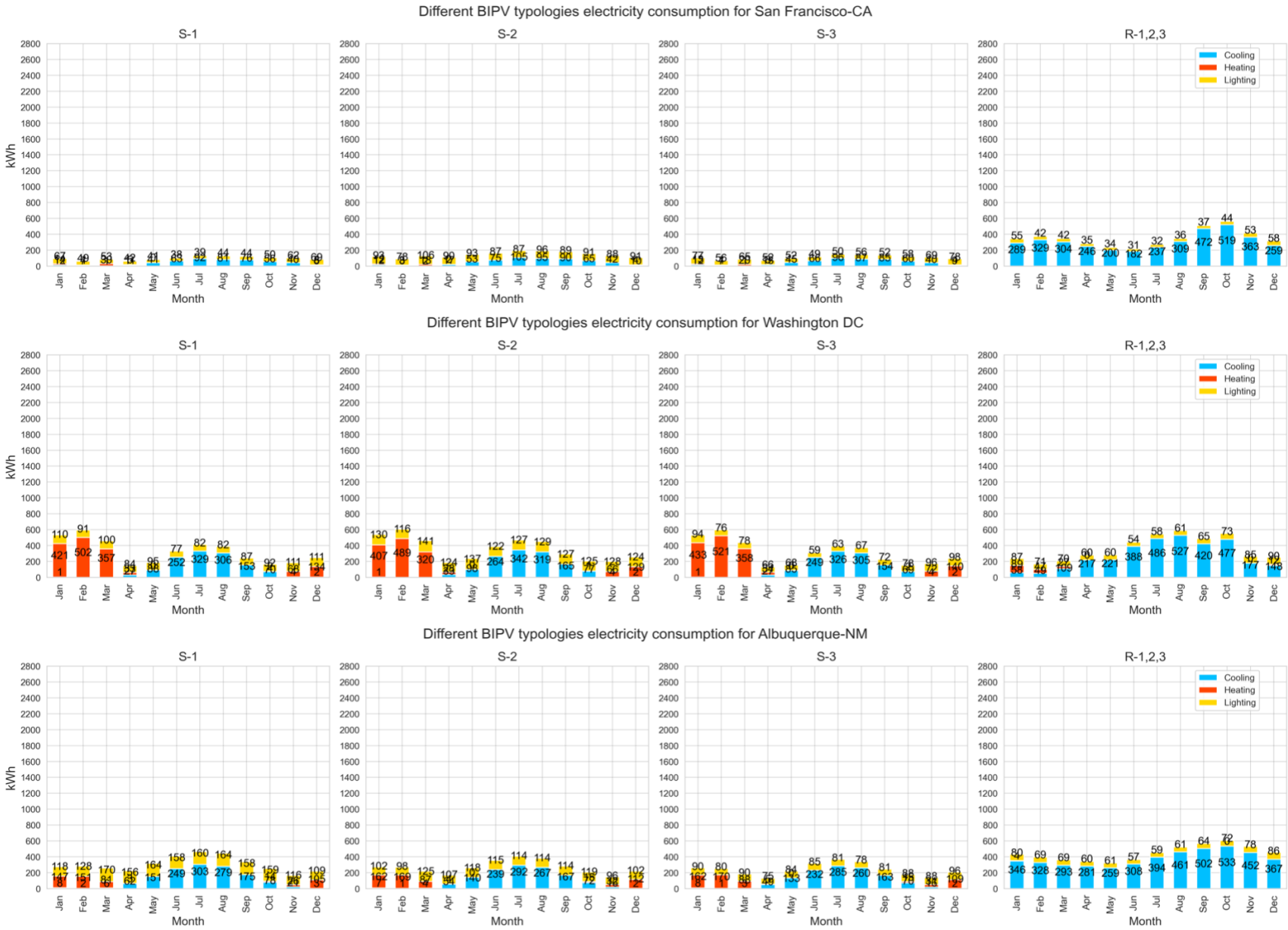
Different BIPV typologies electricity consumption for San Francisco-CA
S-1
S-2
S-3
R-1,2,3
Cooling
Heating
Lighting
kWh
Month
Different BIPV typologies electricity consumption for Washington DC
S-1
S-2
S-3
R-1,2,3
Cooling
Heating
Lighting
kWh
Month
Different BIPV typologies electricity consumption for Albuquerque-NM
S-1
S-2
S-3
R-1,2,3
Cooling
Heating
Lighting
kWh
Month

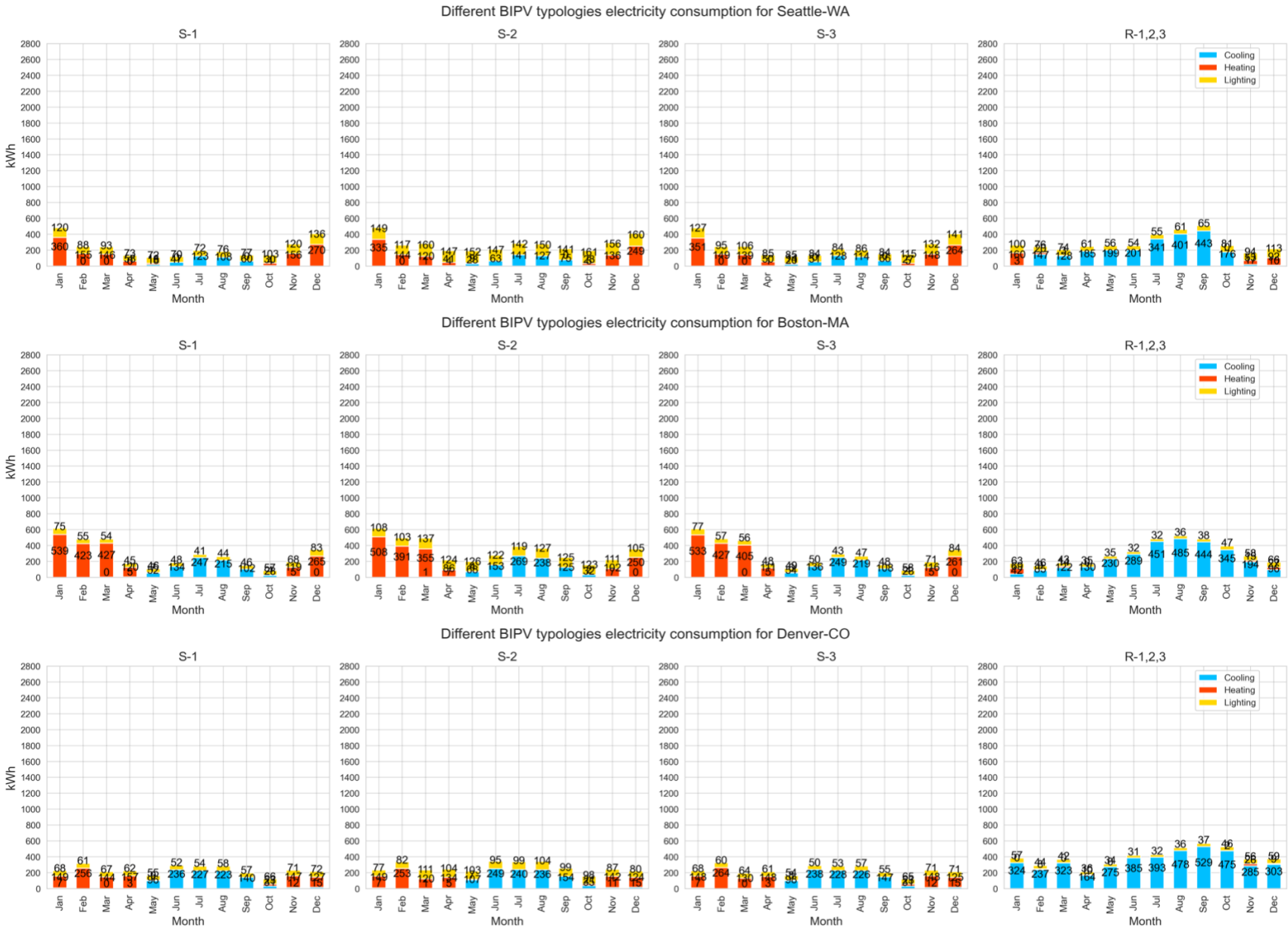
Different BIPV typologies electricity consumption for Seattle-WA
S-1
S-2
S-3
R-1,2,3
Cooling
Heating
Lighting
kWh
Month
Different BIPV typologies electricity consumption for Boston-MA
Different BIPV typologies electricity consumption for Denver-CO

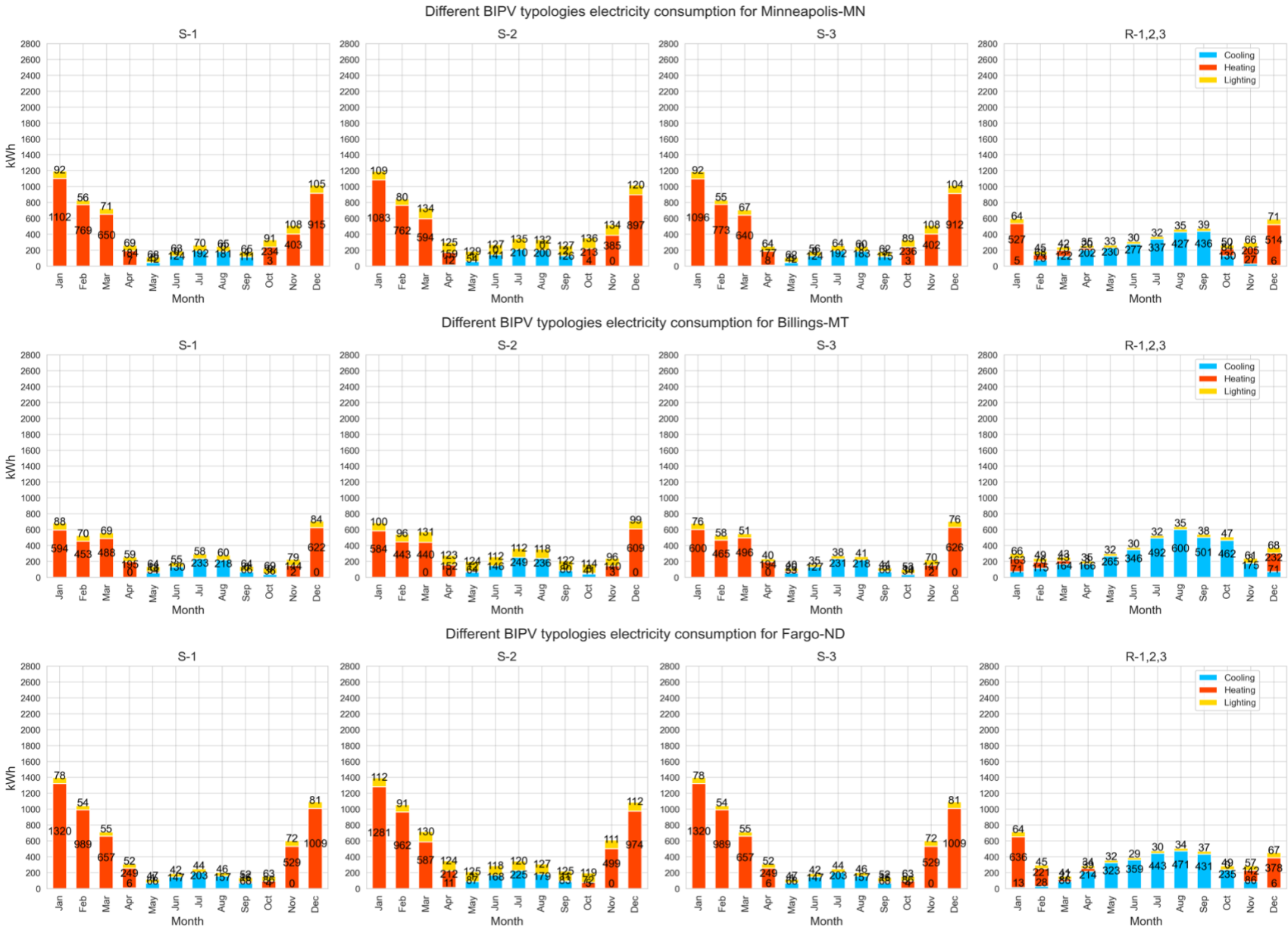
Different BIPV typologies electricity consumption for Minneapolis-MN
S-1
S-2
S-3
R-1,2,3
Cooling
Heating
Lighting
kWh
Month
Jan
Feb
Mar
Apr
May
Jun
Jul
Aug
Sep
Oct
Nov
Dec
Different BIPV typologies electricity consumption for Billings-MT
Different BIPV typologies electricity consumption for Fargo-ND

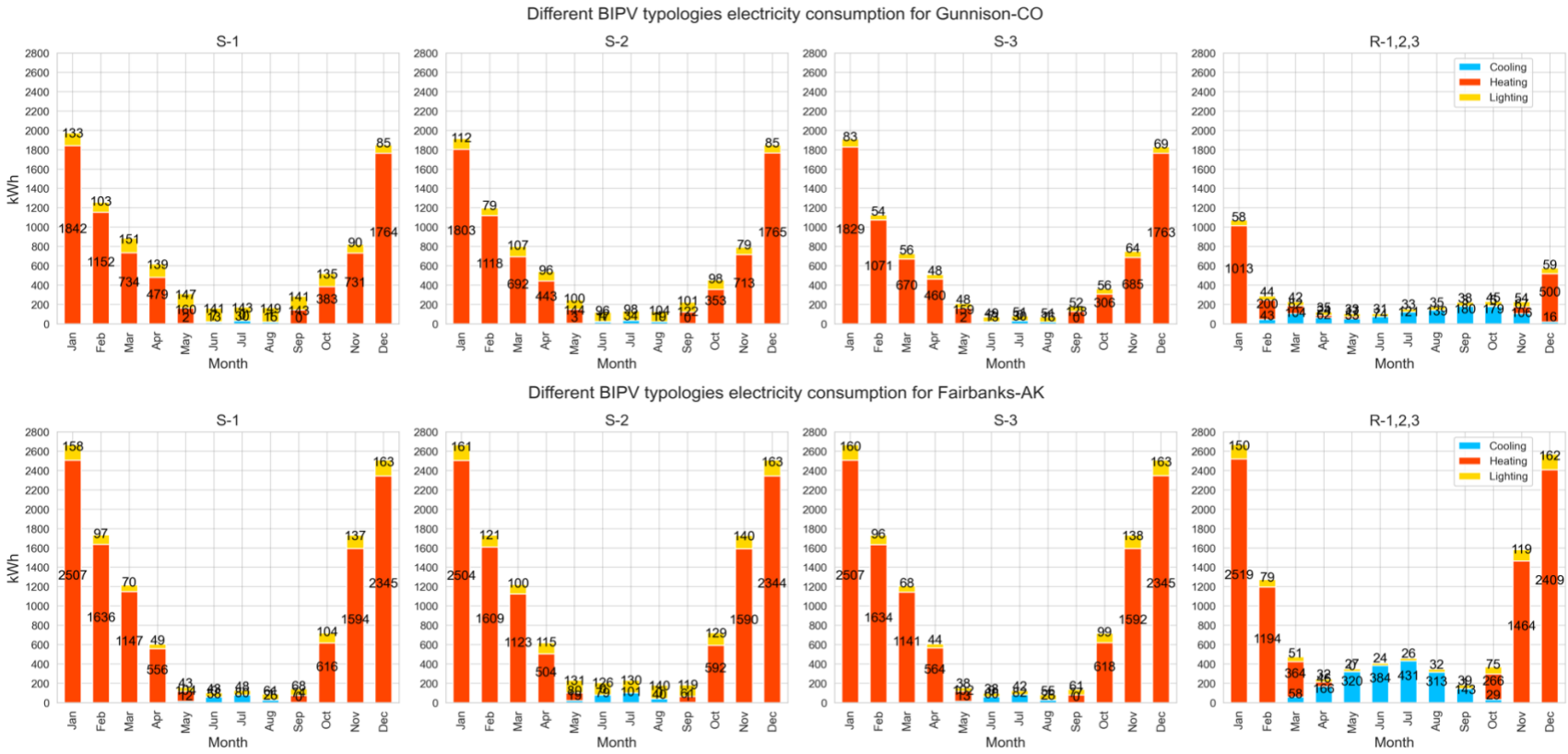

Figure 2.4 Different BIPV typologies energy consumption in selected locations.

Table 2.3, Mean illuminance and disturbing glare on the office working surface across different typologies in variouse latitude levels

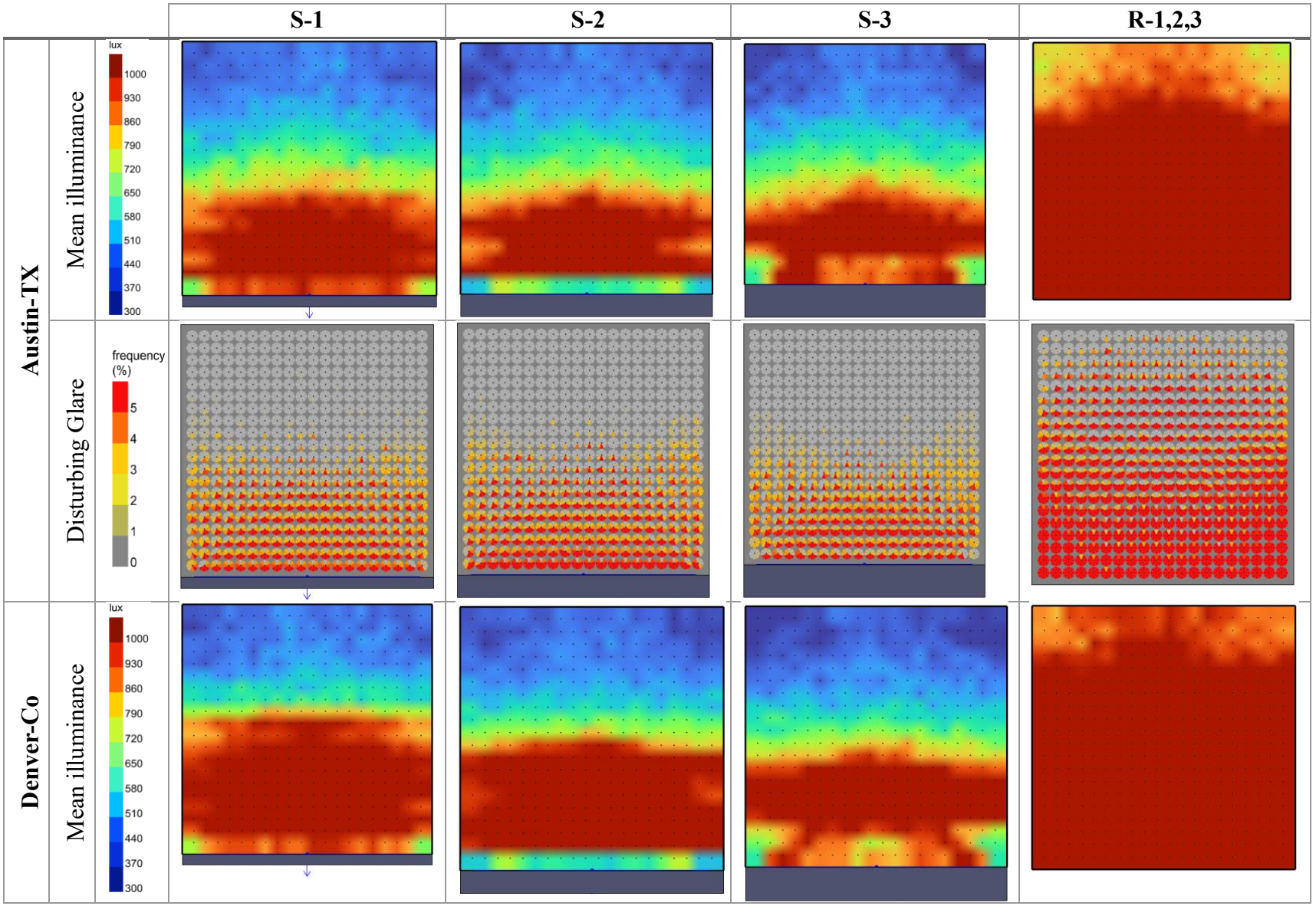

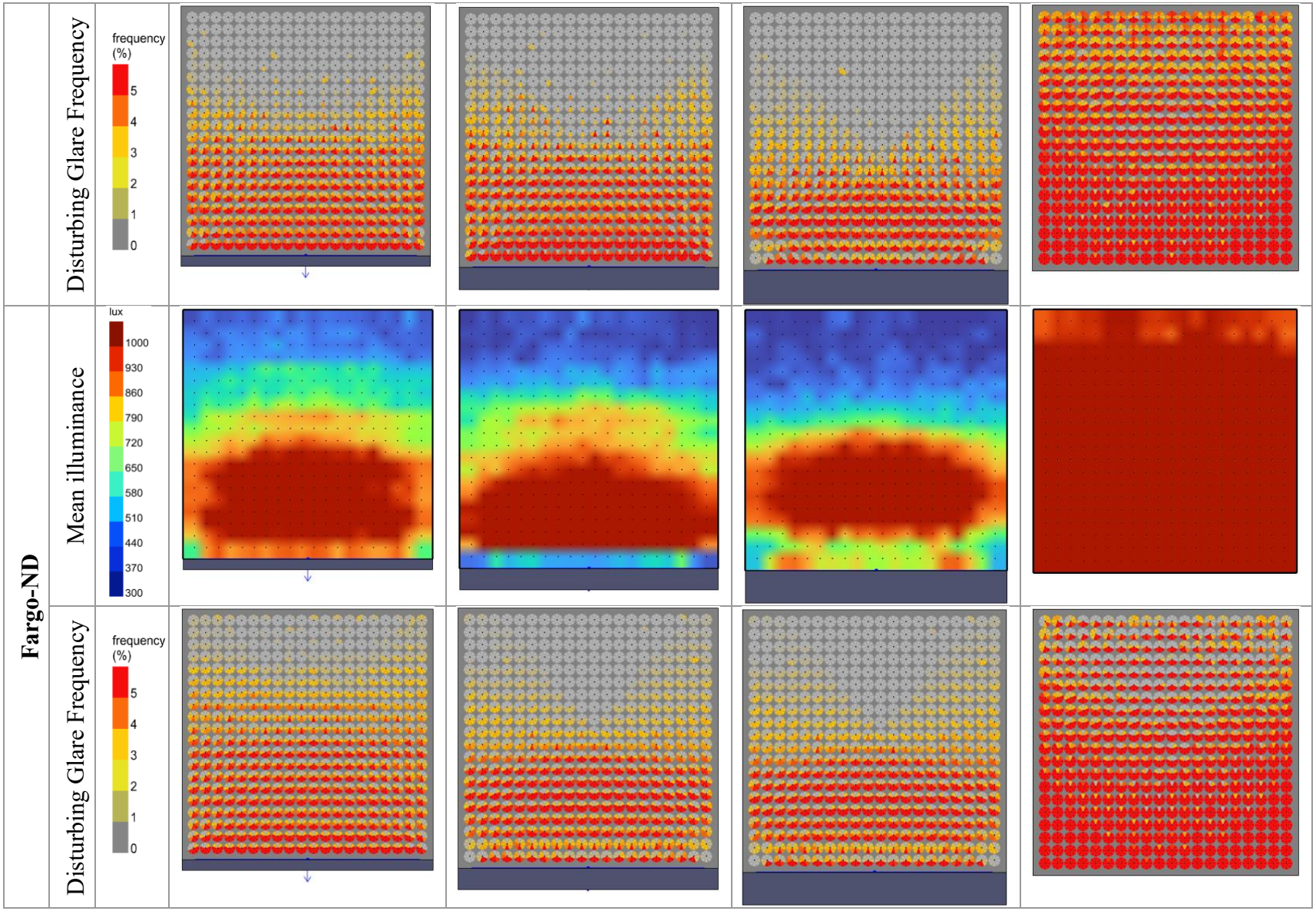
Fargo-ND
Disturbing Glare Frequency
frequency (%)
5
4
3
2
1
0
Mean illuminance
lux
1000
930
860
790
720
650
580
510
440
370
300
Disturbing Glare Frequency
frequency (%)
5
4
3
2
1
0

The mean illuminance levels of all PV-louver typologies were within the standard range of 300 lux to 1000 lux. However, both the mean illuminance levels and the DA index experienced a steep decrease in Fairbanks, AK, which can be attributed to its high latitude and the prevailing sky and weather conditions near the North Pole. Nonetheless, the PV-louver typologies achieved a DA index of 1 or fairly close to 1 in various locations, including Miami, FL, Phoenix, AZ, Austin, TX, Los Angeles, CA, San Francisco, CA, Albuquerque, NM, Denver, CO, and Gunnison, CO.

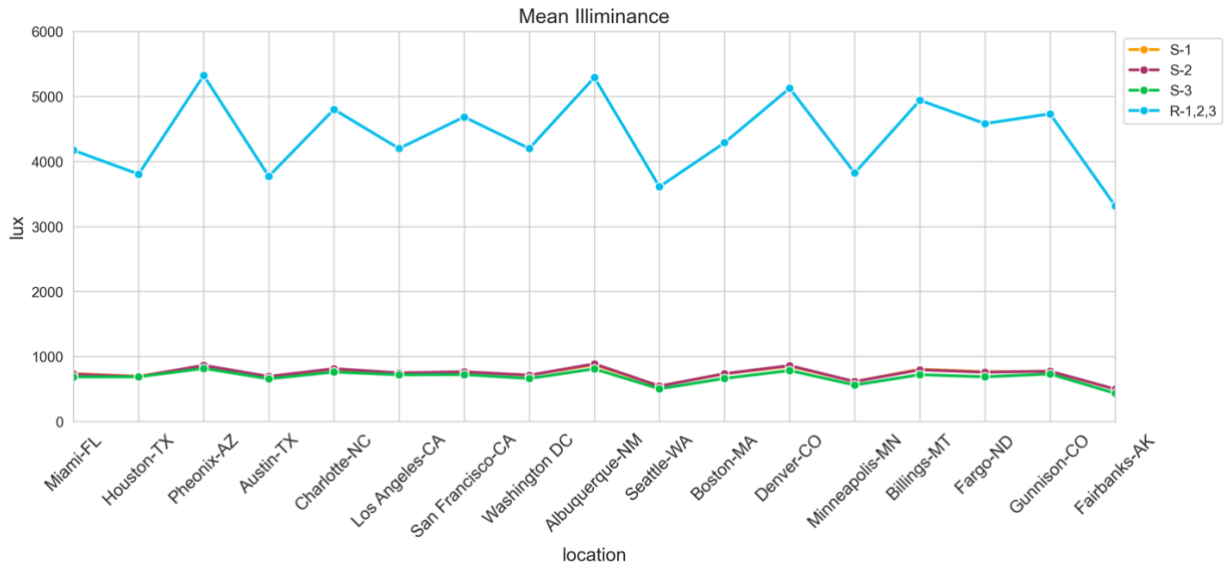

Figure 2.5 Annual mean illuminance levels on office working surface.

Figure 2.7 presents the monthly PV power production for each typology at each location. Comparisons between the south-facing façade typologies and their corresponding roof typologies reveal that roof typologies generally outperformed the façade BIPVs in terms of monthly power production. However, as the depth of the PV panels increased, the power output of the façade typologies progressively approached that of the roof typologies within the same category. A comparison of the monthly PV system power generation across all the typologies and locations revealed a distinct pattern.

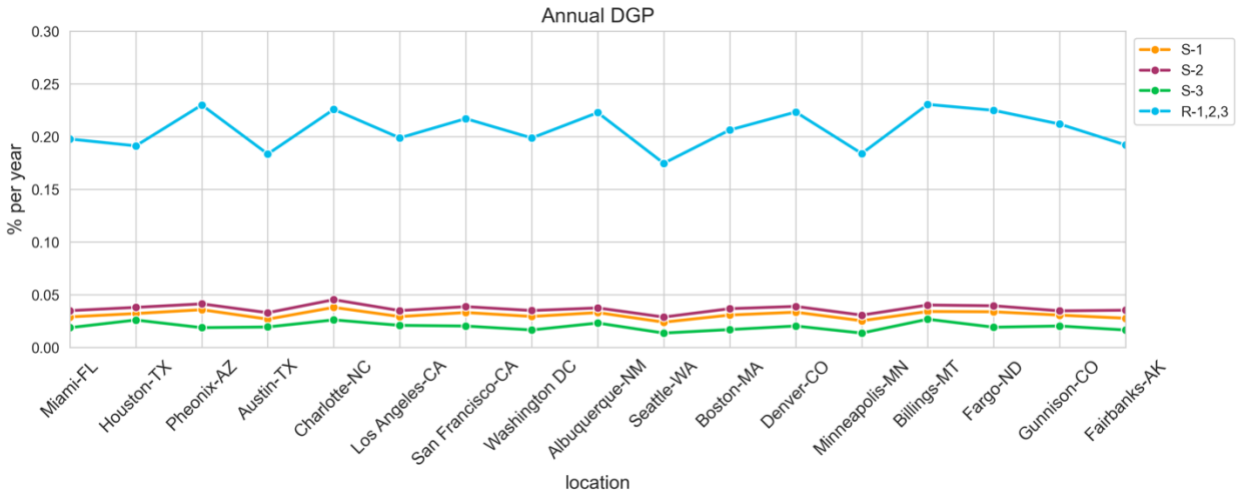

Figure 2.6 Annual GDP levels on office working surface

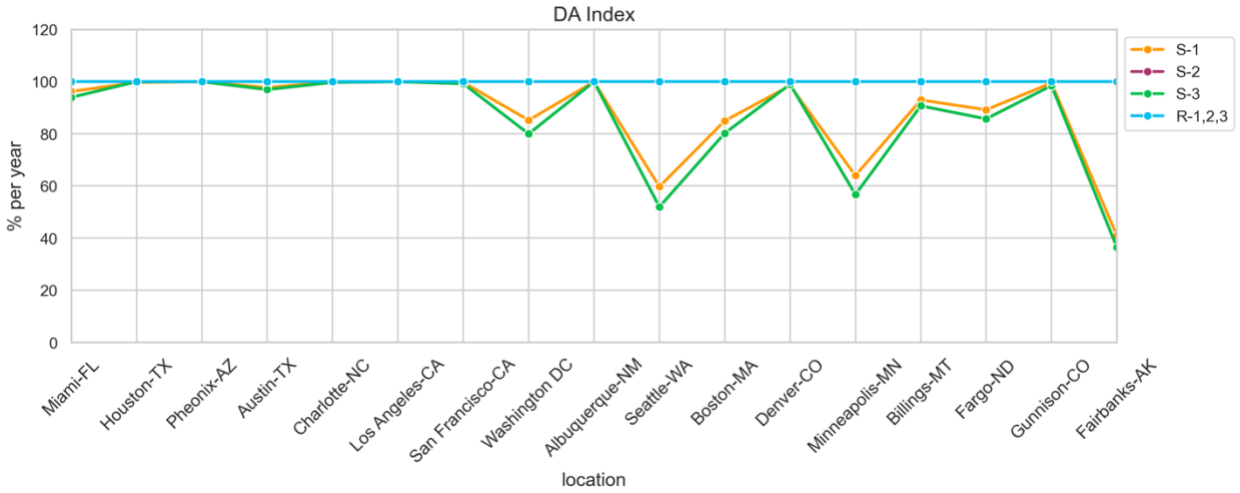

Figure 2.7 DA index in various locations.

Locations situated above 40° North latitude, including Fairbanks, AK, Fargo, ND, Billings, MT, Minneapolis, MN, Boston, MA, and Seattle, WA, typically generated less power during winter months and more power during summer months. Conversely, locations closer to the equator such as Miami, FL, Phoenix, AZ, and Austin, TX exhibited peak power production in winter months and then power production declined around month of June.

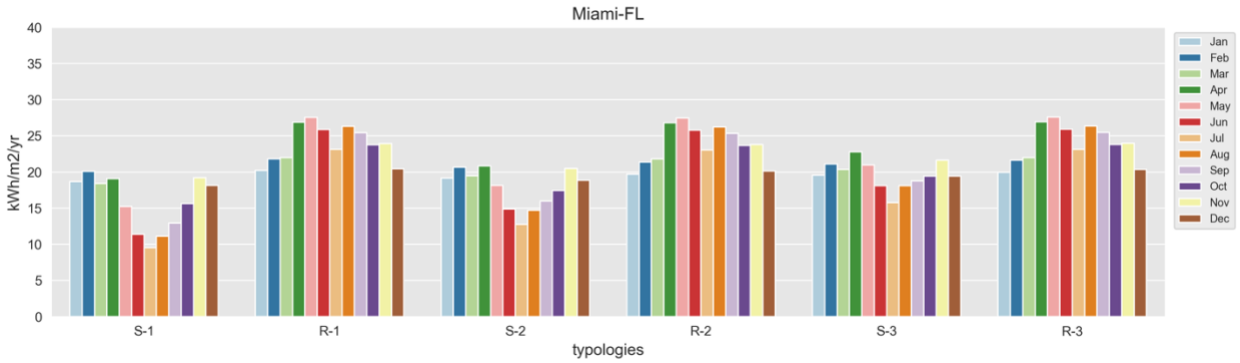
Miami-FL
kWh/m2/yr
typologies
S-1
R-1
S-2
R-2
S-3
R-3
Jan
Feb
Mar
Apr
May
Jun
Jul
Aug
Sep
Oct
Nov
Dec

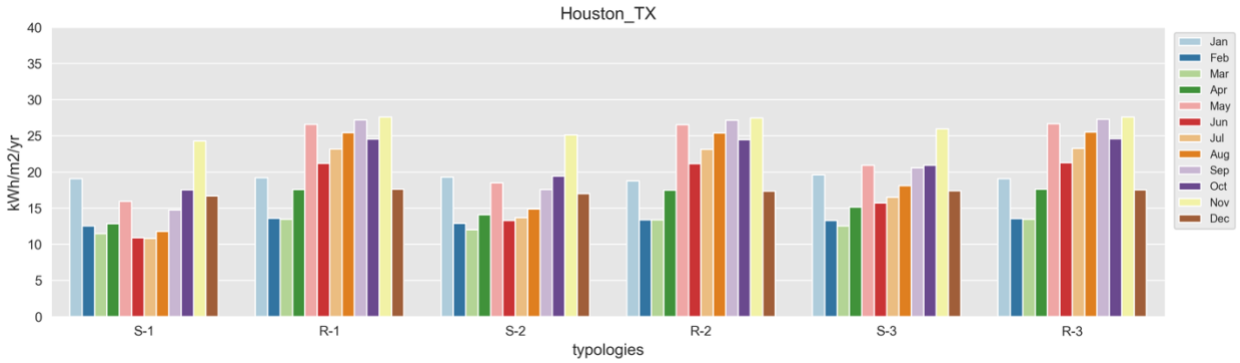
Houston_TX
kWh/m2/yr
typologies
S-1
R-1
S-2
R-2
S-3
R-3
Jan
Feb
Mar
Apr
May
Jun
Jul
Aug
Sep
Oct
Nov
Dec

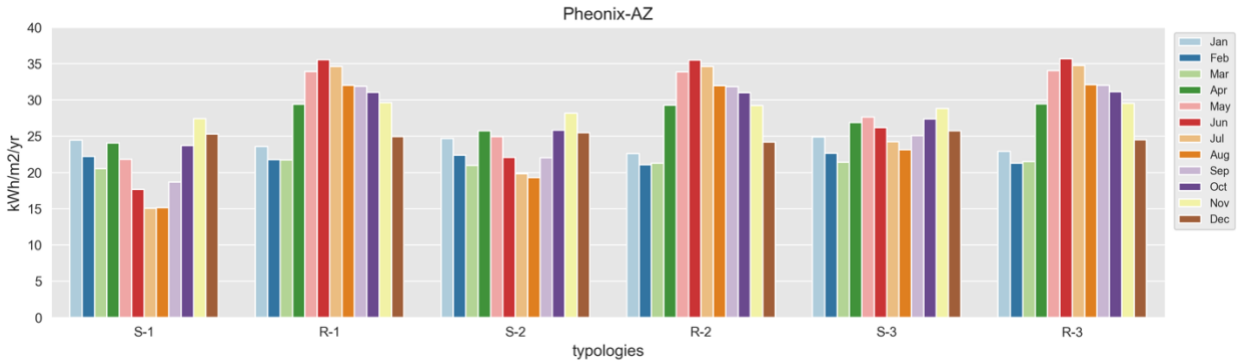
Pheonix-AZ
kWh/m2/yr
typologies
S-1
R-1
S-2
R-2
S-3
R-3
Jan
Feb
Mar
Apr
May
Jun
Jul
Aug
Sep
Oct
Nov
Dec

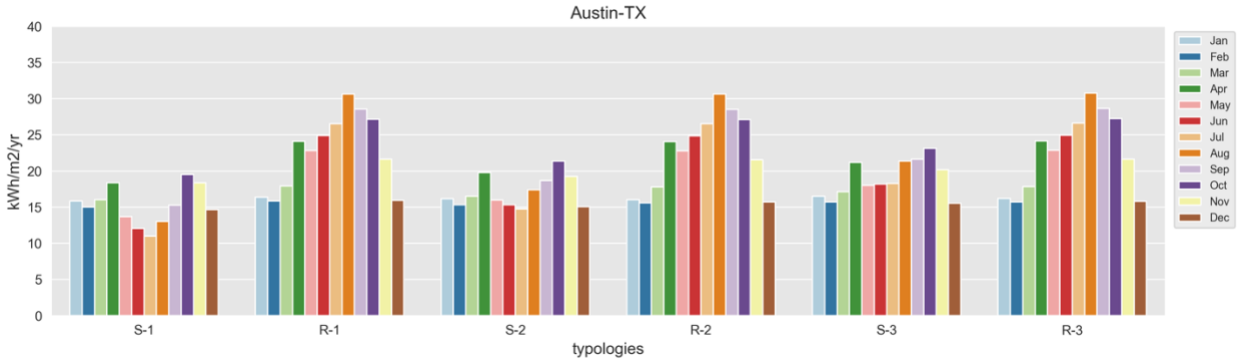
Austin-TX
kWh/m2/yr
typologies
S-1
R-1
S-2
R-2
S-3
R-3
Jan
Feb
Mar
Apr
May
Jun
Jul
Aug
Sep
Oct
Nov
Dec

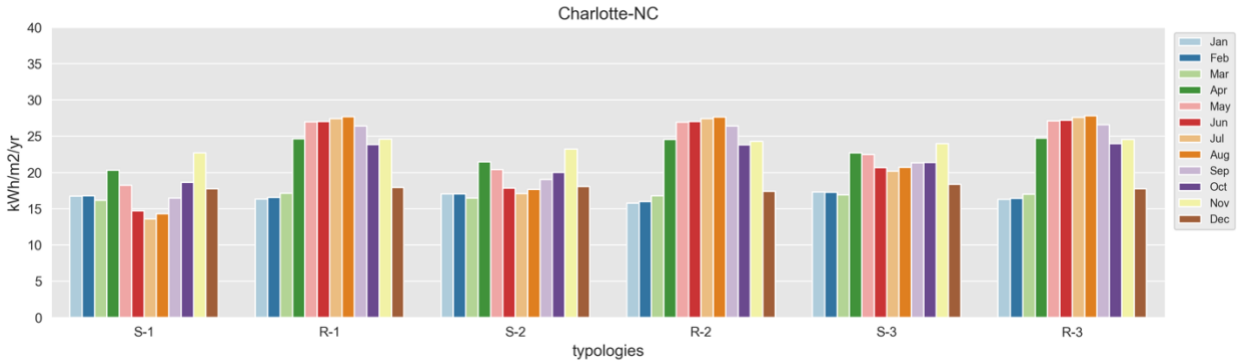
Charlotte-NC
kWh/m2/yr
typologies
S-1
R-1
S-2
R-2
S-3
R-3
Jan
Feb
Mar
Apr
May
Jun
Jul
Aug
Sep
Oct
Nov
Dec

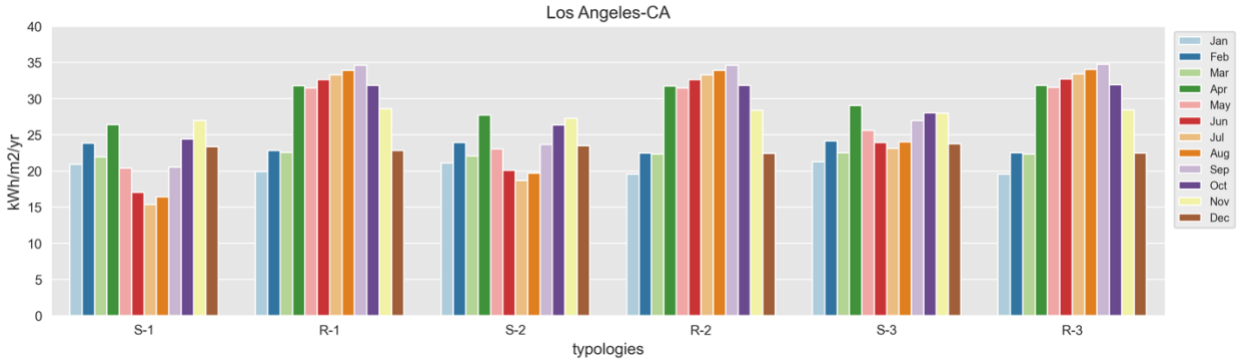
Los Angeles-CA
kWh/m2/yr
typologies
S-1
R-1
S-2
R-2
S-3
R-3
Jan
Feb
Mar
Apr
May
Jun
Jul
Aug
Sep
Oct
Nov
Dec

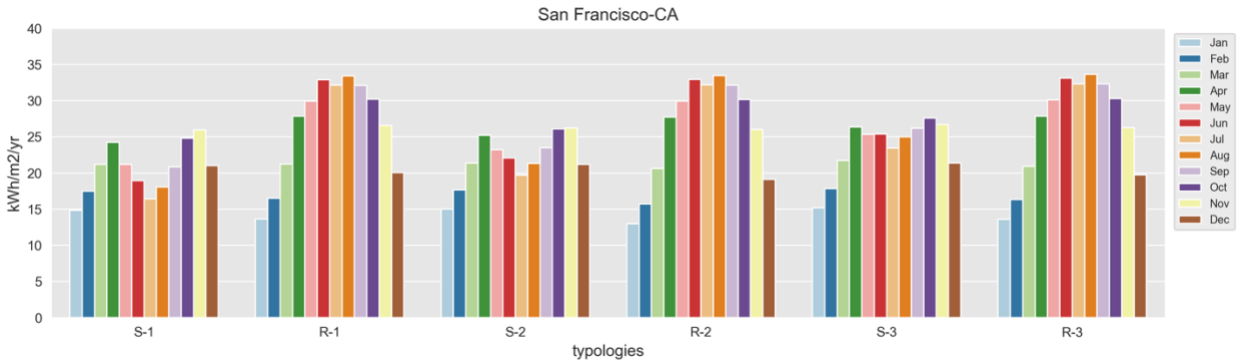
San Francisco-CA
kWh/m2/yr
typologies
S-1
R-1
S-2
R-2
S-3
R-3
Jan
Feb
Mar
Apr
May
Jun
Jul
Aug
Sep
Oct
Nov
Dec

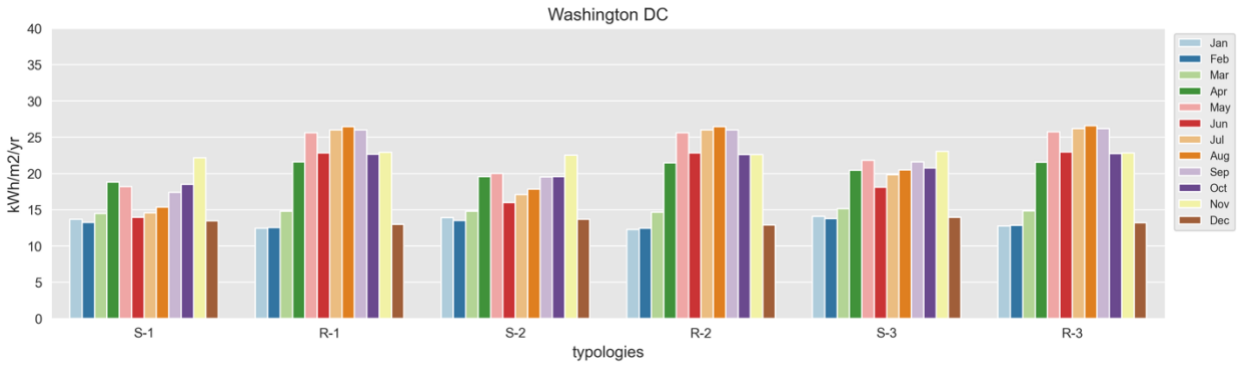
Washington DC
kWh/m2/yr
typologies
S-1
R-1
S-2
R-2
S-3
R-3
Jan
Feb
Mar
Apr
May
Jun
Jul
Aug
Sep
Oct
Nov
Dec

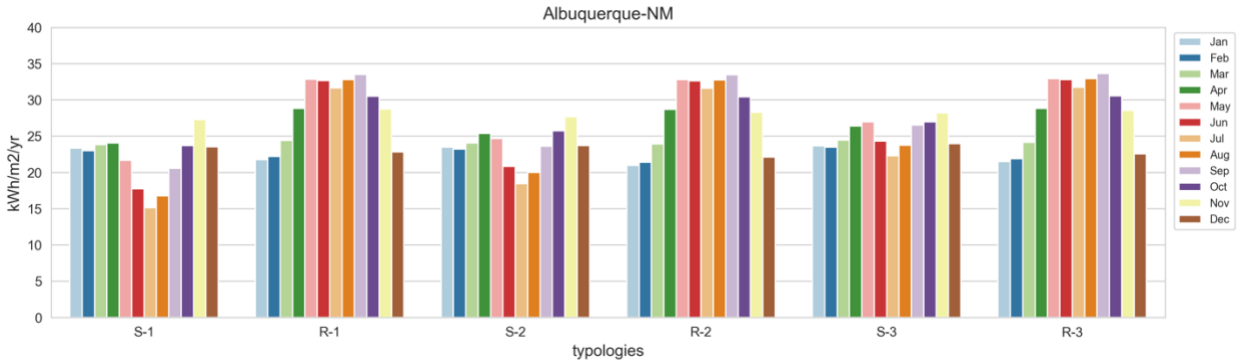
Albuquerque-NM
kWh/m2/yr
typologies
S-1
R-1
S-2
R-2
S-3
R-3
Jan
Feb
Mar
Apr
May
Jun
Jul
Aug
Sep
Oct
Nov
Dec

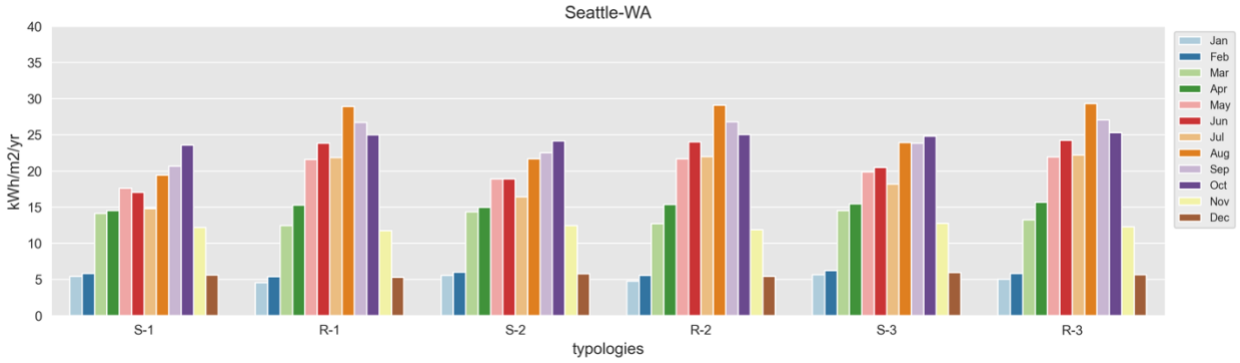
Seattle-WA
kWh/m2/yr
typologies
S-1
R-1
S-2
R-2
S-3
R-3
Jan
Feb
Mar
Apr
May
Jun
Jul
Aug
Sep
Oct
Nov
Dec

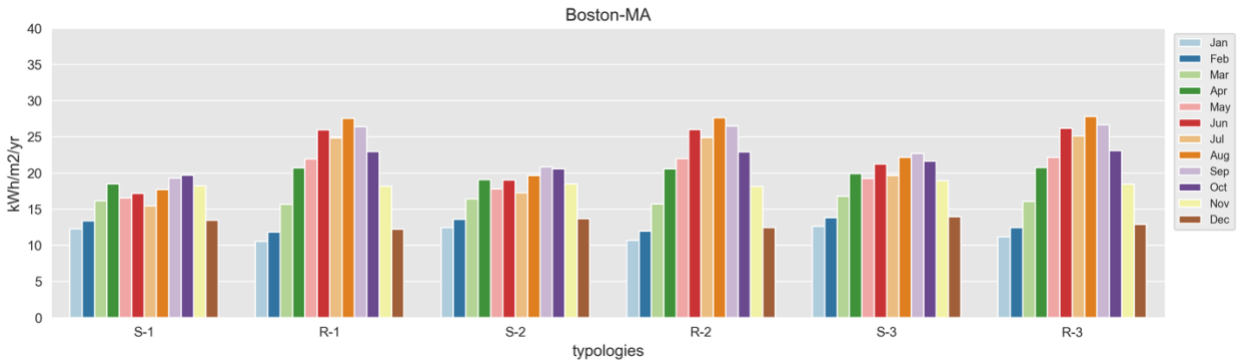
Boston-MA
kWh/m2/yr
typologies
S-1
R-1
S-2
R-2
S-3
R-3
Jan
Feb
Mar
Apr
May
Jun
Jul
Aug
Sep
Oct
Nov
Dec

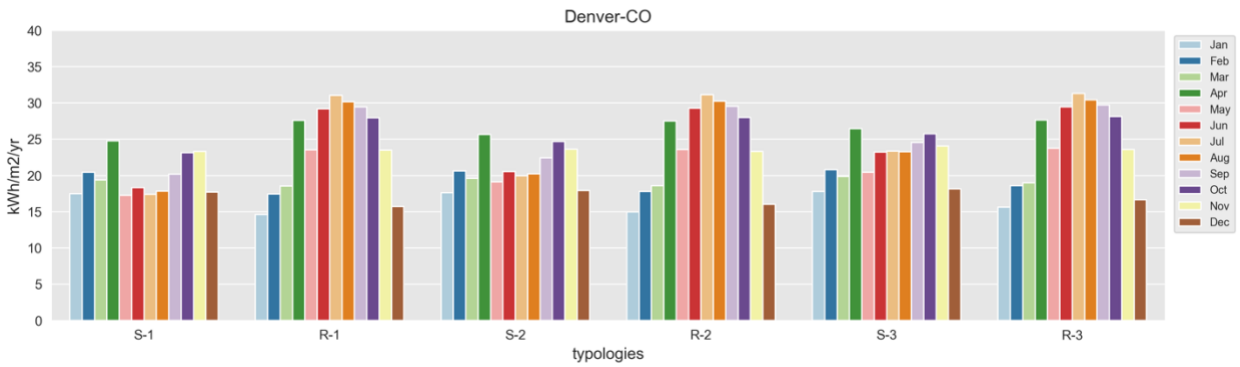
Denver-CO
kWh/m2/yr
typologies
S-1
R-1
S-2
R-2
S-3
R-3
Jan
Feb
Mar
Apr
May
Jun
Jul
Aug
Sep
Oct
Nov
Dec

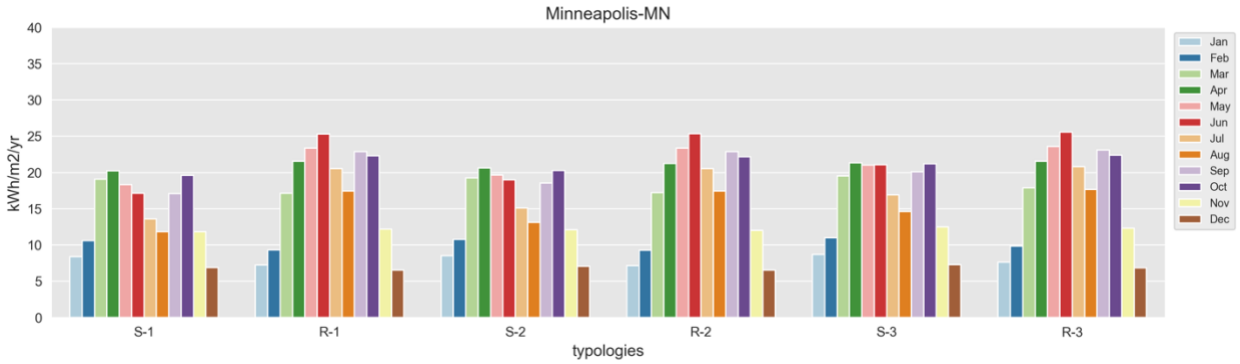
Minneapolis-MN
kWh/m2/yr
typologies
S-1
R-1
S-2
R-2
S-3
R-3
Jan
Feb
Mar
Apr
May
Jun
Jul
Aug
Sep
Oct
Nov
Dec

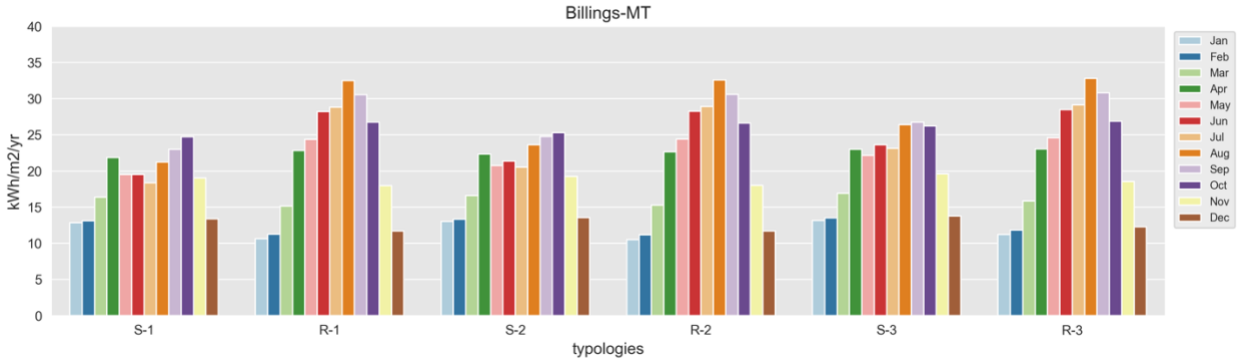
Billings-MT
kWh/m2/yr
typologies
S-1
R-1
S-2
R-2
S-3
R-3
Jan
Feb
Mar
Apr
May
Jun
Jul
Aug
Sep
Oct
Nov
Dec

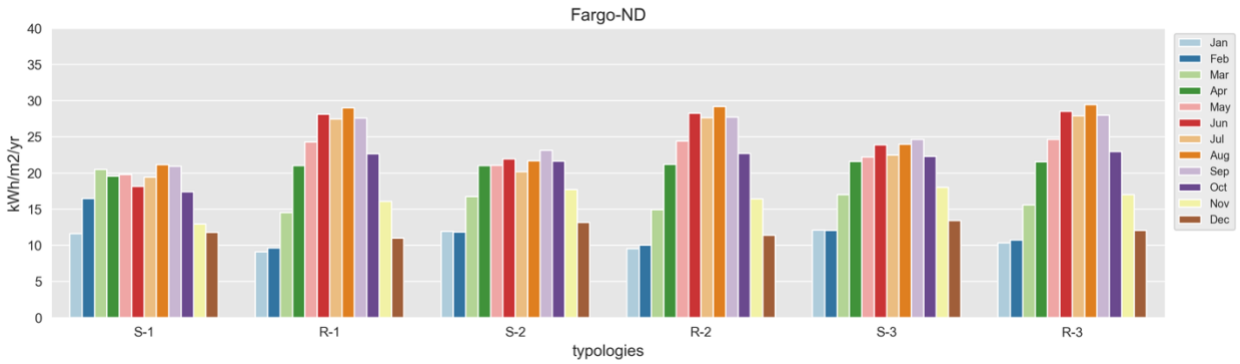
Fargo-ND
kWh/m2/yr
typologies
S-1
R-1
S-2
R-2
S-3
R-3
Jan
Feb
Mar
Apr
May
Jun
Jul
Aug
Sep
Oct
Nov
Dec

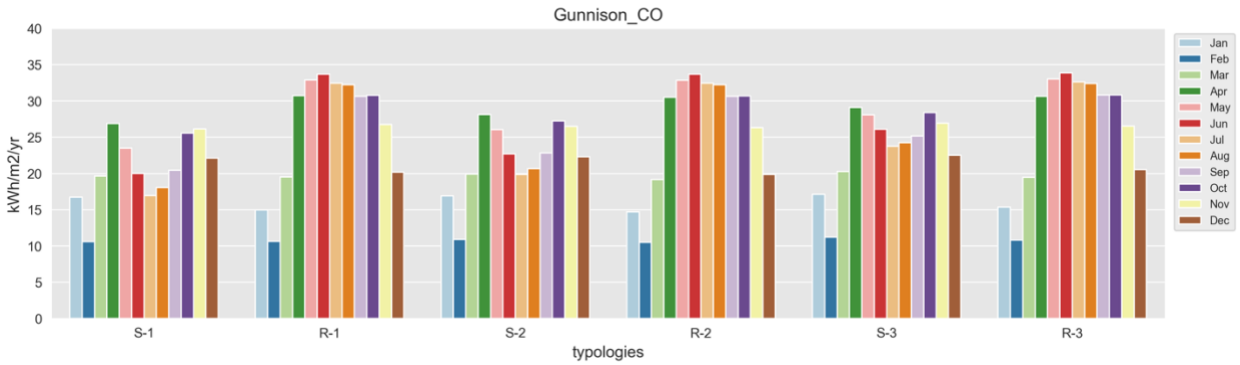
Gunnison_CO
kWh/m2/yr
typologies
S-1
R-1
S-2
R-2
S-3
R-3
Jan
Feb
Mar
Apr
May
Jun
Jul
Aug
Sep
Oct
Nov
Dec

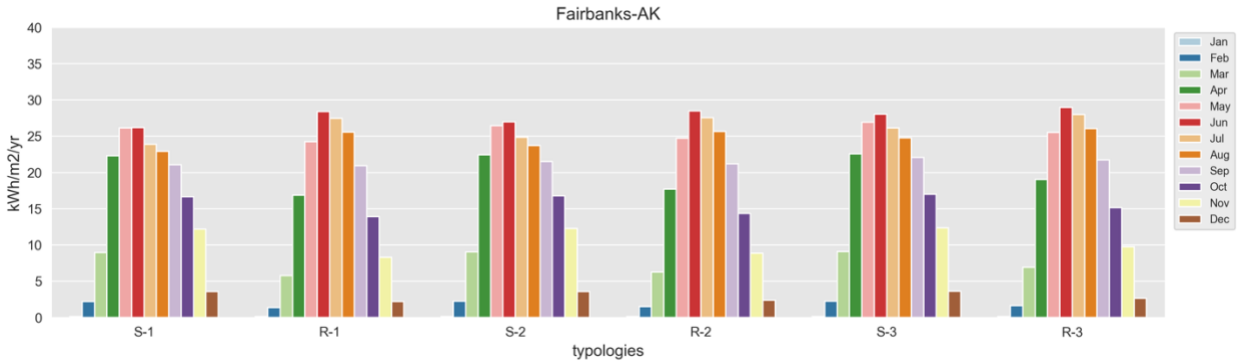

Figure 2.8 Power production of different typologies in selected locations.

Figures 2.9, 2.10, and 2.11 depict the energy consumption, production, and net values for roof and PV-louvers typologies. Building energy consumption of S-1, R-1 and S-2, R-2 typologies was approximately equal at Charlotte, NC, Washington DC, Boston, MA, and Billings MT. However, the S-3 façade typology displayed a slightly better performance in those locations. Except for Minneapolis, MN, the façade typologies reduced building energy consumption in all other locations.

The total building energy consumption which is the sum of cooling, heating, and lighting loads significantly declined in Gunnison, CO, because of a harsh climate, and in Fairbanks, AK, due to both a higher latitude and harsh climate. Increasing the depth of PV panels brought the power production performance closer to that of roof typologies. Additionally, in locations with mild climates like Houston, TX, Phoenix AZ, Austin, TX, Charlotte, NC, Los Angeles, CA, and San Francisco, CA, deeper PV panels in both façade and roof increased the net power output.

The S-1 typology outperformed other façade typologies in San Francesco, CA and Seattle, WA which are in climate zone 3C and 4C.

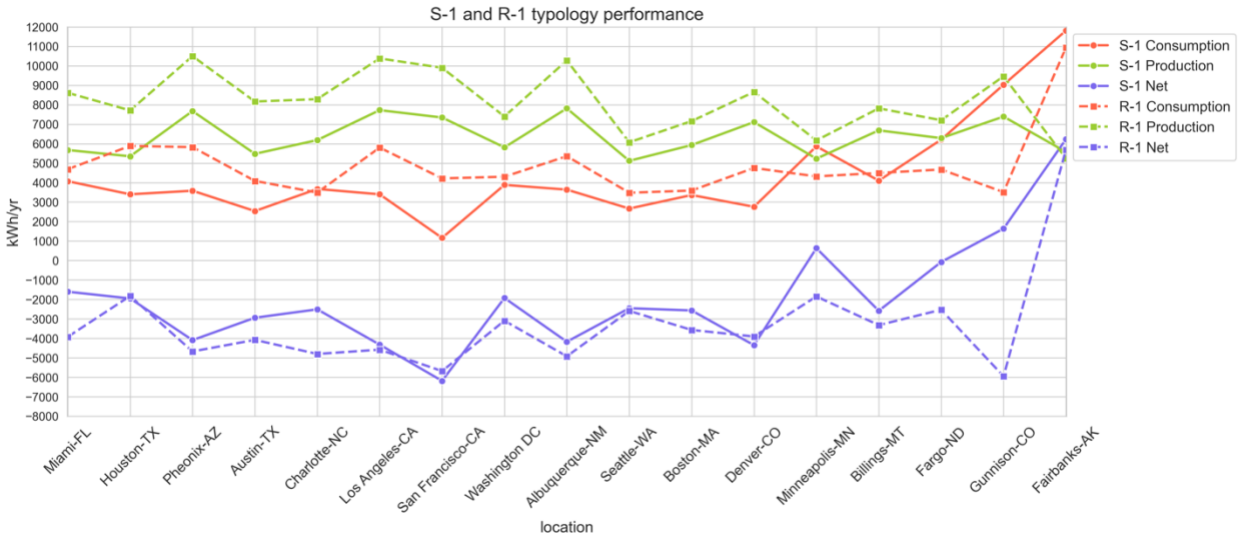

Figure 2.9 S-1 and R-1 typologies electricity production, consumption and net.

4. Conclusion

This study aims to conduct a comprehensive evaluation of the impact of south-facing PV-integrated louvers on not only potential PVPP but also building energy performance and occupants' visual comfort, including glare and mean illuminance levels. The study examined six different BIPV typologies across all ASHRAE climate regions in the U.S. The performance of PV-louvers integrated into the south facade typology is compared with the corresponding roof application to understand the effectiveness of the BIPV facade system in addressing building energy needs. The findings of this study have led to the following conclusions regarding BIPV systems in ASHRAE climate zones:

Climate zone 1: All PV-louver typologies successfully reduced building energy consumption. The percentage of energy savings was higher in S-1 and S-2 typologies compared to S-3. While the roof typologies consumed more energy, the net energy of these typologies was higher, primarily due to increased potential PVPP. Additionally, increasing the depth of the PV

panels enhanced the performance of the potential PVPP and increased the net energy of the facade typologies.

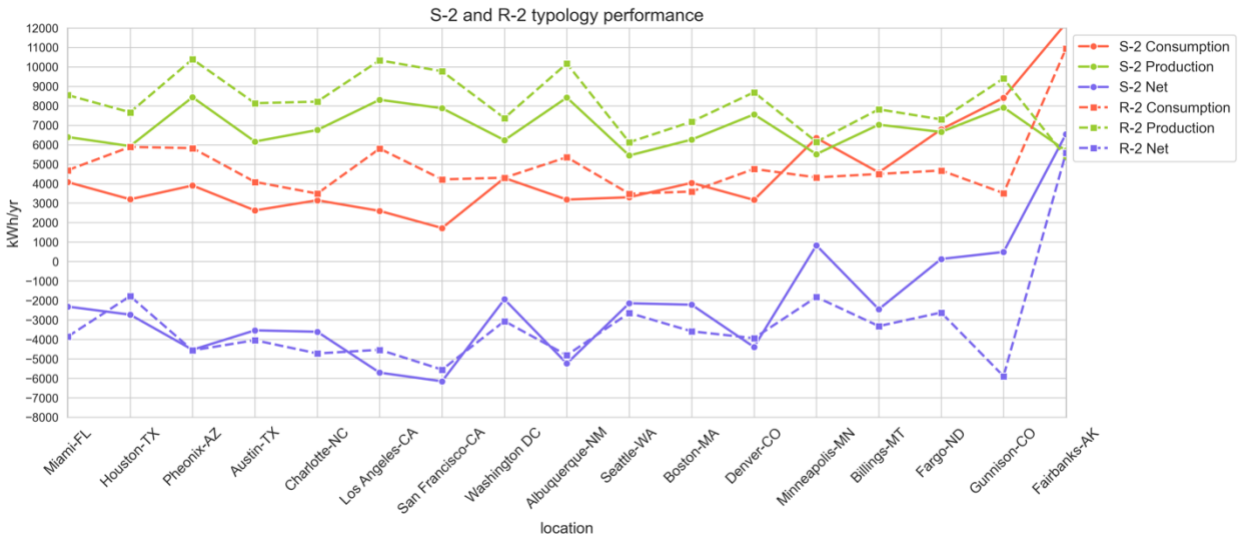

Figure 2.10 , S-2 and R-2 typologies electricity production, consumption and net

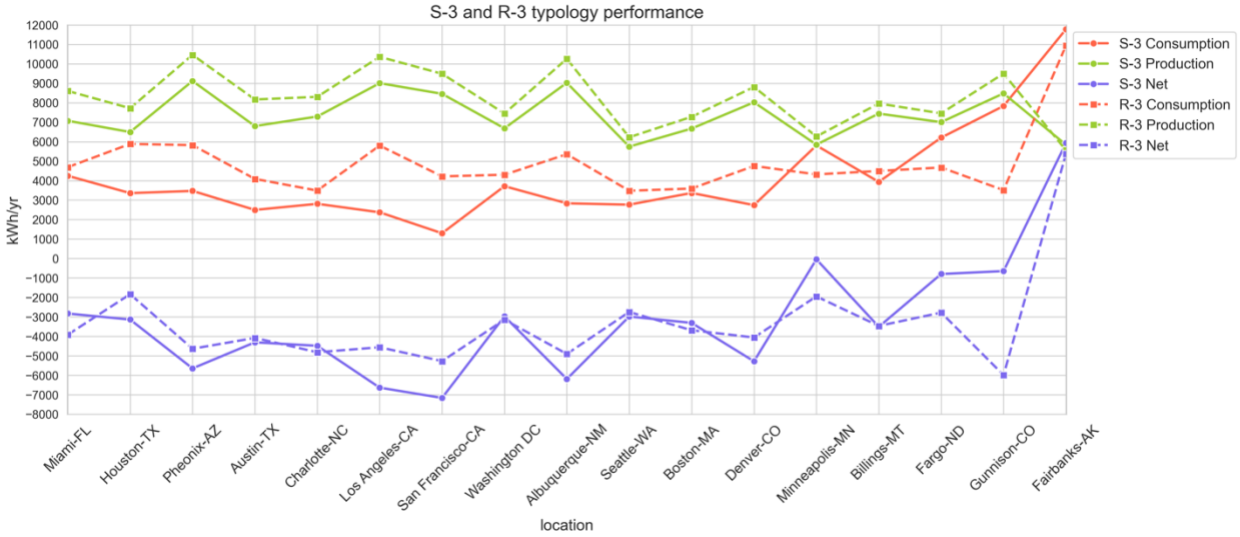

Figure 2.11 S-3 and R-3 typologies electricity production, consumption and net

Climate zone 2: Incorporating PV-louvers into the facade significantly reduced building energy consumption. Increasing the depth of the PV panels boosted PVPP from the PV-louvers, consequently raising the net energy of the S-3 typologies above that of the R-3 typology.

Climate zone 3: PV-louvers proved more effective in reducing building energy consumption in sub-climate types B and C compared to sub-climate type A. Despite lower potential PVPP in S-2 and S-3 typologies compared to roof typologies, the net energy of the facade typologies surpassed that of the roof typologies. Moreover, increasing the depth of the PV panels resulted in higher net energy for the facade typologies.

Climate zone 4: Overall, integrating the PV-louvers into the facade led to a slight reduction in building energy consumption. A direct correlation between the depth of the PV panels and the building's net energy was observed in facade typologies.

Climate zone 5: The building energy consumption remained fairly consistent after integrating PV-louvers into the facade in sub-climate type A. However, it reduced the building energy consumption in sub-climate type B. Specifically, the S-2 typology had adverse effects on building energy consumption in sub-climate type A. On the other hand, PV-louver typologies outperformed roof typologies in sub-climate type B.

Climate zone 6: The PVPP of facade typologies was fairly close to that of roof typologies, and as the depth of the panels increased, the values became even closer. However, facade typologies had an adverse effect on building energy consumption in sub-climate type A. Although the S-2 typology worsened the building energy consumption, S-1 and S-3 improved it in sub-climate type B. Furthermore, S-3 exhibited greater improvement than S-1. Overall, the net energy of the roof typologies was higher than that of the facade typologies across all typologies.

Climate zone 7: The facade typologies led to an increase in building energy consumption, with this adverse effect being more pronounced in sub-climate type B. Additionally, the net energy of the roof typologies was higher.

Climate zone 8: Despite the potential PVPP of the facade and roof typologies being very close, the facade typologies had a negative effect on building energy consumption.

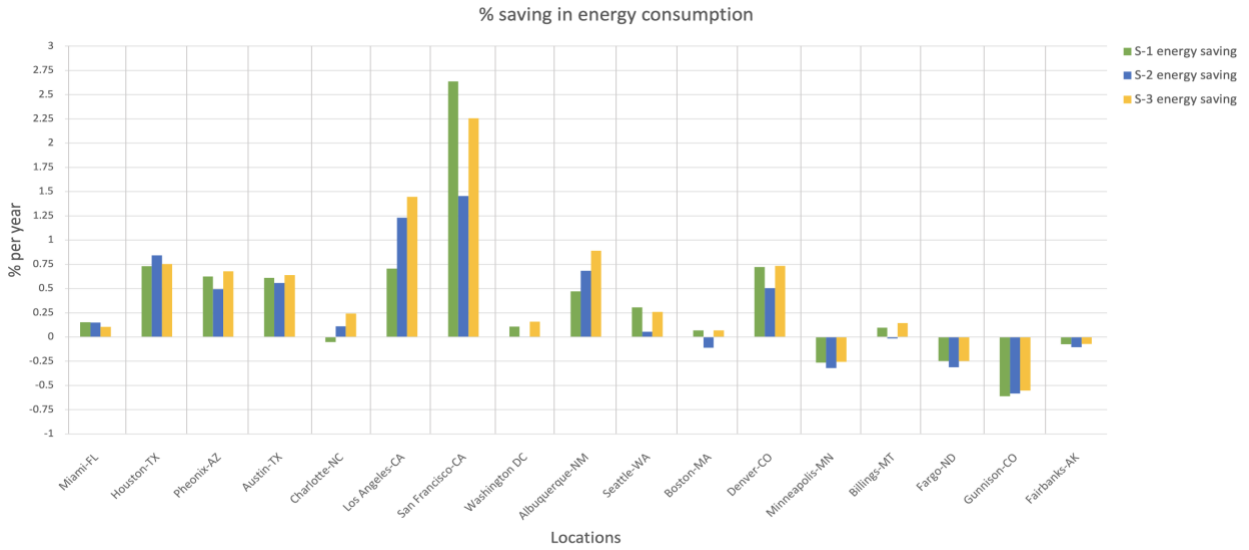

Figure 2.12 Impact of integrating PV-louvers on the south façade in building energy savings.

For further analyzing the efficacy of the façade typologies in offsetting the building electricity consumption, percentage of yearly energy savings across all locations depicted in Figure 2.9. Regardless of the installation location of the PVs in each typology, PV system had a peak in monthly power generation at each location. Table 2.4 shows month of peak power output in each location over a year. This information will be crucial for managing the electricity generated by the PV panels throughout the year and defining the size of other components of the system such as battery storages.

All three PV-louver designs reduced sunlight penetration while achieving the required illuminance levels of 300-1000 lux across most of the floor area. Although less lighting load in roof typologies were observed, the mean illuminance levels on the working surface were on the other hand significantly high which caused disturbing glare for the occupants in a large portion of the floor area.

The applicability of BIPV louvers depends on achieving a balance between maximizing potential power generation and maintaining or improving building energy performance. This study demonstrates that while facade typologies can be effective in reducing energy consumption in some ASHRAE climate zones (1-3, 4B and 5B), they may have an adverse effect in others (6, 7, 8). This underscores the importance of considering climate data and sub-climate variations when designing BIPV louver systems. For instance, in zones with high solar radiation (1-3), deeper facade typologies offer a good balance between energy savings and power generation.

Table 2.4, Peak power output in each location throughout a year

City, State	**Month of peak output**
Miami, FL	November
Houston, TX	October
Phoenix, AZ	October
Austin, TX	October
Charlotte, NC	October
Los Angeles, CA	Varied
San Francisco, CA	September
Washington DC	October
Albuquerque, NM	October
Seattle, WA	September
Boston, MA	August
Denver, CO	March
Minneapolis, MN	March, September

Billings, MT	August
Fargo, ND	August
Gunnison, CO	March
Fairbanks, AK	May

Furthermore, the applicability of BIPV louvers can be viewed through the lens of building use and design objectives. In buildings prioritizing energy savings and occupant comfort, such as office buildings, facade typologies are suitable choices in climate zones of 1-3, 4B and 5B due to their ability to reduce cooling loads and offer shading benefits. Conversely, in buildings where maximizing power generation is the primary goal, like commercial buildings with high electricity demands, roof-mounted typologies may be more applicable across a wider range of climates, considering their generally higher potential power generation observed in this study.

While the impact of building height on energy production with BIPV louvers is not directly addressed in this study, the results suggest that facade typologies can be more competitive with roof-mounted systems in taller buildings. This is because taller buildings offer a larger facade area for BIPV integration, potentially increasing overall power generation. Climate zones with high solar radiation (1-3) seem to benefit most from facade BIPV in this scenario. In these zones, deeper facade profiles effectively balance energy savings through shading with substantial potential power generation due to ample sunlight exposure.

To further enhance the results, using high-resolution weather data customized for each location can better capture recent local climate conditions, thereby improving the accuracy and relevance of the study outcomes.

5. Limitations and future work

In this study, the PV-louver on south façade and PV-mounted rooftop systems were modeled using a combination of software tools, primarily utilizing the EnergyPlus code within the LB. The modeling approach involved defining parameters such as irradiance levels, panel efficiency (η_{PV}), and loss factors (LF). However, it's important to note that our simulation framework has limitations, particularly in accounting for temperature effects of operating such systems in real-world. Due to the constraints of the software used, we focused on key parameters that could provide meaningful insights into the performance of the PV system within the scope of our study. While acknowledging these limitations, we aimed to contribute novel findings regarding the overall energy behavior and potential PVPP of the PV louver system. Future research directions may explore advanced modeling techniques or alternative software tools capable of addressing these factors to enhance the accuracy and comprehensiveness of PV simulations.

6. Acknowledgement

This study was funded by U.S. National Science Foundation (NSF). Award number: 2122014.

7. References

1. EIA. *How much energy is consumed in U.S. buildings?* 2023 [cited 2023; Available from: https://www.eia.gov/tools/faqs/faq.php?id=86&t=1.
2. Freitas, J.d.S., et al., *Modeling and assessing BIPV envelopes using parametric Rhinoceros plugins Grasshopper and Ladybug.* Renewable Energy, 2020. **160**: p. 1468-1479.
3. Aguacil, S., S. Lufkin, and E. Rey, *Active surfaces selection method for building-integrated photovoltaics (BIPV) in renovation projects based on self-consumption and self-sufficiency.* Energy and Buildings, 2019. **193**: p. 15-28.
4. Azami, A. and H. Sevinç, *The energy performance of building integrated photovoltaics (BIPV) by determination of optimal building envelope.* Building and Environment, 2021. **199**: p. 107856.
5. Hwang, T., S. Kang, and J.T. Kim, *Optimization of the building integrated photovoltaic system in office buildings—Focus on the orientation, inclined angle and installed area.* Energy and Buildings, 2012. **46**: p. 92-104.
6. Yang, H. and L. Lu, *The optimum tilt angles and orientations of PV claddings for building-integrated photovoltaic (BIPV) applications.* 2007.
7. Cheng, C., C.S.S. Jimenez, and M.-C. Lee, *Research of BIPV optimal tilted angle, use of latitude concept for south orientated plans.* Renewable energy, 2009. **34**(6): p. 1644-1650.
8. Dimd, B.D., et al., *Quantification of the Impact of Azimuth and Tilt Angle on the Performance of a PV Output Power Forecasting Model for BIPVs.* IEEE Journal of Photovoltaics, 2023.
9. Rambøl, I.B., H.L.S. Vøllestad, and M. Haugen, *Building Integrated Photovoltaics in Residential Areas: A Comparative Study of Energy Performance at Different Orientations*. 2023, NTNU.
10. Kim, K., et al. *Performance Assessment of a Multifunctional 3D BIPV System*. in *ARCC 2023 International Conference THE RESEARCH-DESIGN INTERFACE*. 2023.
11. Mesloub, A., G.A. Albaqawy, and M.Z. Kandar, *The OPTIMUM performance of Building Integrated Photovoltaic (BIPV) windows under a semi-arid climate in algerian office buildings.* Sustainability, 2020. **12**(4): p. 1654.

12. Alhammadi, N., et al., *Building-integrated photovoltaics in hot climates: Experimental study of CIGS and c-Si modules in BIPV ventilated facades.* Energy Conversion and Management, 2022. **274**: p. 116408.
13. Alrashidi, H., et al., *Thermal performance evaluation and energy saving potential of semi-transparent CdTe in Façade BIPV.* Solar Energy, 2022. **232**: p. 84-91.
14. Liu, Z., et al., *A comprehensive study of feasibility and applicability of building integrated photovoltaic (BIPV) systems in regions with high solar irradiance.* Journal of Cleaner Production, 2021. **307**: p. 127240.
15. Sun, Y., et al., *Integrated semi-transparent cadmium telluride photovoltaic glazing into windows: Energy and daylight performance for different architecture designs.* Applied Energy, 2018. **231**: p. 972-984.
16. Cheng, Y., et al., *Investigation on the daylight and overall energy performance of semi-transparent photovoltaic facades in cold climatic regions of China.* Applied Energy, 2018. **232**: p. 517-526.
17. Wang, Y., Y. Chen, and C. Li, *Energy performance and applicability of naturally ventilated double skin façade with Venetian blinds in Yangtze River Area.* Sustainable Cities and Society, 2020. **61**: p. 102348.
18. Liang, S., et al., *Design and performance validation on a solar louver with concentrating-photovoltaic-thermal modules.* Renewable Energy, 2022. **191**: p. 71-83.
19. Luo, Y., et al., *A comparative study on thermal performance evaluation of a new double skin façade system integrated with photovoltaic blinds.* Applied Energy, 2017. **199**: p. 281-293.
20. Zomer, C., et al., *Performance assessment of partially shaded building-integrated photovoltaic (BIPV) systems in a positive-energy solar energy laboratory building: Architecture perspectives.* Solar Energy, 2020. **211**: p. 879-896.
21. Huang, J., et al., *Numerical investigation of a novel vacuum photovoltaic curtain wall and integrated optimization of photovoltaic envelope systems.* Applied Energy, 2018. **229**: p. 1048-1060.
22. Shi, S., et al., *Energy-saving potential comparison of different photovoltaic integrated shading devices (PVSDs) for single-story and multi-story buildings.* Energies, 2022. **15**(23): p. 9196.

23. Kim, J., et al., *Power performance assessment of PV blinds system considering self-shading effects.* Solar Energy, 2023. **262**: p. 111834.
24. Schmid, A.L. and L.K.S. Uehara, *Lighting performance of multifunctional PV windows.* Energy and Buildings, 2017. **154**: p. 590-605.
25. Cannavale, A., et al., *Improving energy and visual performance in offices using building integrated perovskite-based solar cells: A case study in Southern Italy.* Applied Energy, 2017. **205**: p. 834-846.
26. Olivieri, L., et al., *Energy saving potential of semi-transparent photovoltaic elements for building integration.* Energy, 2014. **76**: p. 572-583.
27. Su, X., et al., *Energy performance of a reversible window integrated with photovoltaic blinds in Harbin.* Building and Environment, 2022. **213**.
28. Qiu, C. and H. Yang, *Daylighting and overall energy performance of a novel semi-transparent photovoltaic vacuum glazing in different climate zones.* Applied Energy, 2020. **276**.
29. Riaz, A., et al. *Experimental Study on Electrical Power Generation and Natural Daylighting Illuminance Due to Building-Applied Photovoltaic Façade Application*. in *The International Symposium on Heating, Ventilation and Air Conditioning*. 2019. Springer.
30. Shankar, A., K. Vijayakumar, and B.C. Babu, *Energy saving potential through artificial lighting system in PV integrated smart buildings.* Journal of Building Engineering, 2021. **43**.
31. Roberts, F., et al., *Effect of Semi-Transparent A-Si Pv Glazing within Double-Skin Façades on Visual and Energy Performances Under the UK Climate Condition.* Available at SSRN 4098542, 2023.
32. Chen, H., et al., *Study on natural lighting and electrical performance of louvered photovoltaic windows in hot summer and cold winter areas.* Energy and Buildings, 2022.
33. Xiang, C. and B.S. Matusiak, *Façade Integrated Photovoltaics design for high-rise buildings with balconies, balancing daylight, aesthetic and energy productivity performance.* Journal of Building Engineering, 2022. **57**: p. 104950.
34. Sun, Y., et al., *Analysis of daylight glare and optimal lighting design for comfortable office lighting.* Optik, 2020. **206**: p. 164291.
35. ASHRAE, in *lighting*. 2019.

36. 17037:2019, S.E., *Daylight of buildings*. 2019, European Committee for Standardization.
37. Nabil, A. and J. Mardaljevic, *Useful daylight illuminance: a new paradigm for assessing daylight in buildings.* Lighting Research & Technology, 2005. **37**(1): p. 41-57.
38. power, r.g.e. *Concentrated Solar Power (CSP) Vs Photovoltaic panels (PV)*. 2012 [cited 2024; Available from: https://www.renewablegreenenergypower.com/solar-energy/solar-energy-facts-concentrated-solar-power-csp-vs-photovoltaic-pv-panels.
39. Institute, B., *BIPV Solutions in Europe: Competitiveness Status & Roadmap Towards 2030*. 2021.
40. Cook, J.J., et al., *Observations and Lessons Learned From Installing Residential Roofing-Integrated Photovoltaics*. 2023, National Renewable Energy Lab.(NREL), Golden, CO (United States).
41. pvXchange. *Preisindex*. 2023 [cited 2023; Available from: https://www.pvxchange.com/Preisindex.
42. Jowett, P. *European Parliament approves legal requirement to install solar on buildings*. 2024 [cited 2024; Available from: https://www.pv-magazine.com/2024/03/13/european-parliament-approves-legal-requirement-to-install-solar-on-buildings/.
43. ENERGY, E.S. *Europe's industrial revolution for efficient buildings: shaping the future*. 2024 [cited 2024; Available from: https://www.pv-magazine.com/press-releases/europes-industrial-revolution-for-efficient-buildings-shaping-the-future/.
44. Senate Department for Economic Affairs, E.a.P.E. *Berlin solar law*. 2024 [cited 2024; Available from: https://www.berlin.de/sen/web/en/.
45. Office, S.E.T. *Solar Energy Guide for Homebuilders*. 2023 [cited 2024; Available from: https://www.energy.gov/eere/solar/solar-energy-guide-homebuilders.
46. Curtius, H.C., *The adoption of building-integrated photovoltaics: barriers and facilitators.* Renewable Energy, 2018. **126**: p. 783-790.
47. Feng, W., et al., *A review of net zero energy buildings in hot and humid climates: Experience learned from 34 case study buildings.* Renewable and Sustainable Energy Reviews, 2019. **114**: p. 109303.
48. Hossei, H. and K.-H. Kim. *Circuit Connection Reconfiguration of Partially Shaded BIPV Systems, a Solution for Power Loss Reduction*. in *ACSA Annual Meeting In Common*. 2023.

49. Gao, Y., et al., *A photovoltaic window with sun-tracking shading elements towards maximum power generation and non-glare daylighting.* Applied Energy, 2018. **228**: p. 1454-1472.
50. Taveres-Cachat, E., et al., *A methodology to improve the performance of PV integrated shading devices using multi-objective optimization.* Applied energy, 2019. **247**: p. 731-744.
51. Paydar, M.A., *Optimum design of building integrated PV module as a movable shading device.* Sustainable Cities and Society, 2020. **62**: p. 102368.
52. Ito, R. and S. Lee, *Development of adjustable solar photovoltaic system for integration with solar shading louvers on building façades.* Applied Energy, 2024. **359**: p. 122711.
53. Cheng, Y., et al., *An optimal and comparison study on daylight and overall energy performance of double-glazed photovoltaics windows in cold region of China.* Energy, 2019. **170**: p. 356-366.
54. Akata, A.M.E.A., D. Njomo, and B. Agrawal, *Assessment of Building Integrated Photovoltaic (BIPV) for sustainable energy performance in tropical regions of Cameroon.* Renewable and Sustainable Energy Reviews, 2017. **80**: p. 1138-1152.
55. Li, H., S. Wang, and H. Cheung, *Sensitivity analysis of design parameters and optimal design for zero/low energy buildings in subtropical regions.* Applied energy, 2018. **228**: p. 1280-1291.
56. ASHRAE. *ASHRAE Climate Zones*. 2011 [cited 2024; Available from: https://openei.org/wiki/ASHRAE_Climate_Zones.
57. Goia, F., *Search for the optimal window-to-wall ratio in office buildings in different European climates and the implications on total energy saving potential.* Solar energy, 2016. **132**: p. 467-492.
58. (NREL), N.R.E.L. *PVWatts V8*. 2020 [cited 2024; Available from: https://developer.nrel.gov/docs/solar/pvwatts/v8/.
59. Associates, R.M. *Rhino 8*. 2024 [cited 2024; Available from: https://www.rhino3d.com/.
60. Skandalos, N. and D. Karamanis, *An optimization approach to photovoltaic building integration towards low energy buildings in different climate zones.* Applied Energy, 2021. **295**: p. 117017.
61. Chris Machey. *LADYBUG TOOLS* 2022; Available from: https://www.food4rhino.com/en/app/ladybug-tools.

62. Energy, U.S.D.o., *EnergyPlus™ Version 22.1.0 Documentation*. Engineering Reference. 2022.
63. DOE. *Weather Data*. 2024; Available from: https://energyplus.net/weather.
64. Solemma. *ClimateStudio*. 2022 [cited 2022; Available from: https://www.solemma.com/climatestudio.
65. Jacobson, M.Z. and V. Jadhav, *World estimates of PV optimal tilt angles and ratios of sunlight incident upon tilted and tracked PV panels relative to horizontal panels.* Solar Energy, 2018. **169**: p. 55-66.
66. Alami, A.H., et al., *Management of potential challenges of PV technology proliferation.* Sustainable Energy Technologies and Assessments, 2022. **51**: p. 101942.
67. Dobos, A.P., *PVWatts version 5 manual*. 2014, National Renewable Energy Lab.(NREL), Golden, CO (United States).
68. Milosavljević, D.D., T.S. Kevkić, and S.J. Jovanović, *Review and validation of photovoltaic solar simulation tools/software based on case study.* Open Physics, 2022. **20**(1): p. 431-451.
69. Handbook, I.L., *IES Lighting Handbook.* New York: Illuminating Engineering Society, 1966.

CHAPTER 3 (PAPER 2)

ASSESSING THE PV-INTEGRATED SOUTH FACADE IN MITIGATING THE BIPV SYSTEM OVERSUPPLY

Hamideh Hossei[1], Kyoung-Hee Kim[2]
[1] Department of Infrastructure and Environmental System, UNC Charlotte, USA – 9201 University City Blvd, Charlotte, NC 28223
[2] School of Architecture, UNC Charlotte, USA – 9201 University City Blvd, Charlotte, NC 28223

Abstract

The power generated by PV panels depends on the sunlight reaching their surface, with electricity production peaking at mid-day hours due to abundant solar energy. In places like California, extensive solar PV installations result in electricity generation surpassing mid-day demand. To ensure grid stability, a significant amount of PV-generated power must be curtailed. This loss not only increase ROI period but also diminishes the potential of solar power to efficiently meet energy demand, especially during periods of peak sunlight availability. This study investigates the impact of integrating PV-louvers into the south façade, serving as both shading devices and clean solar power generators, to mitigate PV electricity production curtailment. Simulations were conducted across 10 ASHRAE climate zones, including very hot, hot, warm, and mixed climates. The results demonstrated that south façade PV-louvers can effectively reduce PV system oversupply in very hot, hot, and warm climate zones, with the exception of mixed marine climate zone (3C). In mixed climate zones, a combination of PV-mounted roof and south PV-louvers typologies was effective in mitigating curtailment in different months. Overall, PV-louvers outperformed PV-mounted roof typologies in September and June, suggesting these typologies are particularly effective in addressing curtailment during cooling dominant seasons.

1. Literature review

The California Independent System Operator (CAISO) introduces a phenomenon named duck curve [1]. Imbalanced power flow from PV systems and conventional utilities to respond to demand loads is causing solar power curtailment and an abrupt increase in conventional utility operation load, at mid-day and late evening hours, respectively [2] (Figure 3.1). The duck curve shape can be divided into five primary time sections on its X-axis, each characterized by distinct features related to PV power output, demand load, direct and indirect radiations, and sun availability in the sky.

1- From 3 am to 8 am: This section encompasses nighttime and the early morning hours. As the morning progresses, sun radiation increases. PV panel power output is minimal during this period, and the demand load is primarily fulfilled by the conventional grid system, with a minor contribution from the PV system.
2- From 8 am to noon: Following sunrise, solar power production increases with the growing sun availability. As people start working and use their electrical appliances, the demand load rises. It is highly probable that the PV system integrated into the building can adequately supply the demand load during this time.
3- From noon to 3 pm: During this period, building electricity demand is constant and it can entirely be supplied by PV electricity output. Simultaneously, solar power generation continues to rise.
4- From 3 pm to 8 pm: Sunset occurs during this time frame, resulting in decreased sun availability and a subsequent dramatic drop in the PV system's electricity output. Consumer load profiles rise as they return home and operate electric appliances, necessitating conventional utilities to rapidly increase their power output to meet the demand.

5- From 8 pm to 3 am: This period experiences the peak electricity demand around 9 pm, followed by a gradual decrease as people go to sleep. Solar power generation is nonexistent due to the lack of sunlight, leading the entire demand load to be fulfilled by the grid. The cycle then repeats, starting from time section one for the next day.

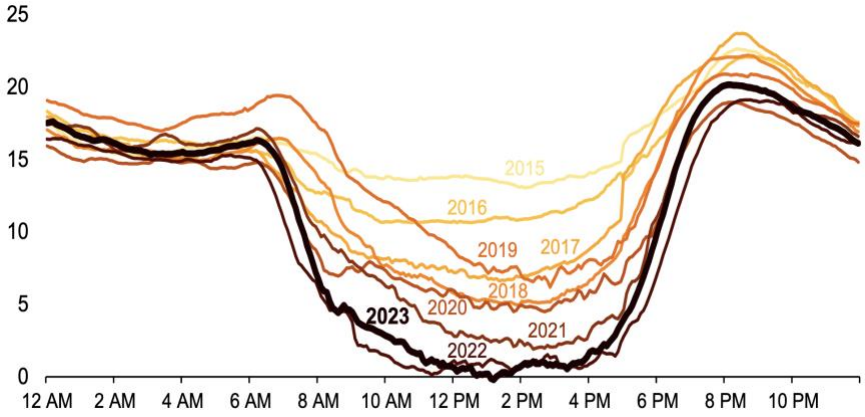

Figure 3.1 Duck curve in a) California, U.S. [3]

Oversupply or power curtailment is a significant issue in regions with high PV systems' power penetration into the grid. This problem is especially pronounced during noon hours in the spring and summer. For instance, in California, high solar penetration led to solar generation peaks at noon and during high-solar-intensity seasons, resulting in overproduction compared to demand. This surplus strained the electricity grid, necessitating curtailment to maintain stability [4]. Regardless of the climate type, by increasing installation of solar farms and rooftop PV systems, the curtailment will increase. In California with warm and moderate climate, the average curtailment of PV-generated electricity was 0.8% in 2015, increasing to 1.5% of total generation in 2018, with about a 6% rise in solar penetration since 2015 [2]. The increased implementation of solar power systems in cold climate zones, such as New England [5], changed the electricity demand profile and increased the surplus solar energy [6].

The installation of rooftop solar systems has been the prevailing approach for buildings on-site solar energy generation, and this trend is projected to contribute to 10%-20% of the total solar deployment by 2050 [7]. Since the rooftop installed PV panels will perform similarly to the solar farms and will intensify the duck curve, with such significant growth of PV systems in the future, it is essential to ensure that BIPV systems are not intensifying the curtailment problem while they are performing at their high efficiency.

Buildings are not only major power consumers but also primary contributors of pollutant emissions in the U.S. [8]. Preliminary findings from the Commercial Buildings Energy Consumption Survey (CBECS) indicate a growing trend in the size of commercial buildings in the United States. As of 2018, the survey estimates there are approximately 5.9 million commercial buildings in the U.S., totaling a whopping 97 billion square feet [9]. This sector represent a significant portion of the U.S. overall consumption, accounting for 18% [10]. Given their substantial energy demands, commercial buildings present a significant opportunity to address the challenges posed by the duck curve phenomenon. Strategic integration of the PV systems into commercial buildings' envelopes, not only offers a solution to mitigate the oversupply challenges of the duck curve, but also supply this sectors electricity demands with clean solar energy. From the utilities standpoint, this approach will ensure reliable and sustainable energy systems for power operators in regions experiencing elevated solar penetration.

Commercial buildings exhibit distinct electricity consumption patterns across seasons. Winter months electricity demand mainly supplied by electric heat pumps [11]. Conversely, summer brings a rise in demand for air conditioning, making it the primary driver of electricity consumption during warmer seasons [11]. Considering these seasonal differences, focusing on mitigating the duck curve challenges specifically during the summer season offers the most

significant benefit. By strategically reducing or eliminating PV power curtailment during summer, buildings can become less reliant on grid electricity, leading to a decrease in overall utility consumption.

The need for efficient, small-scale PV systems that can be seamlessly integrated into buildings is essential for not only offsetting building electricity consumption but also addressing the challenges associated with the duck curve. Currently, solar power generation primarily relies on solar farms or fixed south-facing panels installed on rooftops [12]. This research takes a novel approach by exploring BIPV systems that offer the combined benefit of supplying buildings with solar energy and mitigating PV system oversupply. The hypothesis of this study is that integrating PV-louvers into the south façade will reduce PV system oversupply in very hot, hot, warm, and mixed ASHRAE climate zones. Previous work analyzed the energy performance of BIPV, including building energy consumption and PV power performance [13]. The results showed that south-facing PV-louvers increased heating loads in cool, cold, very cold, and subarctic/arctic climate zones. Therefore, these ASHRAE climate zones were excluded from the current study.

Curtailment is caused by excess solar energy production from the PV system. In PV louver systems, the PV panels serve a dual purpose: generating electricity and providing shade. Therefore, not only does the climate region affect the building's energy consumption, but the installation angle at which the PV-louvers perform optimally significantly impacts the building's energy loads. To comprehensively understand the impact of south-facing PV louvers on minimizing the depth of the lowest point on the BIPV's net energy curve, several factors need to be considered:

- Solar irradiance: The amount of solar radiation hitting the PV louvers throughout the year will affect their energy generation and shading effectiveness. Locations with higher solar irradiance will see a greater impact from both aspects.

- Building energy demand profile: The building's energy use patterns throughout the day will influence how much the PV louvers can offset the cooling or heating needs. For example, if the building's peak cooling demand coincides with peak solar irradiance, PV-louvers can be particularly beneficial.
- Thermal properties of the building envelope: The building's insulation levels, window characteristics, and overall thermal mass will influence how much heat gain needs to be mitigated by the PV louvers.
- PV-louver design: The design of the louvers, such as their width, number, and spacing between them, significantly impacts their ability to generate electricity and provide shade. Optimizing these factors is crucial for maximizing benefits.

One solution that suggested in previse research [14] was to increase the annual solar power injection in the grid but adding a 60% penetration constrain in midday PV power production, manage the curtailment. This method potentially increase the PV power production in the morning and afternoon [14] but the ultimate consequences of this failure will increase costs and reduce the environmental benefits of the PV systems.

A number of studies have focused on battery storage systems as a solution to address the oversupply of PV systems during midday hours. While those systems offer a solution for managing the midday oversupply of PV over generation, they represent a separate strategy distinct from BIPV systems. This study offers valuable insights for architects, engineers, and policymakers to make informed decisions about the optimal BIPV system type for integration with either battery storage or grid connection. By evaluating the performance of south façade PV-louvers in mitigating midday power curtailment, this research guides stakeholders in maximizing system performance and financial returns. For battery-integrated BIPV systems, it highlights how to achieve cost-

effectiveness and high efficiency. For grid-connected BIPV systems without battery storage, it offers strategies to avoid contributing to the duck curve dip and overgeneration, ensuring a reasonable and short return on investment.

Energy consumption and PV power production vary significantly depending on climate, and they do not follow the same pattern. Therefore, a more granular study is needed to investigate the performance of different BIPV typologies in various climate zones and their impact on building energy consumption, including heating, cooling, and lighting. The study aims to close the gap in understanding how different BIPV typologies perform across 10 ASHRAE climate zones. An in-depth search in the literature yielded no research paper investigating the PV-louvers' effectiveness in mitigating PV system oversupply and curtailment, considering various climate conditions and their influence on heating, cooling, and lighting needs. This study aims to provide detailed insights that can inform trade-off decisions in grid electricity consumption, BIPV system performance and ensure reliable and sustainable energy systems in regions with high solar power penetration.

Previous research has explored the performance of south façade PV-louvers and PV-mounted roof systems in generating electricity and reducing building electricity loads across all ASHRAE climate zones [13]. Building on these findings, this study focuses specifically on the impact of those typologies on mitigating the PV power curtailment. By examining the effectiveness of these typologies in addressing PV power curtailment, this research aims to provide new insights into optimizing BIPV systems and enhancing grid stability.

2. Methodology and materials

2.1. Geometry: Simulations were conducted in Rhino, a 3D modeling software [19], using a single room measuring 10m x 10m x 4m (length, depth, and height). Each typology featured a

south-facing window with an 80% window-to-wall ratio (WWR). The overall simulation workflow included six BIPV typologies: three with PV-louvers on the south glass facade and three with roof-mounted PV systems (Figure 3.2). Each typology maintained a consistent PV system surface area of 30m². The depth and number of PV-louvers varied: S-1 and R-1 had 6 louvers at 0.5m depth; S-2 and R-2 had 3 louvers at 1m depth; and S-3 and R-3 had 2 louvers at 1.5m depth.

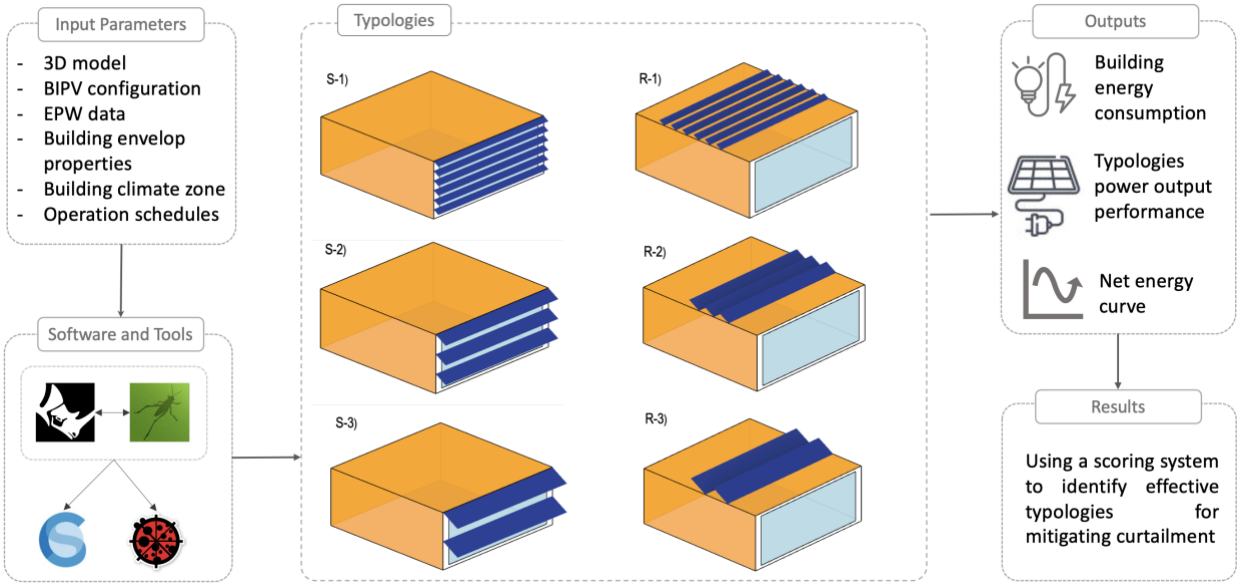

Figure 3.2 Analysis workflow of simulated typologies.

2.2. Building zone and site condition setup: To evaluate the model's performance across various locations, a combination of integrated software tools was employed. Grasshopper (GH), a Rhino plugin, facilitated the simulation workflow [19]. functioned as a bridge, connecting Rhino's 3D modeling with validated simulation engines [20]. LB used the EnergyPlus engine [21] and EnergyPlus Weather (EPW) data [22] to simulate irradiance on PV panels. ClimateStudio [23] (CS version 1.9.8) which is based on Radiance and EnergyPlus, simulated the building's lighting, heating, and cooling loads.

Table 3.1 depicts the selected city-states, their corresponding climate types, ASHRAE climate zones, and the PV tilt angles. ASHRAE 90.1 were used as the building standards in all the energy simulation settings.

For computational efficiency and to focus on key seasonal variations, simulations were conducted in four representative months: March, June, September, and December. These months capture peak and low points in both building yearly electricity consumption and PV power generation.

In all simulation runs, the building program was set up for a medium open-space office, with occupancy schedules tailored to typical office operations. On weekdays, occupancy began at 7 am, gradually ramping up to full occupancy by 9 am, and then started decreasing at 6 pm, reaching vacancy at 10 pm. On the first day of the weekend, operations commenced at 7 am, increased to 30% occupancy by midday, and then started decreasing at 1 pm until fully vacant by 8 pm. The second day of the weekend had no scheduled occupancy.

Table 3.1 Selected locations and their ASHRAE climate zones.

City, State	**Climate type**	**Climate zone**	**PV optimum tilt angle**
Miami, FL	Very hot	1A	24.17
Houston, TX	Hot-humid	2A	26.42
Phoenix, AZ	Hot-dry	2B	28.44
Austin, TX	Warm-humid	3A	26.78
Charlotte, NC	Warm-humid	3A	29.33
Los Angeles, CA	Warm-dry	3B	28.74
San Francisco, CA	Warm-marine	3C	30.46
Washington DC	Mixed-humid	4A	31.02
Albuquerque, NM	Mixed-dry	4B	29.24
Seattle, WA	Mixed-marine	4C	34.57

2.3. BIPV system potential power production: the optimum tilt angle of the PV modules in both PV-louvers and roof-mounted PV typologies were calculated using equation 1 from Jacobson et al. research [24].

$$1.3793 + \theta \times \left(1.2011 + \theta \times (-0.014404 + \theta \times (0.000080509))\right) \quad (1)$$

where θ is the latitude of the location.

The LB plug-in uses the EnergyPlus code to define sky matrix attributes based on the analysis period and local weather data. In this part of the analysis workflow, the Cumulative Sky Matrix component was employed to generate a matrix of direct normal radiation and diffuse horizontal radiation values from each segment of the sky dome. The analysis period was set to one month, allowing for the calculation of average daily irradiance levels (kWh/m²/day) on the PV surface for each month. Nonuniform irradiance levels, often caused by self-shading of panels, are a common issue in PV-louver systems. This results in a significant voltage drop, leading to a dramatic reduction in PVPP performance. Previous research [25] proposed a new circuit connection for partially shaded BIPV systems. According to their study, a hybrid series and parallel cell connection mitigated the voltage drop from 98% to 21%. Since LB simulates the irradiance levels on the PV surface, incorporating this hybrid circuit connection approach could potentially convert a majority of the received irradiance into power. Therefore, the calculation of potential power production for the PV system in this study relies on the irradiance levels, as demonstrated in equation 2.

$$P_{PV} = E \times \eta_{PV} \times (1 - \mathrm{LSF}) \times \eta_{inv} \quad (2)$$

Where

PVPP is potential power production,

E is irradiance on PV surface,

η_{PV} is PV panels efficiency,

LSF is loss factor

η_{inv} is nominal rated DC-to-AC conversion efficiency of the inverter

Mono crystalline silicon (c-Si) PV cells were considered for the PV material in all typologies. While in laboratory conditions c-Si PVs exhibit an efficiency range of 25%-27%, their real-world efficiency varies from 16% to 22% [26]. In this study, the efficiency of the PV system (η_{PV}) was assumed to be 19%, the median value of the real-world efficiency range for c-Si PVs. For the loss factor (LF), accounting for losses due to soiling, shading, snow, mismatch, wiring, connectors, light-induced degradation, nameplate rating, age, and availability, a reduction of 14.08% was considered [27]. he inverter efficiency factor (η_{inv}) as established by the National Renewable Energy Lab (NREL), was assumed to be 96% [27].

2.4. Building energy consumption: In this simulation workflow, the PV-louvers were defined as shading devices, whereas the roof-mounted PV typologies did not provide any shading for the south façade window. U-value (W/m^2K), SHGC and Tvis of the windows were set to align with ASHRAE 90.1 requirements and contemporary recommendations in each locations' climate zone (Table 3.2). A double-glazing system in accordance with ASRHAE 90.1 window requirements were used in respective locations. Lighting availability schedules were set to the office schedule with the power density of 6.5 W/m according to ASHRAE 90.1 requirements. The working surface height for daylight and glare analysis was set at 0.75m above the floor.

The heating ($E_{Heating}$), cooling ($E_{Cooling}$) and lighting ($E_{Lighting}$) loads of the room were simulated in all building typologies using CS.

The net energy use was calculated by subtracting power generated by PV system (E_{PV}) from sum of the loads using the equation below:

$$E_{net} = E_{Heating} + E_{Cooling} + E_{Lighting} - P_{PV} \quad (3)$$

2.5. Impact on Duck curve valley: To assess the typologies' net energy use behavior during peak PV power production, the analysis focused on the hours from 10 am to 2 pm. The y-values within this time range were extracted for each monthly curve of each typology. Numerical integration was then used to compute the area under each monthly curve for all typologies. The resulting area values served as quantitative scores to determine which typologies best mitigated BIPV curtailment. A lower score indicated less PV power curtailment.

Table 3.2 The building envelops parameters in different climate zones.

		Climate Zones			
Envelop Surface	**Parameter**	**1**	**2**	**3**	**4**
Double-glazing window	U-value (W/m^{2}K)	2.84	2.56	2.39	2.04
	SHGC	0.23	0.25	0.25	0.36
	Tvis	0.25	0.28	0.28	0.40
Exterior walls	U-value (W/m^{2}K)	2.11	0.75	0.62	0.54
	Thermal Capacity (kJ/K/m^2)	532.30	538.50	540.40	542.28
Roof	U-value (W/m^{2}K)	0.26	0.22	0.22	0.18
	Thermal Capacity (kJ/K/m^2)	469.70	471.13	471.13	472.78
Ground	U-value (W/m^{2}K)	0.81	0.73	0.70	0.69
	Thermal Capacity (kJ/K/m^2)	471.60	471.91	472.00	472.00

3. Results

The power production and energy consumption, including equipment, heating, cooling, and lighting, of six different BIPV typologies were simulated across ten ASHRAE climate zones, ranging from very hot to mixed climates. Figures 3.2 to 3.5 depict the net energy use curves of the typologies for the months of March, June, September, and December. The impact of south facade PV-louvers and PV-mounted roofs on mitigating PV power curtailment was assessed by calculating the area under each typology's net energy curve between 10 am and 2 pm (Figure 3.6). The impact

of the south façade on mitigating curtailment can be evaluated by comparing typology performance in each month and each climate zone. The comparison based on climate zones is as follows:

Climate Zone 1: S3 consistently received higher score than other typologies across all four months indicating that it successfully mitigated the PV power curtailment.

Climate Zone 2: S1 and R1 performed similarly in cold month, but the performance gap widened as the months became warmer. For example, their scores were identical in December but diverged significantly by June, with S1 scoring notably higher than R1. Typology S3 generally outperformed the others in both climate zone 2A and 2B. Interestingly, in sub-climate zone 2A, S2 performed best in all four months.

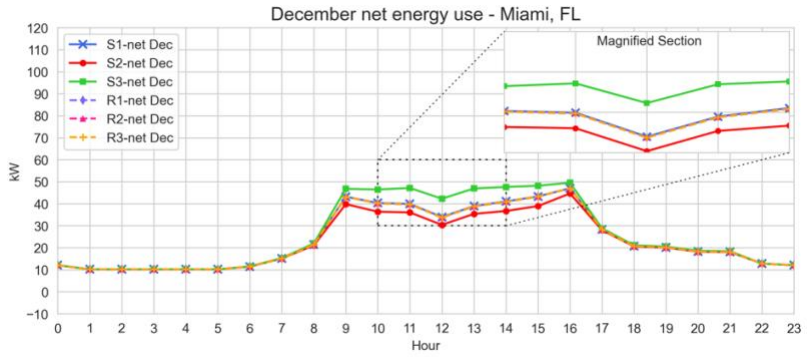
December net energy use - Miami, FL
S1-net Dec
S2-net Dec
S3-net Dec
R1-net Dec
R2-net Dec
R3-net Dec
Magnified Section
kW
Hour

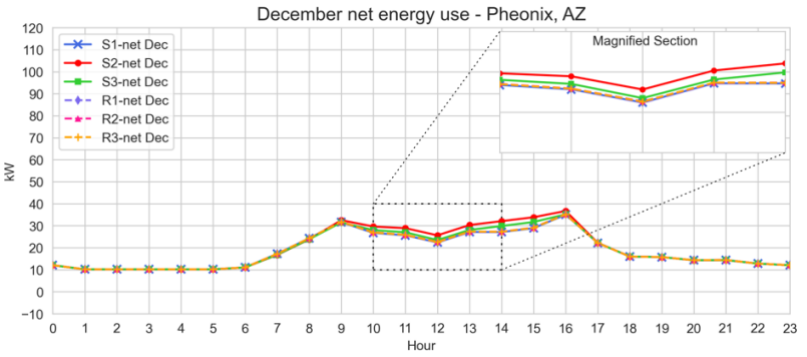
December net energy use - Pheonix, AZ
S1-net Dec
S2-net Dec
S3-net Dec
R1-net Dec
R2-net Dec
R3-net Dec
Magnified Section
kW
Hour

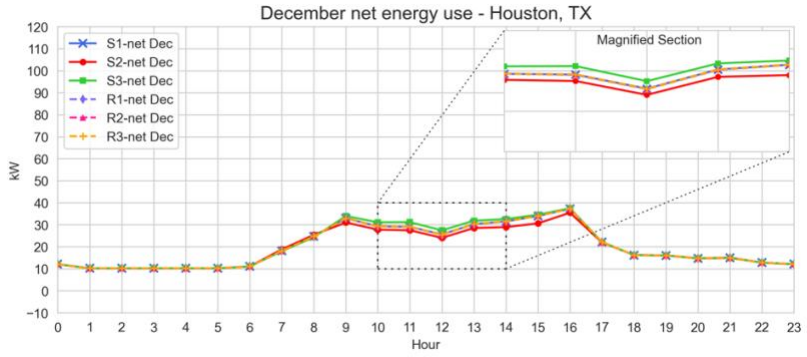
December net energy use - Houston, TX
S1-net Dec
S2-net Dec
S3-net Dec
R1-net Dec
R2-net Dec
R3-net Dec
Magnified Section
kW
Hour

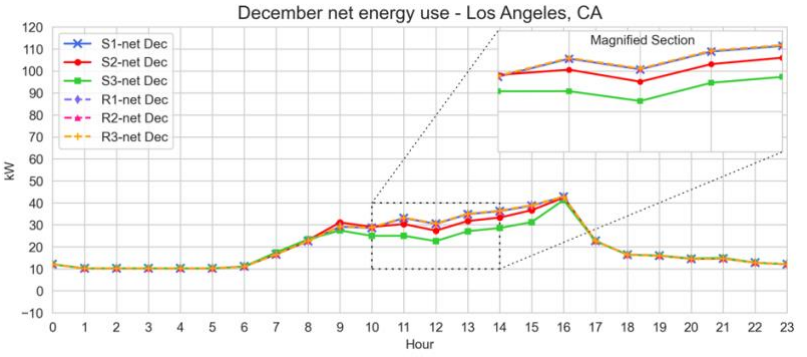
December net energy use - Los Angeles, CA
S1-net Dec
S2-net Dec
S3-net Dec
R1-net Dec
R2-net Dec
R3-net Dec
Magnified Section
kW
Hour

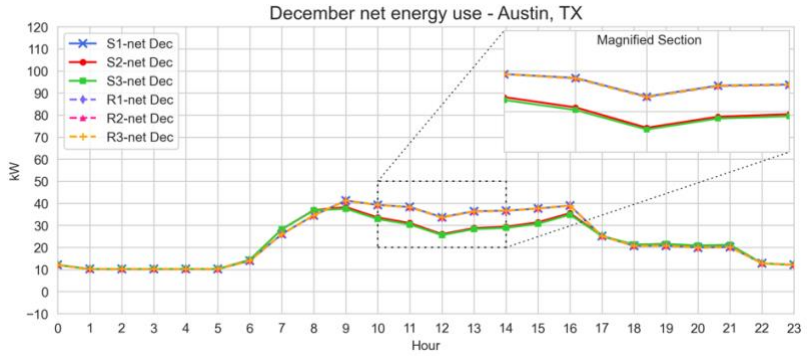
December net energy use - Austin, TX
S1-net Dec
S2-net Dec
S3-net Dec
R1-net Dec
R2-net Dec
R3-net Dec
Magnified Section
kW
Hour

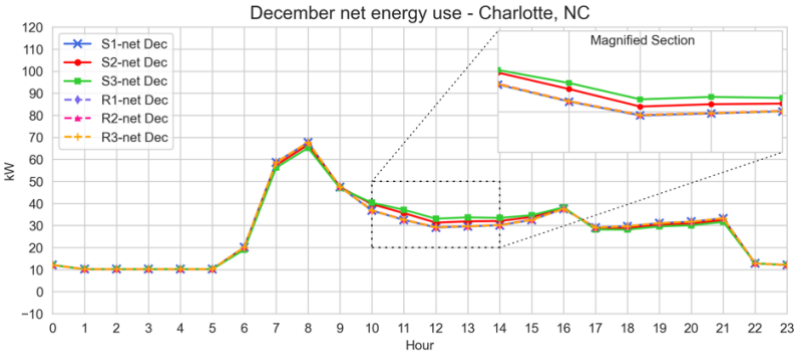
December net energy use - Charlotte, NC
S1-net Dec
S2-net Dec
S3-net Dec
R1-net Dec
R2-net Dec
R3-net Dec
Magnified Section
kW
Hour

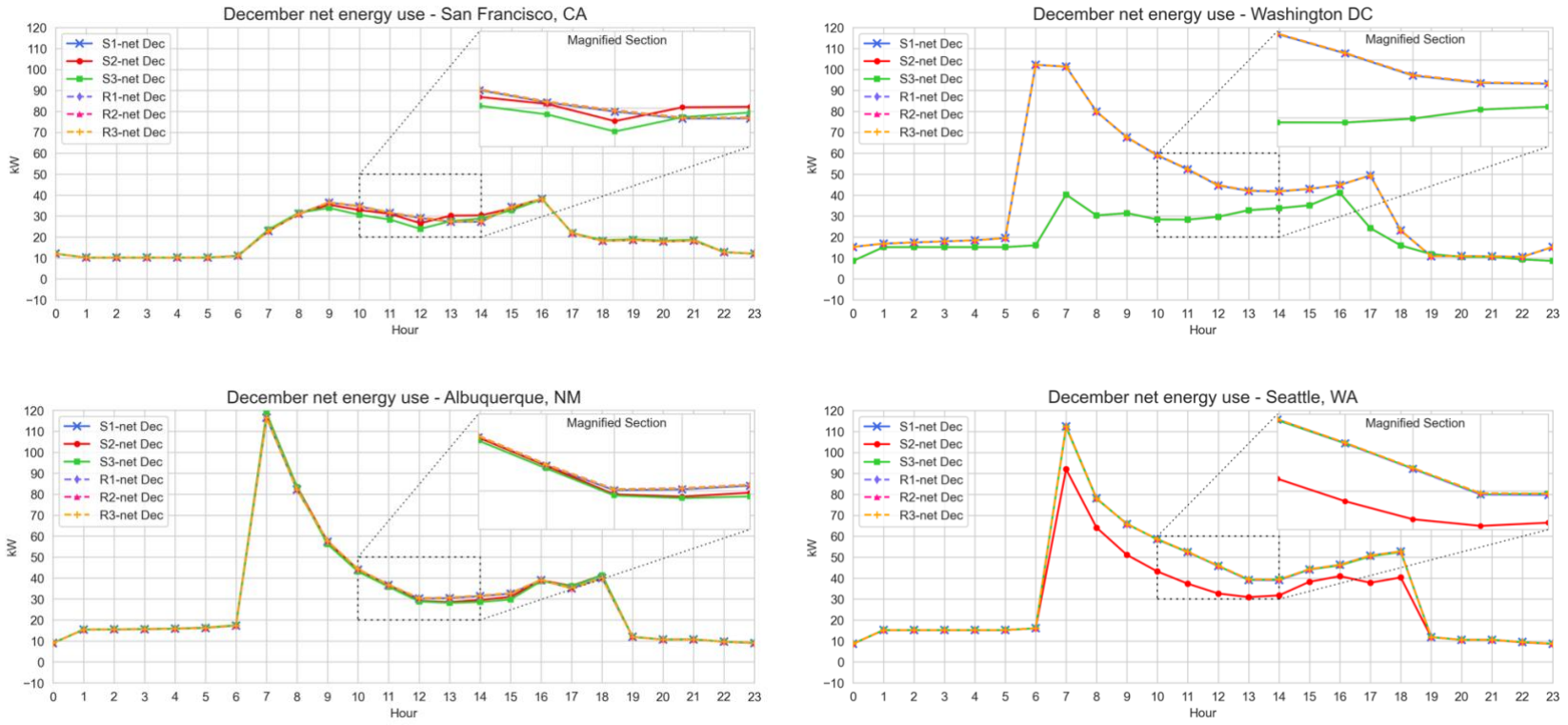

Figure 3.3 Net energy use of the typologies in selected locations in December.

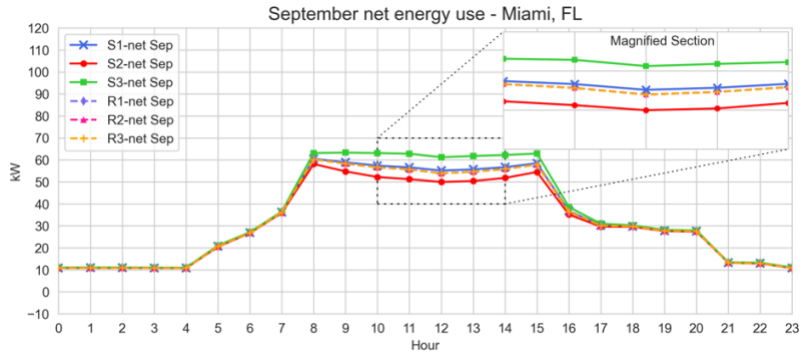
September net energy use - Miami, FL
S1-net Sep
S2-net Sep
S3-net Sep
R1-net Sep
R2-net Sep
R3-net Sep
Magnified Section
kW
Hour

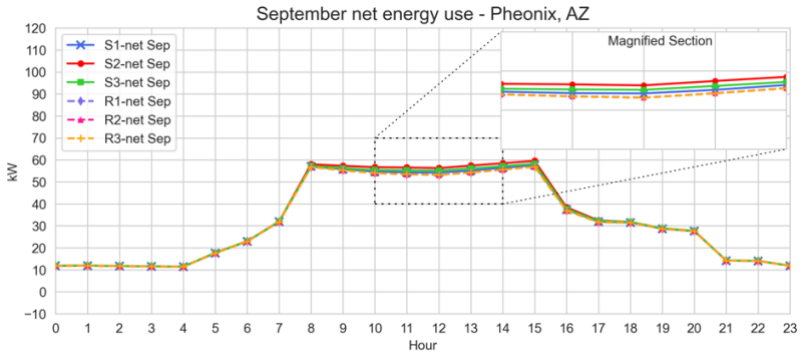
September net energy use - Pheonix, AZ
S1-net Sep
S2-net Sep
S3-net Sep
R1-net Sep
R2-net Sep
R3-net Sep
Magnified Section
kW
Hour

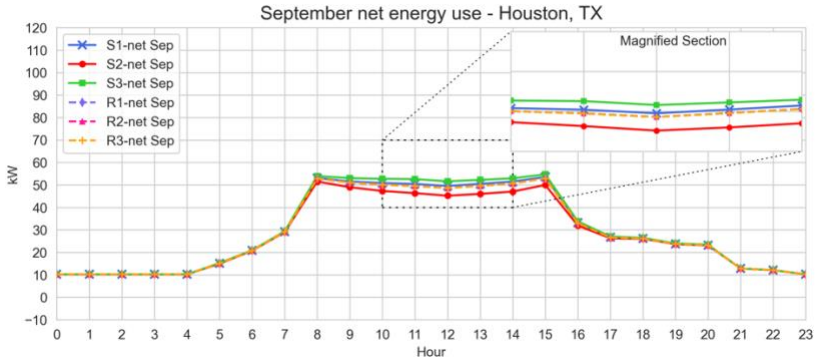
September net energy use - Houston, TX
S1-net Sep
S2-net Sep
S3-net Sep
R1-net Sep
R2-net Sep
R3-net Sep
Magnified Section
kW
Hour

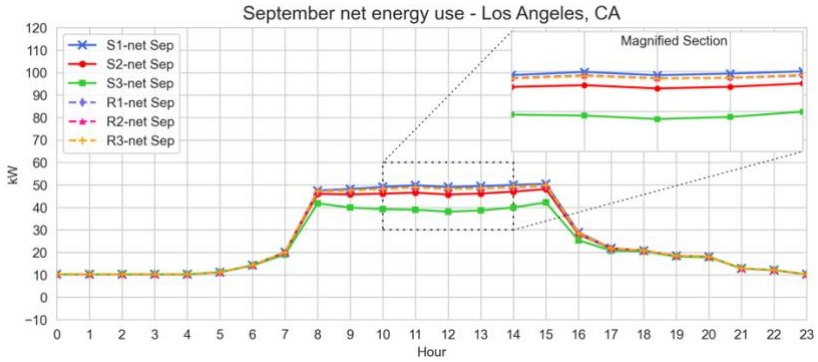
September net energy use - Los Angeles, CA
S1-net Sep
S2-net Sep
S3-net Sep
R1-net Sep
R2-net Sep
R3-net Sep
Magnified Section
kW
Hour

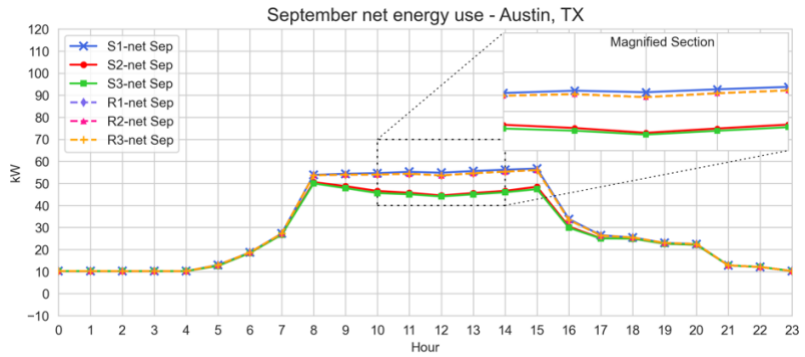
September net energy use - Austin, TX
S1-net Sep
S2-net Sep
S3-net Sep
R1-net Sep
R2-net Sep
R3-net Sep
Magnified Section
kW
Hour

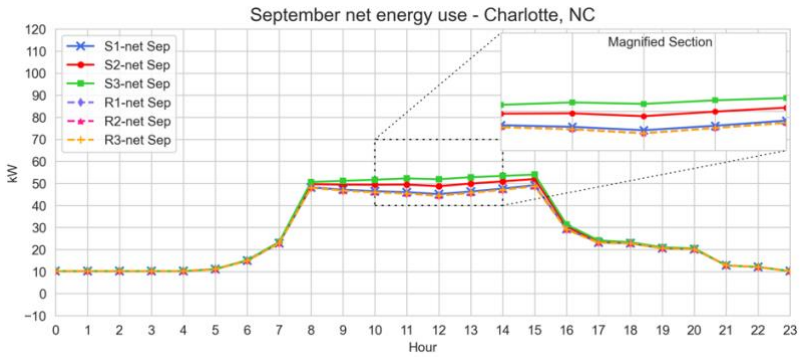
September net energy use - Charlotte, NC
S1-net Sep
S2-net Sep
S3-net Sep
R1-net Sep
R2-net Sep
R3-net Sep
Magnified Section
kW
Hour

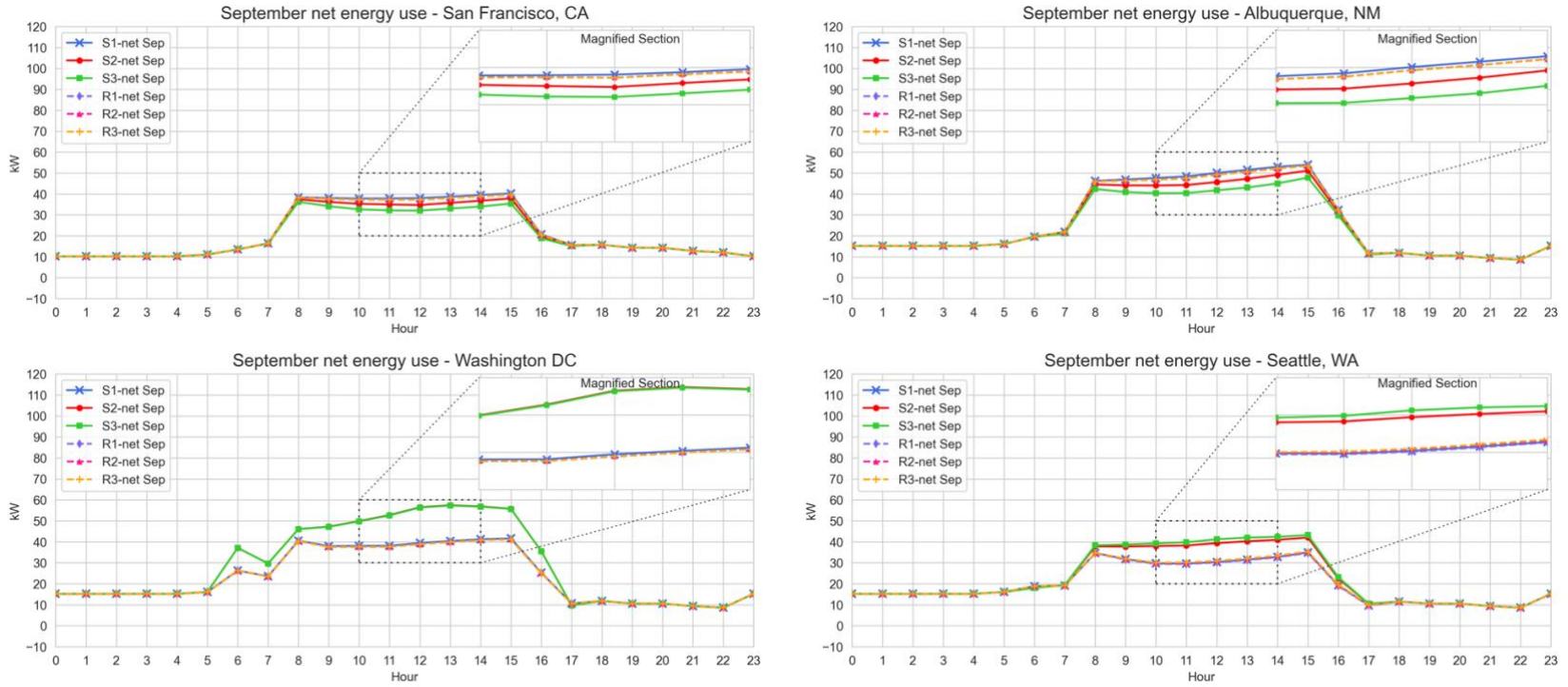

Figure 3.4 Net energy use of the typologies in selected locations in September.

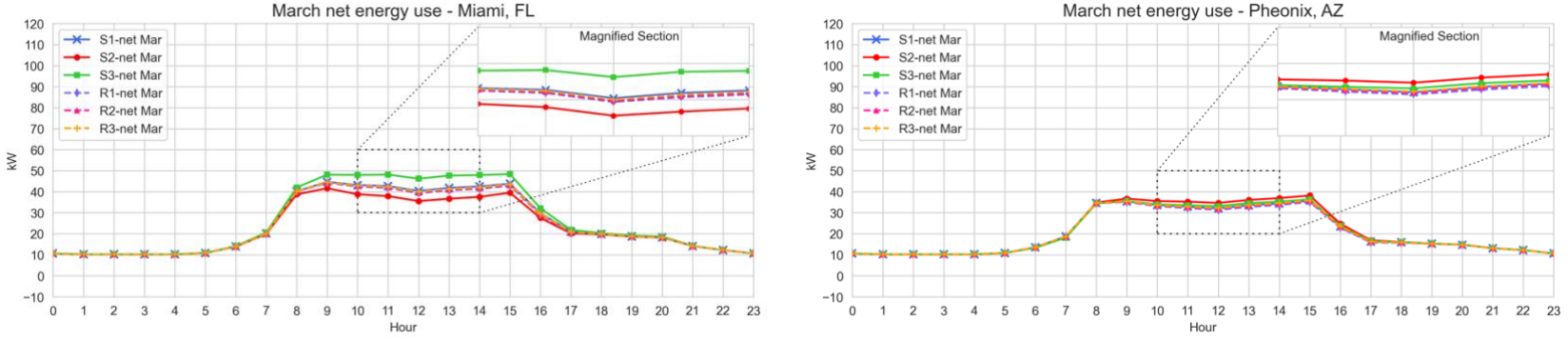

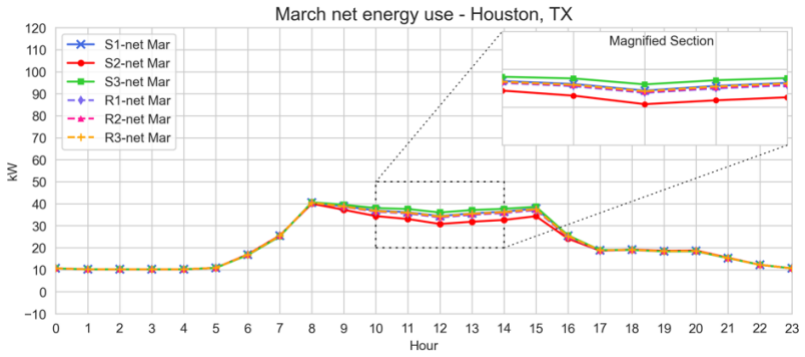
March net energy use - Houston, TX
S1-net Mar
S2-net Mar
S3-net Mar
R1-net Mar
R2-net Mar
R3-net Mar
Magnified Section
kW
Hour

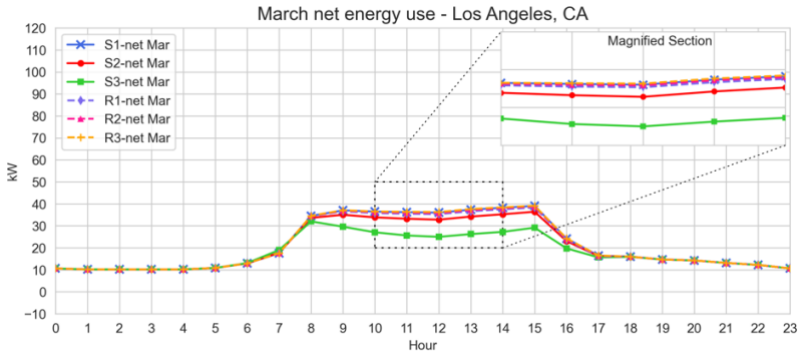
March net energy use - Los Angeles, CA
S1-net Mar
S2-net Mar
S3-net Mar
R1-net Mar
R2-net Mar
R3-net Mar
Magnified Section
kW
Hour

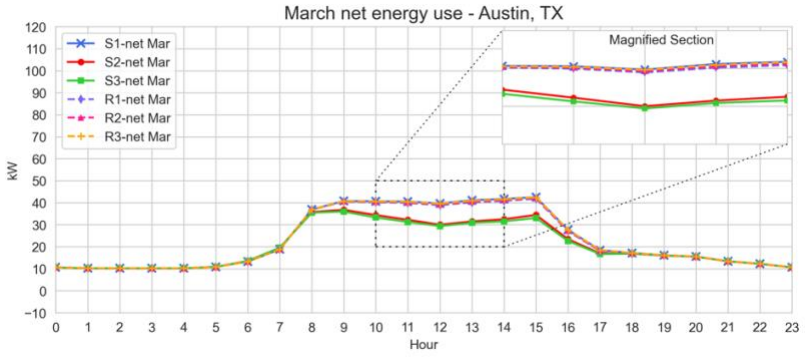
March net energy use - Austin, TX
S1-net Mar
S2-net Mar
S3-net Mar
R1-net Mar
R2-net Mar
R3-net Mar
Magnified Section
kW
Hour

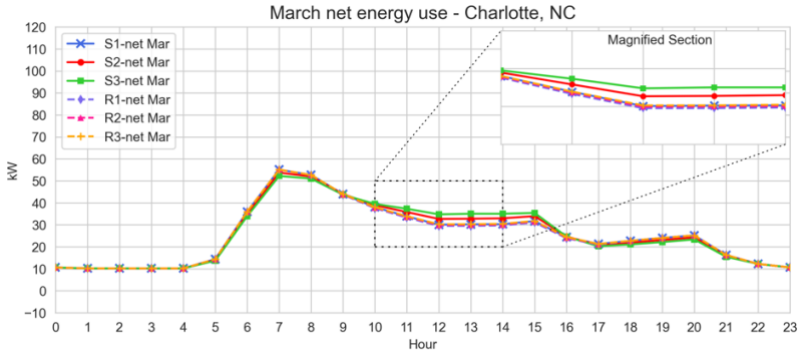
March net energy use - Charlotte, NC
S1-net Mar
S2-net Mar
S3-net Mar
R1-net Mar
R2-net Mar
R3-net Mar
Magnified Section
kW
Hour

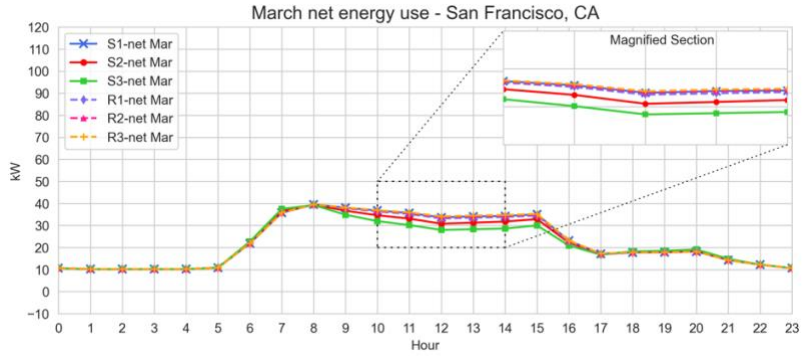
March net energy use - San Francisco, CA
S1-net Mar
S2-net Mar
S3-net Mar
R1-net Mar
R2-net Mar
R3-net Mar
Magnified Section
kW
Hour

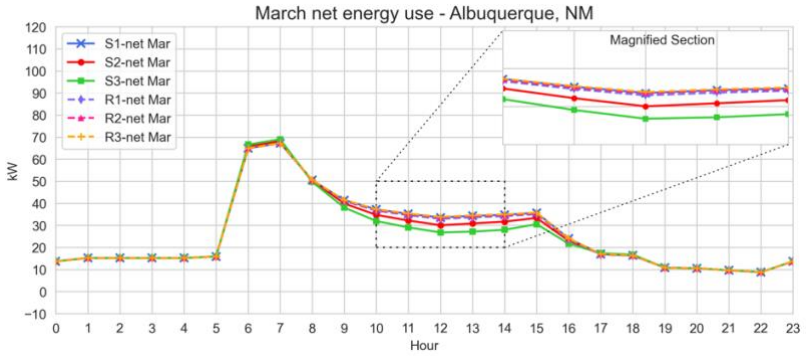
March net energy use - Albuquerque, NM
S1-net Mar
S2-net Mar
S3-net Mar
R1-net Mar
R2-net Mar
R3-net Mar
Magnified Section
kW
Hour

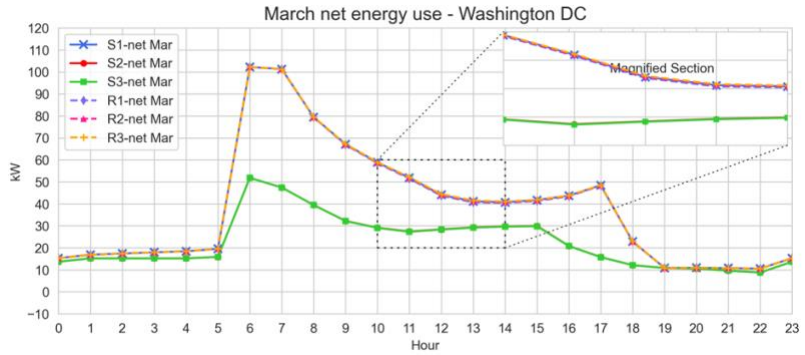

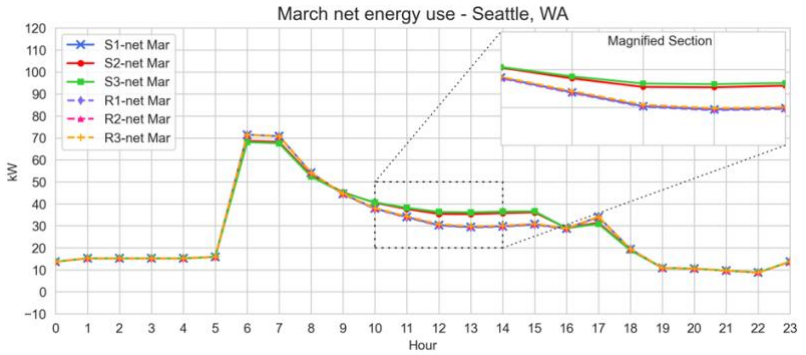

Figure 3.5 Net energy use of the typologies in selected locations in March.

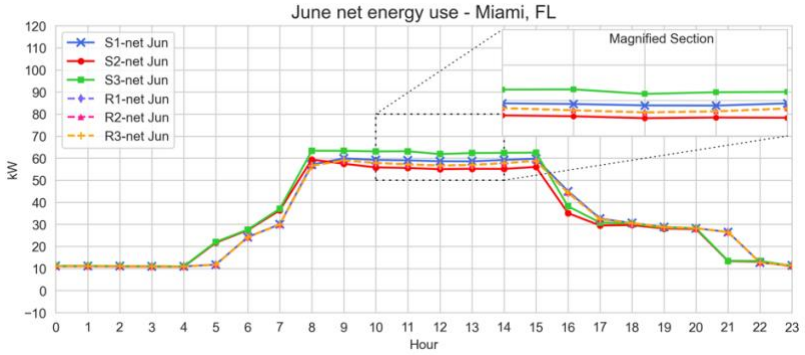

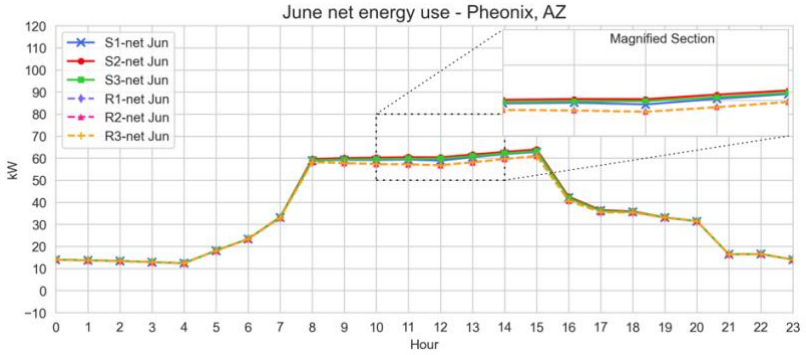

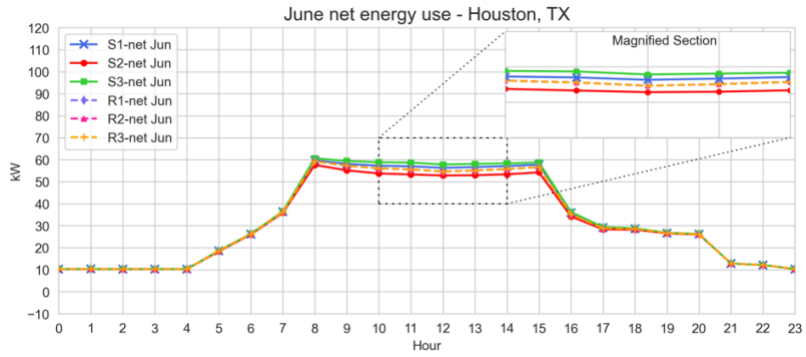
June net energy use - Houston, TX
S1-net Jun
S2-net Jun
S3-net Jun
R1-net Jun
R2-net Jun
R3-net Jun
Magnified Section
kW
Hour

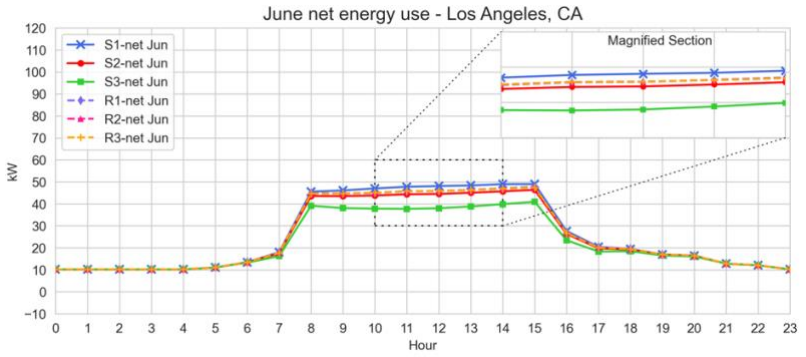
June net energy use - Los Angeles, CA
S1-net Jun
S2-net Jun
S3-net Jun
R1-net Jun
R2-net Jun
R3-net Jun
Magnified Section
kW
Hour

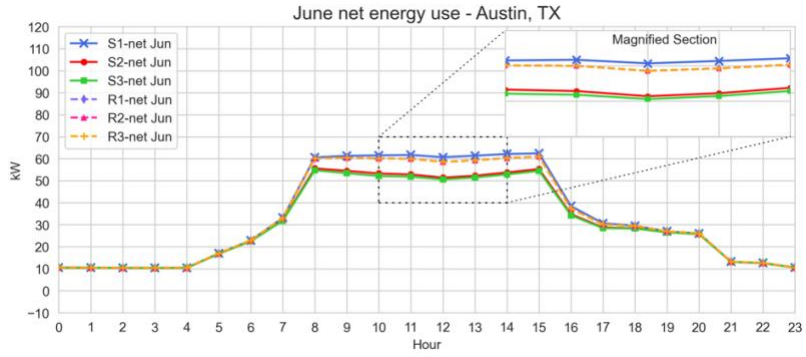
June net energy use - Austin, TX
S1-net Jun
S2-net Jun
S3-net Jun
R1-net Jun
R2-net Jun
R3-net Jun
Magnified Section
kW
Hour

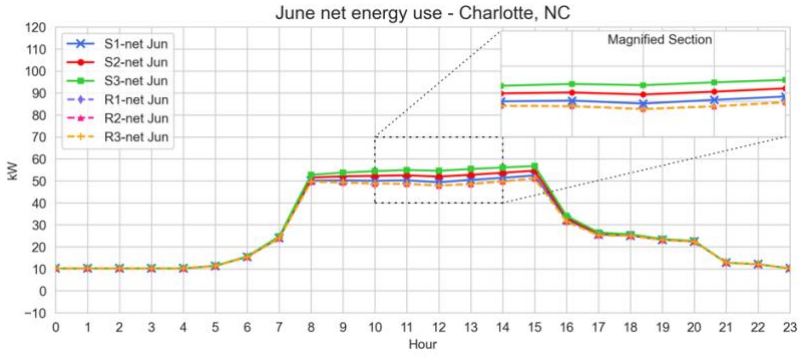
June net energy use - Charlotte, NC
S1-net Jun
S2-net Jun
S3-net Jun
R1-net Jun
R2-net Jun
R3-net Jun
Magnified Section
kW
Hour

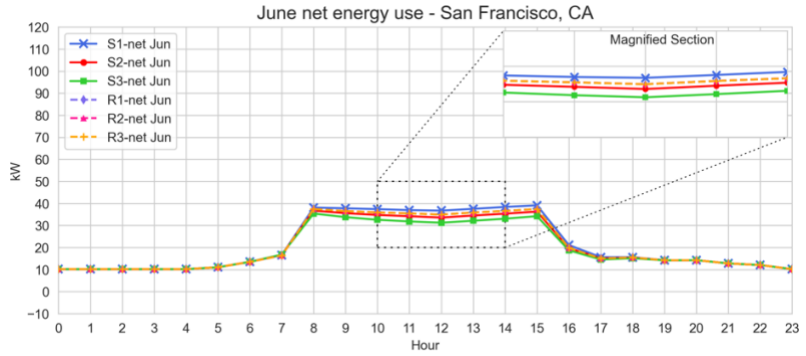
June net energy use - San Francisco, CA
S1-net Jun
S2-net Jun
S3-net Jun
R1-net Jun
R2-net Jun
R3-net Jun
Magnified Section
kW
Hour

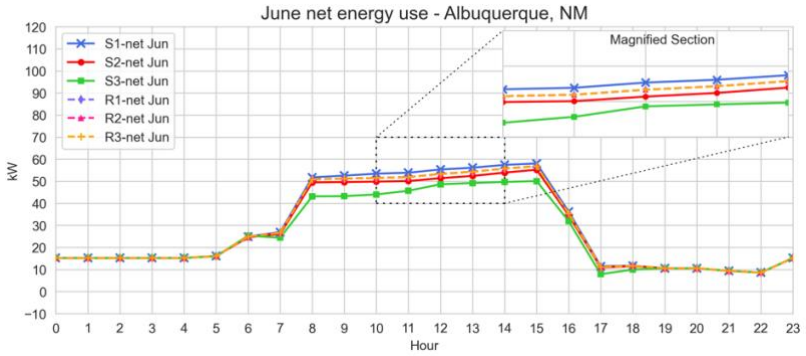
June net energy use - Albuquerque, NM
S1-net Jun
S2-net Jun
S3-net Jun
R1-net Jun
R2-net Jun
R3-net Jun
Magnified Section
kW
Hour

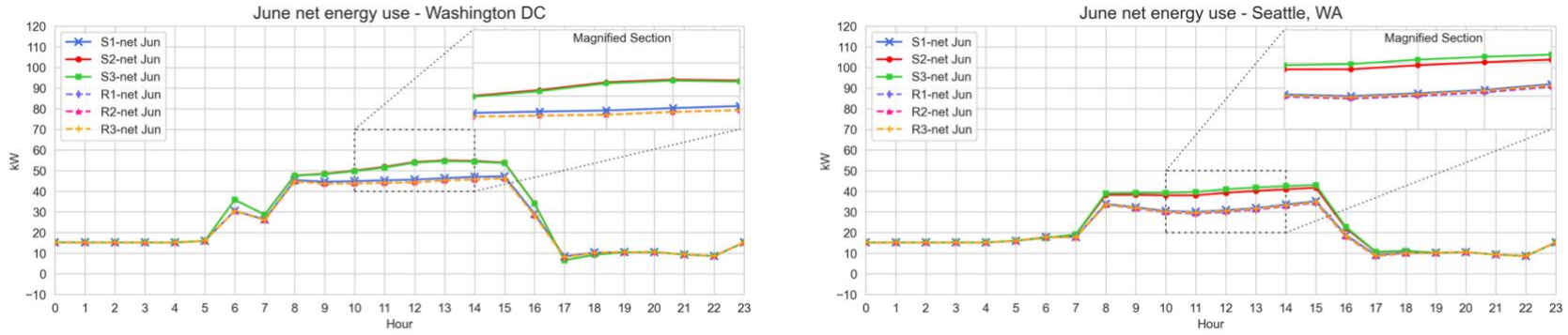

Figure 3.6 Net energy use of the typologies in selected locations in June.

Climate Zone 3: S1 outperformed other typologies in Los Angeles, CA (sub-climate zone 3B) and Austin, TX (sub-climate zone 3B). S3 received higher scores than the rest in Charlotte, NC (sub-climate zone 3A). In San Francisco (sub-climate zone 3C), the performance of both roof-mounted PV and south mounted PV-louvers was inconsistent, making it difficult to identify a single optimal typology for year-round use in this sub-climate.

Climate Zone 4: In Washington DC (sub-climate zone 4A), S2 outperformed in September and June, while R2 and R3 had very close scores and outperformed others in March and December. In Albuquerque, NM (sub-climate zone 4B), S1 outperformed in all four months except December. In Seattle (sub-climate zone 4C), S3 outperformed in all four months except December.

The efficacy of the typologies in mitigating PV system overgeneration for each month is demonstrated in Table 3.3 In locations with very hot, hot, and warm climates, the PV-louvers on the south façade performed best. However, in mixed climates, roof typologies were more effective.

Table 3.3 Outperforming typologies in each month at selected locations.

City, State	December	September	March	June
Miami, FL	S3	S3	S3	S3
Phoenix, AZ	S2	S2	S2	S3
Houston, TX	S1and R2	S3	S3	S3
Austin, TX	S1	S1	S1	S1
Los Angeles, CA	S1	S1	S1	S1
Charlotte, NC	S3	S3	S3	S3
San Francisco, CA	R2	R2	R3	S1
Washington DC	R2	S2	R3	S2
Albuquerque, NM	R2	S1	S1	S1
Seattle, WA	R2 and R3	S3	S3	S3

4. Conclusion

PV power oversupply or curtailment underscores the need for energy efficiency measures to manage demand during peak times. This study's results show that the effectiveness of south façade PV-louvers in mitigating PV system overgeneration depends significantly on the location's solar irradiance levels and building energy consumption. Other key factors include PV-louver design and climate type. Considering that PV overproduction is mainly problematic during warmer seasons, the higher scores of PV-louver typologies in September and June indicate their efficacy in mitigating PV power curtailment. Even for typologies with lower scores, which means that the PV system generated more than the building's electricity demand, these represent good potential for integrating battery storage systems to store surplus energy.

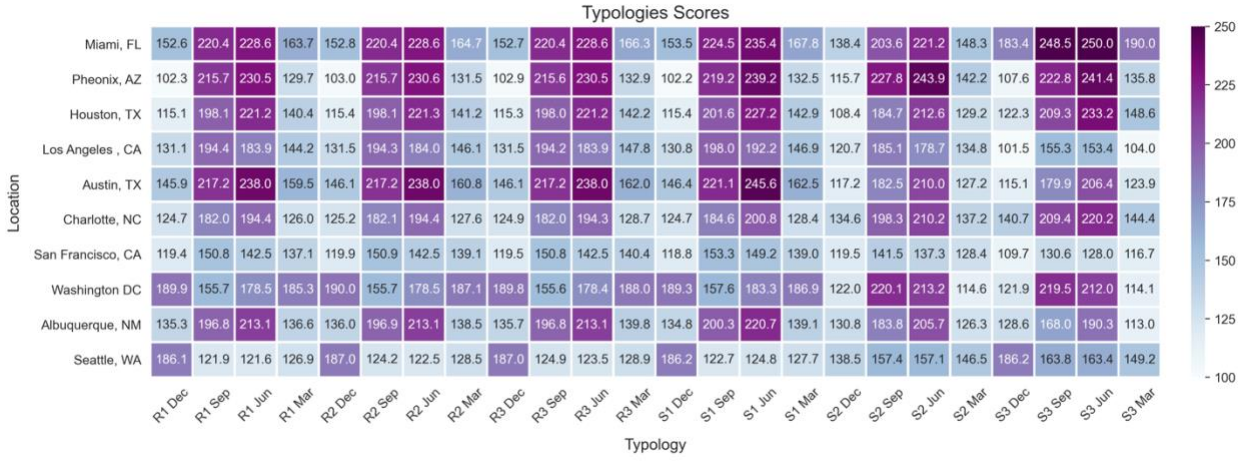

Figure 3.7 Scores of each typology in mitigating the curtailment.

Some climates and locations had a consistently best-performing typology throughout all four months, making the decision-making process straightforward for architects, engineers, and building owners. However, sub-climate zone 3C requires further investigation in other locations and over a yearly analysis period due to the lack of a consistent leader among the typologies. While

this study does not directly address the impact of building height on energy production with BIPV louvers, the results suggest that façade typologies, particularly S1 and S3, which showed energy production close to R1, could be more beneficial for offsetting electricity consumption in tall buildings.

5. Acknowledgement

This study was funded by U.S. National Science Foundation (NSF). Award number: 2122014.

6. References

1. Operator., C.I.S., *Demand Response and Energy Efficiency Roadmap: Maximizing Preferred Resources*. 2013, California Independent Systems Operator Folsom, CA.
2. Sun, Y., et al., *2018 renewable energy grid integration data book*. 2020, National Renewable Energy Lab.(NREL), Golden, CO (United States).
3. Richard Bowers, E.F., Katherine Antonio. *As solar capacity grows, duck curves are getting deeper in California*. 2023 [cited 2024; Available from: https://www.eia.gov/todayinenergy/detail.php?id=56880.
4. EIA. *Hourly electricity consumption varies throughout the day and across seasons*. 2020 [cited 2024; Available from: https://www.eia.gov/todayinenergy/detail.php?id=42915.
5. DOE. *Guide to Determining Climate Regions by County*. 2015 [cited 2022; Available from: https://www.energy.gov/sites/prod/files/2015/10/f27/ba_climate_region_guide_7.3.pdf.
6. ISO-NE. *Solar Power in New England: Concentration and Impact*. 2018 [cited 2022; Available from: https://www.iso-ne.com/about/what-we-do/in-depth/solar-power-in-new-england-locations-and-impact.
7. EERE. *Solar Futures Study*. 2021 [cited 2022; Available from: https://www.energy.gov/eere/solar/solar-futures-study.
8. Shoemaker, S. *How much energy is consumed in U.S. buildings?* 2023 [cited 2023; Available from: https://www.eia.gov/tools/faqs/faq.php?id=86&t=1.
9. Zack Marohl, J.T., Chrishelle Lawrence. *Commercial buildings have gotten larger in the United States, with implications for energy*. 2020 [cited 2022; Available from: https://www.eia.gov/todayinenergy/detail.php?id=46118#:~:text=CBECS%20estimates%20that%205.9%20million,was%20last%20conducted%20in%202012.
10. Energy, U.S.D.o. *Annual Energy Outlook 2020. Table A2 Energy Consumption by Sector and Source*. 2020 [cited 2024; Available from: https://www.eia.gov/outlooks/aeo/.
11. Comstock, O. *U.S. natural gas consumption has both winter and summer peaks*. 2020 [cited 2023; Available from: https://www.eia.gov/todayinenergy/detail.php?id=42815#:~:text=During%20winter%2C%20homes%20and%20businesses,gas%20in%20the%20winter%20months.

12. EIA. *Solar photovoltaic output depends on orientation, tilt, and tracking*. 2014 [cited 2022; Available from: https://www.eia.gov/todayinenergy/detail.php?id=18871.
13. Hossei, H. and K.-H. Kim, *Comprehensive analysis of energy and visual performance of building-integrated photovoltaics in various climate zones.* Energy and Buildings, under review.
14. Denholm, P., et al., *Overgeneration from solar energy in California. a field guide to the duck chart*. 2015, National Renewable Energy Lab.(NREL), Golden, CO (United States).
15. Hernández-Callejo, L., S. Gallardo-Saavedra, and V. Alonso-Gómez, *A review of photovoltaic systems: Design, operation and maintenance.* Solar Energy, 2019. **188**: p. 426-440.
16. Ayeng'o, S.P., et al., *Comparison of off-grid power supply systems using lead-acid and lithium-ion batteries.* Solar Energy, 2018. **162**: p. 140-152.
17. Zhao, G., et al., *Economic analysis of integrating photovoltaics and battery energy storage system in an office building.* Energy and Buildings, 2023. **284**: p. 112885.
18. Judkoff, R. and J. Neymark, *International Energy Agency building energy simulation test (BESTEST) and diagnostic method*. 1995, National Renewable Energy Lab.(NREL), Golden, CO (United States).
19. Associates, R.M. *Rhino 8*. 2024 [cited 2024; Available from: https://www.rhino3d.com/.
20. Chris Machey. *LADYBUG TOOLS* 2022; Available from: https://www.food4rhino.com/en/app/ladybug-tools.
21. Energy, U.S.D.o., *EnergyPlus™ Version 22.1.0 Documentation*. Engineering Reference. 2022.
22. DOE. *Weather Data*. 2024; Available from: https://energyplus.net/weather.
23. Solemma. *ClimateStudio*. 2022 [cited 2022; Available from: https://www.solemma.com/climatestudio.
24. Jacobson, M.Z. and V. Jadhav, *World estimates of PV optimal tilt angles and ratios of sunlight incident upon tilted and tracked PV panels relative to horizontal panels.* Solar Energy, 2018. **169**: p. 55-66.
25. Hossei, H. and K.-H. Kim. *Circuit Connection Reconfiguration of Partially Shaded BIPV Systems, a Solution for Power Loss Reduction*. in *ACSA Annual Meeting In Common*. 2023.

26. Alami, A.H., et al., *Management of potential challenges of PV technology proliferation.* Sustainable Energy Technologies and Assessments, 2022. **51**: p. 101942.
27. Dobos, A.P., *PVWatts version 5 manual*. 2014, National Renewable Energy Lab.(NREL), Golden, CO (United States).

CHAPTER 4 (PAPER 3)

ASSESSING THE IMPACT OF PV-INTEGRATED WEST FACADE IN ALLEVIATING THE DUCK CURVE STEEP RAMP IN ALL ASHRAE CLIMATE ZONES

Hamideh Hossei[1], Kyoung-Hee Kim[2]
[1] Department of Infrastructure and Environmental System, UNC Charlotte, USA – 9201 University City Blvd, Charlotte, NC 28223
[2] School of Architecture, UNC Charlotte, USA – 9201 University City Blvd, Charlotte, NC 28223

Abstract

PV systems experience a rapid decline in power production at sunset. This requires utility plants to quickly increase electricity production to meet demand, raising grid stability problems. This paper investigates the impact of 19 BIPV typologies including PV-west façade and PV-mounted roof across all ASHRAE climate zones during March, June, September, and December in alleviating the duck curve steep ramp. The novel finding of this study revealed that the west-PV façade was able to supply the building in late afternoon hours by generated electricity during few hours before the sun set. The findings of this study reveal that the west-PV façade can effectively supply building electricity demand during the late afternoon hours. The effectiveness of PV-west facades in alleviating the steep ramp of the duck curve varied significantly across different climate zones. In very hot and hot climates, the impact was limited. Warm, mixed, and cool climates demonstrated more potential, particularly in climate zones 3 and 4 during June, December, and March. Cold, very cold, and Arctic climates exhibited higher effectiveness during warmer months. This solution offers a promising avenue for mitigating grid instability and optimizing solar energy integration within the built environment.

Nomenclature

Symbols

α	Latitude
P	potential power production
E	irradiance on PV surface
η_{PV}	PV panels efficiency
LF	PV system loss factor
η_{inv}	Nominal rated DC-to-AC conversion efficiency of the inverter
U Value	Heat transfer coefficient or thermal transmittance
P (δ)	Power production of PV-west façade that installed in δ angle
ω	Normalized weight of PVPP in each hour
t	Hour
$P(t)_{net}$	Net energy consumption of the building in t hour
EC	Building electricity consumption
SUH_{mon}	Useful sunlight hours of a month

Abbreviations

PV	Photovoltaic panels
PVPP	PV power production
BIPV	Building integrated PV panels
BESS	Battery energy storage systems
EIA	U.S. energy information administration
GW	Gigawatts
MWh	Megawatt hour
kWh	Kilowatt hour
3D	Three dimensions
SHGC	Solar heat gain coefficient
EPW	EnergyPlus weather file
GH	Grasshopper, a plugin for Rhino software
LB	Ladybug, an environmental analysis plugin for Grasshopper for Rhino software
WWR	Window-to-wall ratio

1. Introduction and literature review

Solar-grid integration has become widespread in many countries worldwide, driven by the increasing demand for clean alternative energy sources in place of fossil fuels [1]. The emergence of the duck curve phenomenon originated in California as a consequence of the significant adoption of solar photovoltaic (PV) systems. The curve represents the daily electricity demand and generation patterns, illustrating a pronounced dip in net demand during midday when solar generation is at its peak, resembling a duck's profile.

As solar panel installations increase, the challenge posed by the duck curve becomes more significant, especially in areas where solar energy penetration into the grid is high. Olczak et al. developed a tool to assess how the growing number of solar panel installations affects the grid [2]. As solar penetration increased globally, the duck curve phenomenon extended beyond California, occurring in regions with high solar capacity. The widespread adoption of solar energy, coupled with the intermittent nature of sunlight, raises concerns that traditional energy generators will not be able to balance supply and demand, especially on days characterized by the duck graph.

To achieve the decarbonization target of 80% by 2050 [7], the US must source 44% - 45% of its electricity from solar energy [8]. However, such a high level of solar penetration could exacerbate the challenges associated with the duck curve and require additional grid infrastructure. Due to the high penetration of distributed PV systems like rooftop PV and small ground-mounted PV systems, the fluctuations in PV power generation are on the rise.

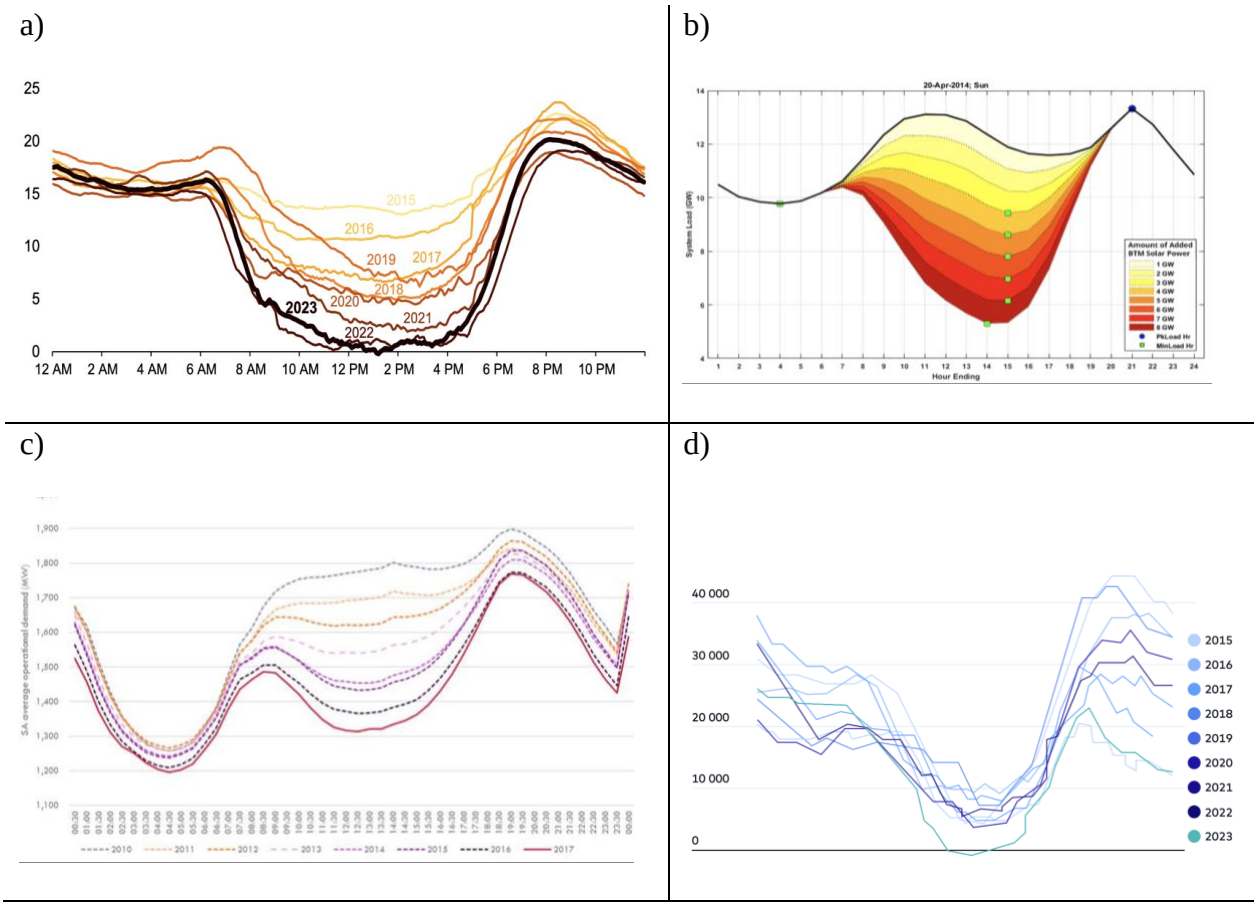

Figure 4.1 Duck curve in a) California, U.S. [3], b) New England, U.S. [4] , c) Australia [5] d) Germany [6]

Managing these fluctuations presents challenges due to unpredictable weather changes [9], disparities between solar energy production and demand [10], and limited bi-directional grid infrastructure [11]. In the existing infrastructure, ensuring grid reliability becomes challenging with increased solar power integration, as traditional utilities like coal and nuclear plants have slow response times and cannot quickly adjust their operating parameters or shut down when needed [12]. While implementing the PV system is rapidly growing, a stable grid is essential for maintaining reliable electricity supply, which is crucial for the functioning of modern cities and societies.

Additionally, widespread deployment of ground-mounted solar systems raises concerns about land-use changes. Clearing large, forested areas and altering terrain can disrupt natural ecosystems, potentially contradicting the environmental benefits of solar energy as a clean energy source. These challenges could lead to increased costs, hinder further PV deployment, or both [13].

Two main concerns of the duck curve are overgeneration and the steep ramp towards the later hours of the day. To make the steep ramp closer to flat, first, the solar power generation needs to shift more toward the later hours of the day, as it will provide more flexibility for the utilities to ramp up their power generation gradually and second, reducing the peak hours electricity consumption.

Although battery energy storage systems (BESS) are currently an option, they come with various drawbacks and challenges, primarily revolving around costs, that rule them out in many smaller scale PV systems. Implementing an effective storage system is not only costly in terms of initial investment [14] but also requires ongoing maintenance [15], posing economic challenges that hinder widespread BESS adoption, particularly in small-scale PV applications. As a result, current battery storage solutions struggle to fully bridge the gap between surplus solar generation and peak demand periods. Therefore, the search for environmentally friendly and sustainable alternatives becomes crucial for ensuring the long-term viability of solar PV energy for cities.

Several studies have investigated different PV systems as a solution to mitigate the duck curve. Researchers were investigated implementing vertical bi-facial PV modules as their peak power production is at 9 am and at 4 pm. They concluded that a combination of the vertical bi-facial PVs with ground-mounted mono-facial PV modules can distribute the PVPP throughout the day and flatten the duck curve [16] [17].

U.S. energy information administration (EIA) published a chart that was comparing the energy production of tracking PV panels, with no-tracking 20° tilt angle in different orientations [18]. Solar power generation primarily relies on solar farms or fixed south-facing panels installed on the rooftops. As a result, peak power production occurs around noon. This presents a challenge for traditional utilities, as they must rapidly increase production in the few hours leading up to sunset. However, during the late afternoon, west-facing PV panels outperform south-facing PV systems due to their orientation toward the setting sun. This maximizes energy capture during the final hours of daylight which will be particularly advantageous for grid operators because it aligns with peak demand periods, helping to maintain a balanced electricity supply [18].

Hassan et al. investigated the PVPP and building energy consumption reduction by integrating PV system into facades of the building. Their research revealed that integrating PV panels into the west-facing facade shifted peak power production to later hours in the day [19]. Similarly, testing the irradiance levels on the vertical PV surface in south and south-west orientation showed that south-west orientation shift the maximum irradiance levels in the afternoon hours between 3 pm to 7 pm [20].

Addressing the duck curve can yield significant economic benefits for cities and societies. For most utilities, the marginal costs of electricity fluctuate across various time dimensions, including minutes, hours, days, months, and seasons. As electricity demand rises, higher-cost power plants are often activated to meet the increased demand. Additionally, the variable nature of certain renewable generation technologies can also contribute to fluctuations in power costs [21]. The price of electricity curve closely follows the shape of the duck curve [22]. These price hikes particularly occur during warm weather and on weekdays, with the super-peak period being 4:00 p.m. to 9:00 p.m. on July and August weekdays [23].

The small-scale solar capacity, including BIPVs, in the U.S. expanded significantly from 7.3 GW in 2014 to 39.5 GW in 2022, representing a substantial growth. Small-scale solar installations now constitute approximately one-third of the total solar capacity across the United States [24]. This ascending trend signifies a growing path for solar energy, particularly in the form of BIPV systems.

As of 2018, there were approximately 5.9 million commercial buildings in the U.S. [25], accounting for 18% of the total energy usage in 2022 [26]. While integrating PV panels onto building roofs is a common approach to offset grid electricity consumption, this practice, along with solar farms, contributes to the grid fluctuation challenges. Nonetheless, the rooftop of high-rise buildings do not have enough area to install the PV panels that can offset the electricity consumption of the entire building [27].

Commercial buildings are the second-largest consumers of electricity in the United States [26]. Given their substantial energy demands, these buildings present a significant opportunity to address the challenges posed by the duck curve phenomenon. The strategic integration of PV systems into commercial building envelopes not only helps mitigate the steep ramp challenges of the duck curve but also supplies clean solar energy to meet this sector's electricity demands. Therefore, this study aims to address the need for small-scale PV systems that can be seamlessly integrated into buildings and alleviate the steep ramp of the duck curve by investigating the following hypothesis: integrating PV panels into the west facades of commercial buildings provides utilities with a buffer to gradually ramp up their production in the later hours of the day.

Previous research has explored the performance of south façade PV-louvers and PV-mounted roof systems in generating electricity and reducing building electricity loads across all ASHRAE climate zones [28]. This study focuses specifically on PV-west facades and PV-mounted

roofs in supplying the building's afternoon peak demand and mitigating the duck curve's steep ramp. By examining the effectiveness of these facades in addressing late afternoon energy demands, this research aims to provide new insights into optimizing solar energy integration and enhancing grid stability.

With growing need to supply the building sector with solar energy and the challenges associated with grid integration, exploring innovative solutions like west-facing PV systems offers a promising avenue for a more sustainable and efficient energy future in cities and societies. Substantial literature review found no research investigating the efficacy of PV-integrated west facades in alleviating the steep ramp of the duck curve, which highlights the gap that this study aims to address. The novelty of this research lies in investigating the optimum BIPV system that not only provides on-site clean energy for the buildings, but also help mitigate the challenges associated with high solar penetration into the grid.

2. Methodology

This section outlines the study's workflow, detailing the data, tools, and assumptions used throughout the research. The software and tools were used to conduct the simulation were Ladybug (LB version 1.7.0) [29], Honeybee (HB), Grasshopper (GH) and Rhino (version 7). LB plug-in utilizes the Energyplus engine [30] and HB employs the OpenStudio [31], using EnergyPlus (version 23.2.0) Weather (EPW) data [32], they simulate irradiance levels on the PV surface and the building energy consumption. Rhino and GH served as user-friendly interfaces for setting up simulations and visualizing data [33]. Analysis period in all of the simulation workflows were set to four months of March, July, September and December. A total of 31536 simulations conducted to examine the impact of the PV-integrated west facade on the duck curve in 17 U.S. locations

across all ASHRAE climate zones [34] (Table 4.1). The following sections explain each steps' workflow in detail.

2.1. Solar radiation on west oriented PV: In the northern hemisphere, the sun rises in the east in the morning, reaches its highest point in the south around midday, and sets in the west in the afternoon. Consequently, locations with a westward orientation receive the most direct sunlight during the later hours of the day. To determine the optimal angle for maximizing power production during these later hours, it is essential to assess the levels of irradiance in west-facing orientations. To this end, sun radiations in different azimuth angles of the west orientation in four months of March, June, September and December across all ASHRAE climate zones were studied. Using LB, the amount of solar energy received by a vertical surface facing each of the directions of the compass azimuth angles was calculated (Figure 4.2). This preliminary study evaluated the amount of solar radiation rows (SRR_{mon}) reaching the surfaces facing campus azimuth angles at 10° intervals.

Table 4.1 List of the locations, their corresponding climate type and zone.

City, State	**Climate type**	**Sub climate type**	**Climate zone**
Miami, FL	Very hot	Humid	1A
Houston, TX	Hot	Humid	2A
Phoenix, AZ		Dry	2B
Austin, TX	Warm	Humid	3A
Charlotte, NC		Humid	3A
Los Angeles, CA		Dry	3B
San Francisco, CA		Marine	3C
Washington DC	Mixed	Humid	4A
Albuquerque, NM		Dry	4B
Seattle, WA		Marine	4C
Boston, MA	Cool	Humid	5A
Denver, CO		Dry	5B

Minneapolis, MN	Cold	Humid	6A
Billings, MT		Very cold	6B
Fargo, ND	Very Cold	Subarctic	7A
Gunnison, CO		Polar	7B
Fairbanks, AK	Arctic	Subarctic	8

The steep rise in electricity demand during peak hours, coupled with insufficient PVPP, contributes steep ramp of the duck curve. Depending on factors such as the specific climate zone and the energy demands of the building, different azimuth angles may have varying effects on the severity of the duck curve's steep ramp. To comprehensively understand which angle will contribute to mitigating the steep ramp of the duck curve, it is necessary to consider building energy consumption patterns as well. Therefore, this study also conducted calculations to assess building energy consumption in relation to different climate zones.

2.2. Geometry: To conduct the PVPP and building energy consumption simulations, a single room model was created in Rhino with dimensions measured 10 m x 10 m x 4 m in length, depth, and height, respectively (Figure 4.3). Each typology included a south-facing window with a window-to-wall ratio (WWR) of 80%. Six PV panels, with dimensions of 1m x 4m (depth x height), were installed on the west façade, providing a total PV area of 24m^2. To isolate the impact of PV-west facades on mitigating the duck curve's steep ramp, we assumed the PV-west façade to be installed on the opaque west-facing façade. To maintain consistency in system size across all typologies, the roof typology's PV panels were considered to have a length of 4m and a width of 1m.

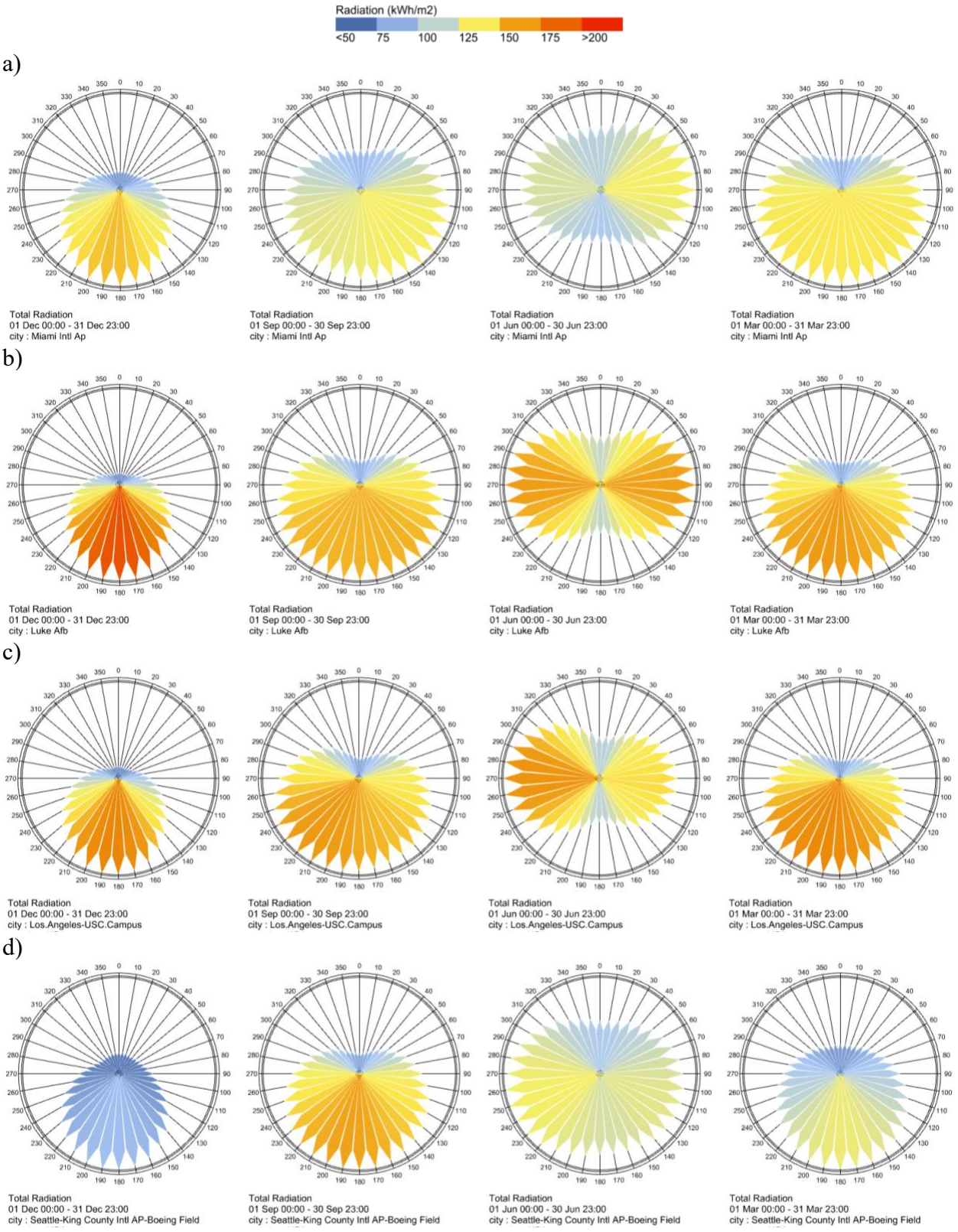
Radiation (kWh/m2)
<50 75 100 125 150 175 >200
a)
Total Radiation
01 Dec 00:00 - 31 Dec 23:00
city : Miami Intl Ap
Total Radiation
01 Sep 00:00 - 30 Sep 23:00
city : Miami Intl Ap
Total Radiation
01 Jun 00:00 - 30 Jun 23:00
city : Miami Intl Ap
Total Radiation
01 Mar 00:00 - 31 Mar 23:00
city : Miami Intl Ap
b)
Total Radiation
01 Dec 00:00 - 31 Dec 23:00
city : Luke Afb
Total Radiation
01 Sep 00:00 - 30 Sep 23:00
city : Luke Afb
Total Radiation
01 Jun 00:00 - 30 Jun 23:00
city : Luke Afb
Total Radiation
01 Mar 00:00 - 31 Mar 23:00
city : Luke Afb
c)
Total Radiation
01 Dec 00:00 - 31 Dec 23:00
city : Los.Angeles-USC.Campus
Total Radiation
01 Sep 00:00 - 30 Sep 23:00
city : Los.Angeles-USC.Campus
Total Radiation
01 Jun 00:00 - 30 Jun 23:00
city : Los.Angeles-USC.Campus
Total Radiation
01 Mar 00:00 - 31 Mar 23:00
city : Los.Angeles-USC.Campus
d)
Total Radiation
01 Dec 00:00 - 31 Dec 23:00
city : Seattle-King County Intl AP-Boeing Field
Total Radiation
01 Sep 00:00 - 30 Sep 23:00
city : Seattle-King County Intl AP-Boeing Field
Total Radiation
01 Jun 00:00 - 30 Jun 23:00
city : Seattle-King County Intl AP-Boeing Field
Total Radiation
01 Mar 00:00 - 31 Mar 23:00
city : Seattle-King County Intl AP-Boeing Field

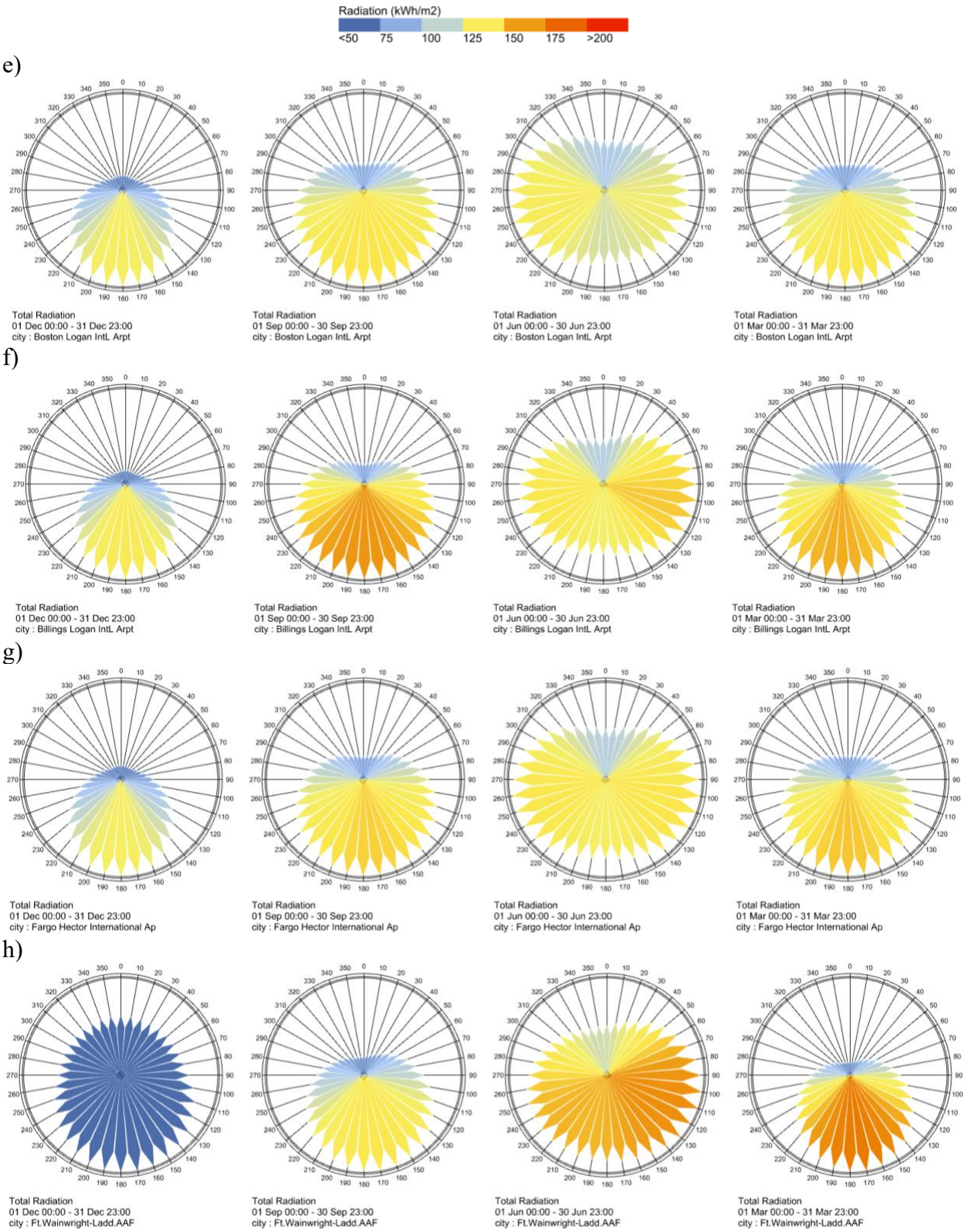

Figure 4.2 SSR on the different orientations at 10° intervals.

To conduct the PVPP and building energy consumption simulations, a single room model was created in Rhino with dimensions measured 10 m x 10 m x 4 m in length, depth, and height, respectively (Figure 4.3). Each typology included a south-facing window with a window-to-wall ratio (WWR) of 80%. Six PV panels, with dimensions of 1m x 4m (depth x height), were installed on the west façade, providing a total PV area of 24m^2. To isolate the impact of PV-west facades on mitigating the duck curve's steep ramp, we assumed the PV-west façade to be installed on the opaque west-facing façade. To maintain consistency in system size across all typologies, the roof typology's PV panels were considered to have a length of 4m and a width of 1m.

2.3. PVPP: The PVPP workflow comprised three parts. In the first part, the LB plug-in utilized the EnergyPlus code and EnergyPlus Weather (EPW) data to define sky matrix attributes based on the analysis period and location. The second part involved calculating the irradiance levels on the PV surface. This calculation was performed for both typologies of PV-mounted roof and PV-west facade in different azimuth angles. The Cumulative Sky Matrix component was used in this step to create a matrix of both direct normal radiation and diffuse horizontal radiation values from each path of the sky dome.

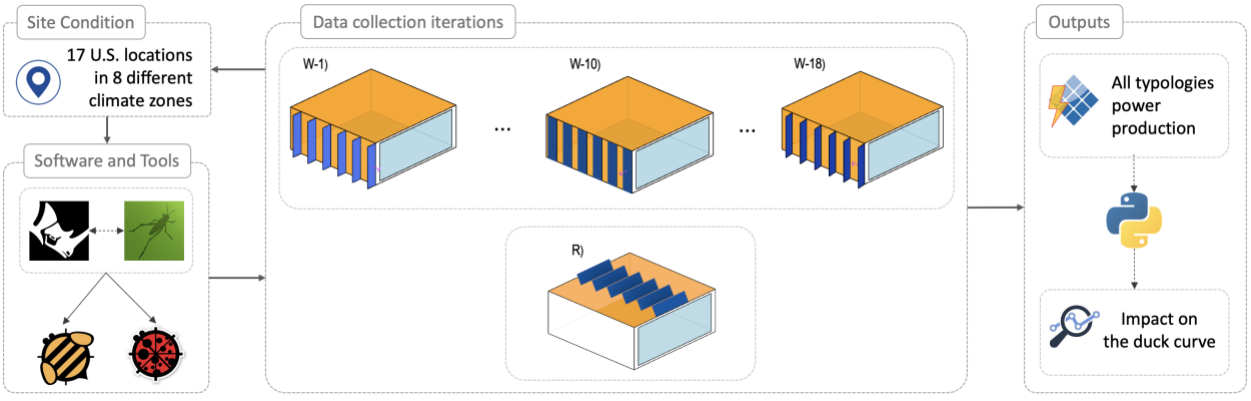

Figure 4.3 Data collection and analysis workflow of simulated typologies.

Based on the findings from the initial sun ray study conducted in section 3-1, the PV-west facade was categorized into 18 typologies. These typologies varied in their PV azimuth angles (δ), ranging from 180° to 350° (Figure 4.4). As illustrated in Figure 4.4, the arrow on the PV-west indicates the PV surface normal vector, which points in the direction of the azimuth angles. The tilt angle of the roof-mounted PVs was determined using the formula in Equation 1 from Jacobson et al.'s research [35].

$$1.3793 + \alpha \times \left(1.2011 + \alpha \times (-0.014404 + \alpha \times (0.000080509))\right) \quad (1)$$

where α is the latitude of the location.

In the third part, the potential power production of the typologies was calculated using Equation 2. Mono Crystalline Silicon (c-Si) PV cells were chosen as the PV material in all typologies. While in laboratory conditions, c-Si PVs have an efficiency range of 25%-27%, their real-world efficiency varies from 16% to 22% [36]. In this study, the efficiency, η_{PV} was considered to be 19%, which was the median of the real-world c-Si PV efficiency range. For the LF factor, accounting for losses due to soiling, shading, snow, mismatch, wiring, connectors, light-induced degradation, nameplate rating, age, and availability, a value of 14.08% was used [37]. The η_{inv} factor established by the NREL, was considered to be 96% [37].

$$P = E \times \eta_{PV} \times (1 - \mathrm{LF}) \times \eta_{inv} \quad (2)$$

Where

P is potential power production,

E is irradiance on PV surface,

η_{PV} is PV panels efficiency,

LF is loss factor

η_{inv} is nominal rated DC-to-AC conversion efficiency of the inverter

2.4. Building Energy Consumption: Building energy consumption simulations in our study consisted of energy use for heating (E_H), cooling (E_C), hot water (E_{HW}), lighting (E_L), and electrical equipment (E_E). Hourly building energy consumption were simulated using HB.

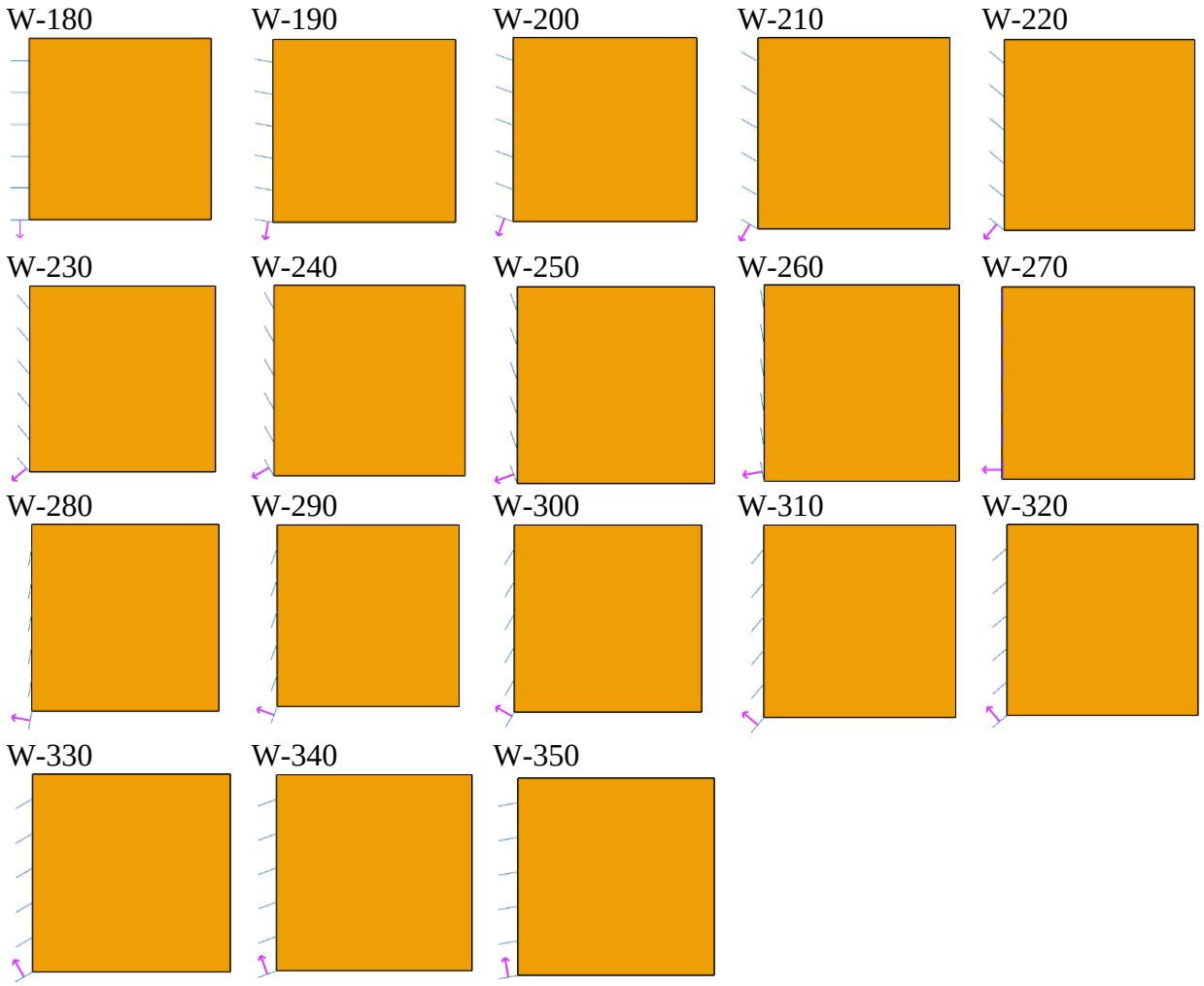

Figure 4.4 Plan view of the PV-west typologies azimuth angle.

In addition to EPW data, this step of the analysis workflow conducted considering building program, climate zone and occupancy schedules. Glazing attributes such as the U Value (W/m^2K) and solar heat gain coefficient (SHGC) were set according to ASRHAE 90.1 requirements. Occupancy schedules were set according to the office setting operation where weekdays start from

6 am and ramp up until fully occupied by 9am and at 3 pm start decreasing until it reached to vacancy at 7 pm. All the opaque walls as well as ground and roof surfaces were set to be adiabatic. building heating and cooling temperature set points were inputted as 15°C and 24°C in the simulations. The analysis model was validated before each simulation iteration using the HB Validate Model component to check all extension attributes for Energy and Radiance, ensuring correct simulation in these engines.

2.5. Impact on duck curve steep ramp: The workflow comprised three primary steps: First, the net energy use for both PV-west facade and PV-mounted roof typologies was calculated. Second, a mathematical equation was used to score and assess each point on the typologies' monthly net energy use curve to understand their impact on the existing curve's steep ramp. Third, weighted average of each typologies performance was calculated to define the optimum angle for the fixed PV-west façade system. In the first step, the PVPP subtracted from the electricity demand for each time interval (t) (Equation 3). This yielded the net load ($P(t)_{net}$) curve, indicating the additional electricity required from conventional power sources to meet remaining demand after accounting for PVs power generation.

$$P(t)_{net} = E_H + E_C + E_{HW} + E_L + E_E - PVPP(\theta) \quad (3)$$

In the second step, a mathematical equation was devised to precisely evaluate the net energy use curve of various system typologies and measure their impact on mitigating the existing duck curve steep ramp. To this end, it is crucial for the power generated from solar panels to offset or exceed the building's electricity consumption during afternoon hours. This reduces the reliance on electricity from power plants, thereby alleviating the magnitude of the utilities' power

generation ramp up. Ideally, any surplus power generated by the PV system can be fed back into the grid to supply surplus power to buildings in need. This strategy acts as a buffer, allowing utilities to gradually adjust their power production to meet the building's electricity demand. To evaluate the effectiveness of different typologies in achieving this goal, a weighting system was implemented. Weights are determined by normalizing the PVPP values for each typology at each hour of the day by the maximum PVPP observed in that typology (Equation 4). This ensures that all values are on a similar scale and contribute proportionally to the analysis. The resulting normalized hourly PVPP values were organized as tuples, with each tuple corresponding to a specific installation angle.

$$\omega_t = \frac{PVPP\ (\theta)}{PVPP_{max}^{(\theta)}} \tag{4}$$

Where

ω is normalized weight of PVPP in each hour,

PVPP is potential power production,

θ is PV panels' installation angle, which is equal to azimuth angle (δ) in PV-west façade typologies and varies from 180° to 350° in different PV-west typologies. θ for PV-mounted roof in each location was one angle value and calculated using Equation 1 explained in section 3-2.

Regardless of orientation, all PV systems eventually cease generating power as sunset approaches, ultimately reaching zero power output when the sun sets. Thus, a system that can effectively mitigate the steep ramp of the existing duck curve will be one that slowly decreases power production near sunset. This criterion ensures that while the PV system is generating power during later hours of the day, its net energy use will not cause a problem similar to the existing

duck curve's steep ramp. In the typologies' net energy use curve, this can be evaluated by the slope of the curve in the later hours of the day. The smoother the slope of the curve, the more favorable and manageable it becomes for utilities to meet demand requirements efficiently, meaning $\frac{1}{dy/dx}$ which is dx/dy. By summing the multiplication of the weight of each point to the slop of the line between each point on the net energy use curve, a thorough assessment is obtained. However, only points corresponding to later hours of the day are relevant to the duck curve's steep rise. Therefore, values associated with earlier hours need to be filtered out. Since the net energy use curve typically has a positive slope in the later hours, the most effective way to filter is to exclude negative $^{dx}/_{dy}$ values, denoted as $\omega_t \times {}^{dx}/_{dy}\ 1_{\frac{dx}{dy}>0}$.

Another criterion for evaluating the net energy use curve of typologies is the minimum point on the curve. As the position on the x-axis approaches higher numbers, it indicates that the PV system generated more power during later hours of the day, making it more effective in mitigating the steep ramp of the existing duck curve. Considering that the steep ramp of the existing duck curve typically starts around 4 pm, typologies that provide maximum surplus prior to that time will not effectively impact the mitigation of the steep ramp. Thus, by focusing only on net energy use curves that their minimum point happens on 4 pm or after, we isolate the relevant data and concentrate on how each typology's power output impacts the existing duck curve steep ramp in four months of March, June, September and December. Finally, the mathematical equation to score each typologies monthly performance ($f(x, \delta)_{mon}$) is defined as follows.

$$f(x,\delta)_{mon} = (t_{max} - 15)_+ \sum_{x_i} \left(\omega_t \times {}^{dx}/_{dy}\ 1_{\frac{dx}{dy}>0} \right). \quad (7)$$

the decision variables are:

t_{max} the time on the x axis where the surplus is maximum

d_x/d_y the slope of the curve at each hour on the x axis

Next, the impact of each typology on the duck curve steep ramp were evaluated by Equation 8.

$$ArgeMax_{\delta} \quad f(x,\delta)_{mon} \tag{8}$$

Considering that commercial buildings' electricity demand is primarily supplied by electric heat pumps during winter months, while summer sees a surge in air conditioning demand, becoming the primary driver of electricity consumption [38]. In addition to that, the challenges associated with the duck curve phenomenon are most pronounced during warmer months [39]. Therefore, selecting a PV-west typology that performs optimally during the warm seasons and consistently throughout the year is crucial. To achieve this, a weighted average method was employed (see Equation 9). The weights were define based on the amount of SRR_{mon} reaching to the PV modules oriented toward each specific azimuth angle.

$$f(x,\delta)_{yr} = \tag{9}$$

$$\frac{f(x,\delta)_{Mar} \times SRR_{Mar} + f(x,\delta)_{Jul} \times SRR_{Jul} + f(x,\delta)_{Sep} \times SRR_{Sep} + f(x,\delta)_{Dec} \times SRR_{Dec}}{SRR_{Mar} + SRR_{Jul} + SRR_{Sep} + SRR_{Dec}}$$

Equation 10 determines the angle that performs optimally throughout the year.

$$ArgeMax_{\delta} \quad f(x,\delta)_{yr} \tag{10}$$

3. Results

This study focused on assessing the impact of the PV-mounted roofs and PV-integrated west façade typologies with 18 varying azimuth angles across 17 different locations spanning all ASHRAE climate zones. PV-west façade typologies featured PV modules oriented toward various azimuth angles. Simulations were conducted for PVPP and building energy consumption over four

months: March, June, September, and December. Additionally, SRR reaching vertical planes facing different west azimuth angles was analyzed.

A mathematical equation was formulated and applied to evaluate the effectiveness of each typology in mitigating the steep ramp of the duck curve during the above-mentioned months. Next, a weighted average was utilized to identify the best performing tilted angle with the highest potential to mitigate the duck curve's steep ramp throughout the entire year for a fixed BIPV system.

The analysis of SRR patterns revealed interesting trends. In March, most locations received the most SRR at an angle of 180°. However, Los Angeles (CA) and Fairbanks (AK) deviated slightly, with peak SRR occurring around 190° and 170°, respectively. In June, the distribution of maximum SRR angles varied significantly across locations. In Miami (FL), east-facing panels received the highest SRR, followed closely by west-facing ones. Phoenix (AZ) had significant SRR levels for both east and west orientations. Los Angeles (CA), Seattle (WA), and Boston (MA) recorded maximum SRR in the west direction. Billings (MT) and Fairbanks (AK) observed the highest SRR in the east and southeast directions. Notably, Fargo (ND) exhibited relatively uniform SRR across all orientations except for north.

September showed a shift in SRR patterns. Simulations revealed that Miami (FL) and Phoenix (AZ) receiving the highest SRR in the southeast and south directions, respectively. Los Angeles observed peak SRR in the south and southwest directions. Similarly, Seattle (WA), Boston (MA), Billings (MT) experienced maximum SRR in the south direction, while Fairbanks (AK) saw it in the south and southeast directions. Finally, in December, a consistent pattern emerged across all locations. Miami (FL), Phoenix (AZ), Los Angeles (CA), Seattle (WA), Boston (MA), and Billings (MT) consistently recorded maximum SRR at an angle of 180°.

While SRR studies provide valuable insights into sunlight radiation intensity across various azimuth angles, understanding the building energy use behavior is crucial for addressing the steep ramp of the duck curve. Hence, this paper delved into a thorough examination of hourly energy consumption across all ASHRAE climate zones. The goal was to identify BIPV typologies, including PV-west façade and PV-mounted roof systems, that effectively mitigate the steep ramp of the duck curve.

Following simulations of PVPP and building energy consumption, net energy use data was computed. Figure 4.5 illustrates the simulated net energy use of building integrated PV-west façade in San Francisco (CA). To enhance readability and provide clearer visualization of data trends, the charts for other locations were limited to display the net energy use of PV-west façades at 180°, 220°, and 270° angles in March, September, December and 220°, 270°, and 300° angles in June. In addition, the net energy use of roof typologies was visualized alongside these angles for the same four months (figure 4.5).

Figures 4.6 to 4.9 display the results of scoring for each PV-west façade and PV-mounted roof in mitigating the steep ramp of the duck curve. While PV-mounted Roof typologies scored zero in all four months, while most PV-west façade configurations showed notable scores, except for the 350° PV-west typology, which scored zero. Similarly, in December, the 320°, 330°, and 340° PV-west typologies also scored zero. Overall, lower scores were observed during the colder months compared to the warmer months.

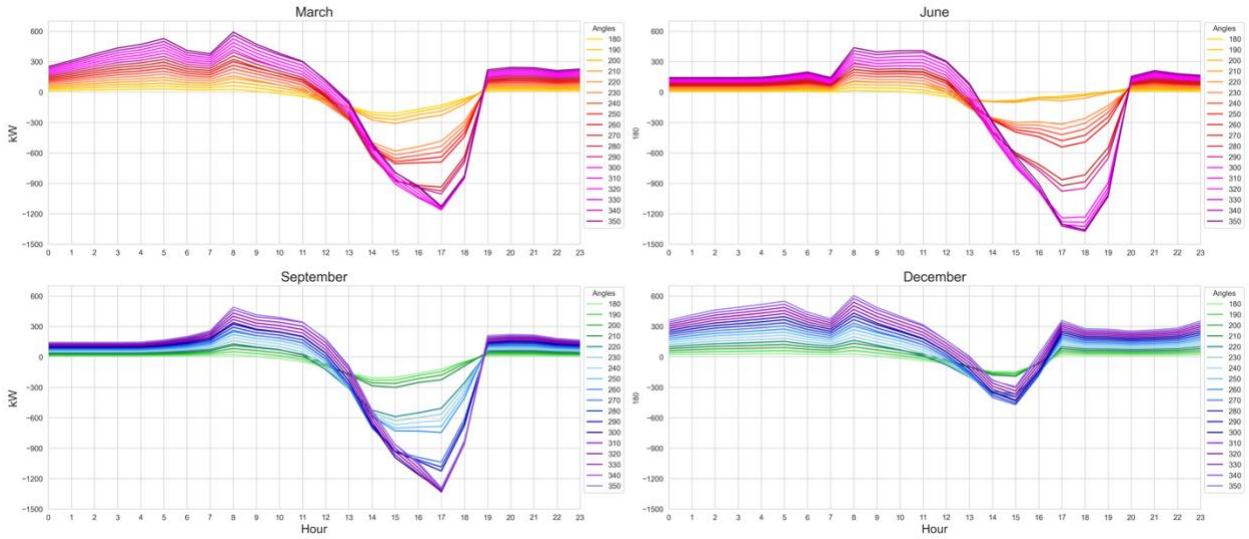

Figure 4.5 Net energy use of building integrated PV-west façade in San Francisco (CA).

Table 4.2 depicts the results of scoring for each PV-west façade and PV-mounted roof in mitigating the steep ramp of the duck curve for a fixed system throughout a year. Figures 4.6 to 4.9 display the results of scoring for all the typologies in mitigating the steep ramp of the duck curve during the four months of analysis period. All four months of simulations resulted in zero scores for the PV-mounted roof typologies. This is primarily because the peak PVPP of those typologies (t_{max}) occurred before 4 pm. As a result, in the $(f(x, \delta)_{mon})$ calculations $t_{max} - 15$ resulted in zero for all iterations.

On the other hand, most PV-west façade configurations showed notable scores, except for the 350° PV-west typology, which scored zero. Similarly, in December, the 320°, 330°, and 340° PV-west typologies also scored zero. Overall, lower scores were observed during the colder months compared to the warmer months.

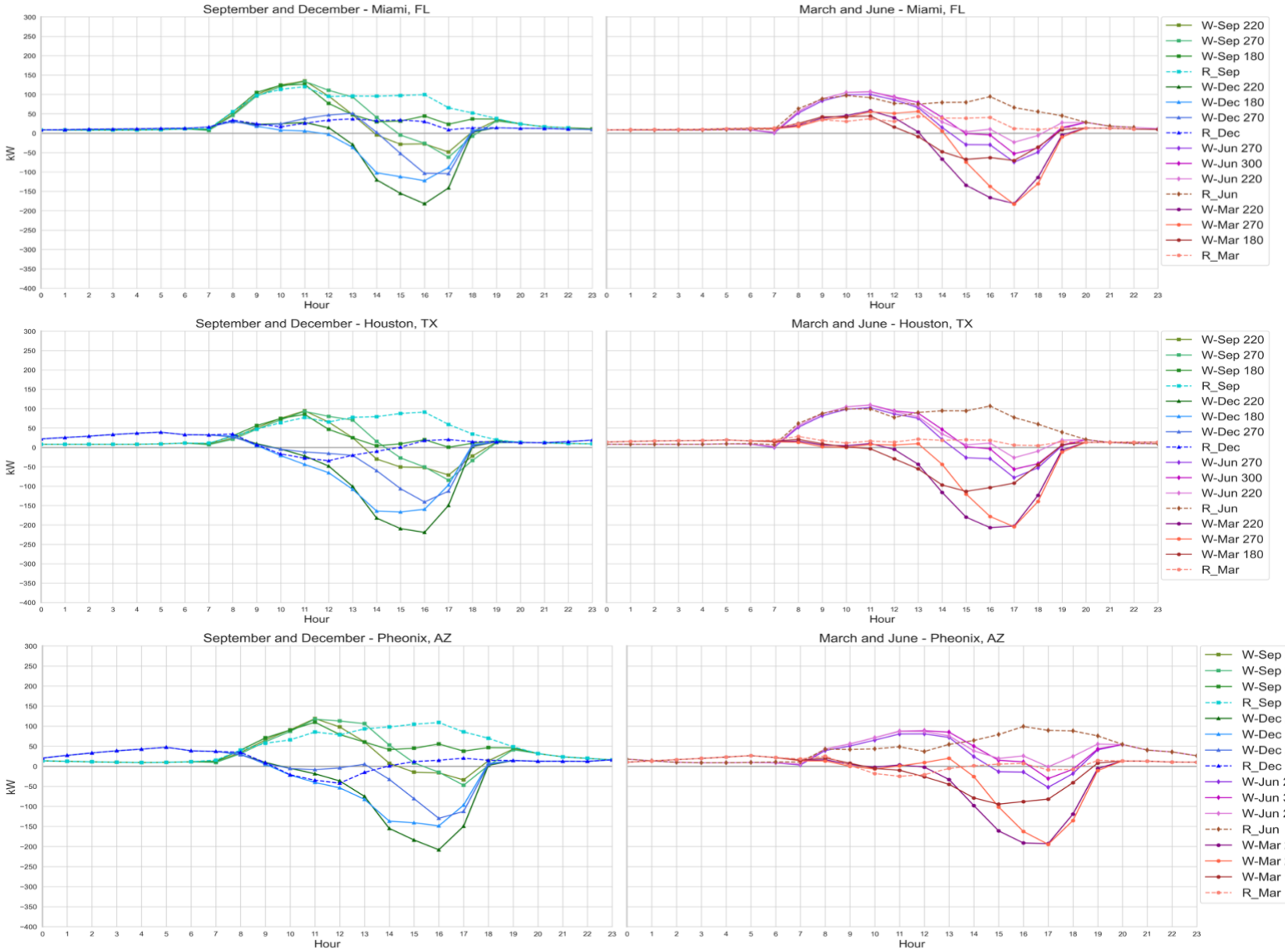
September and December - Miami, FL
March and June - Miami, FL
September and December - Houston, TX
March and June - Houston, TX
September and December - Pheonix, AZ
March and June - Pheonix, AZ
kW
Hour
W-Sep 220
W-Sep 270
W-Sep 180
R_Sep
W-Dec 220
W-Dec 180
W-Dec 270
R_Dec
W-Jun 270
W-Jun 300
W-Jun 220
R_Jun
W-Mar 220
W-Mar 270
W-Mar 180
R_Mar

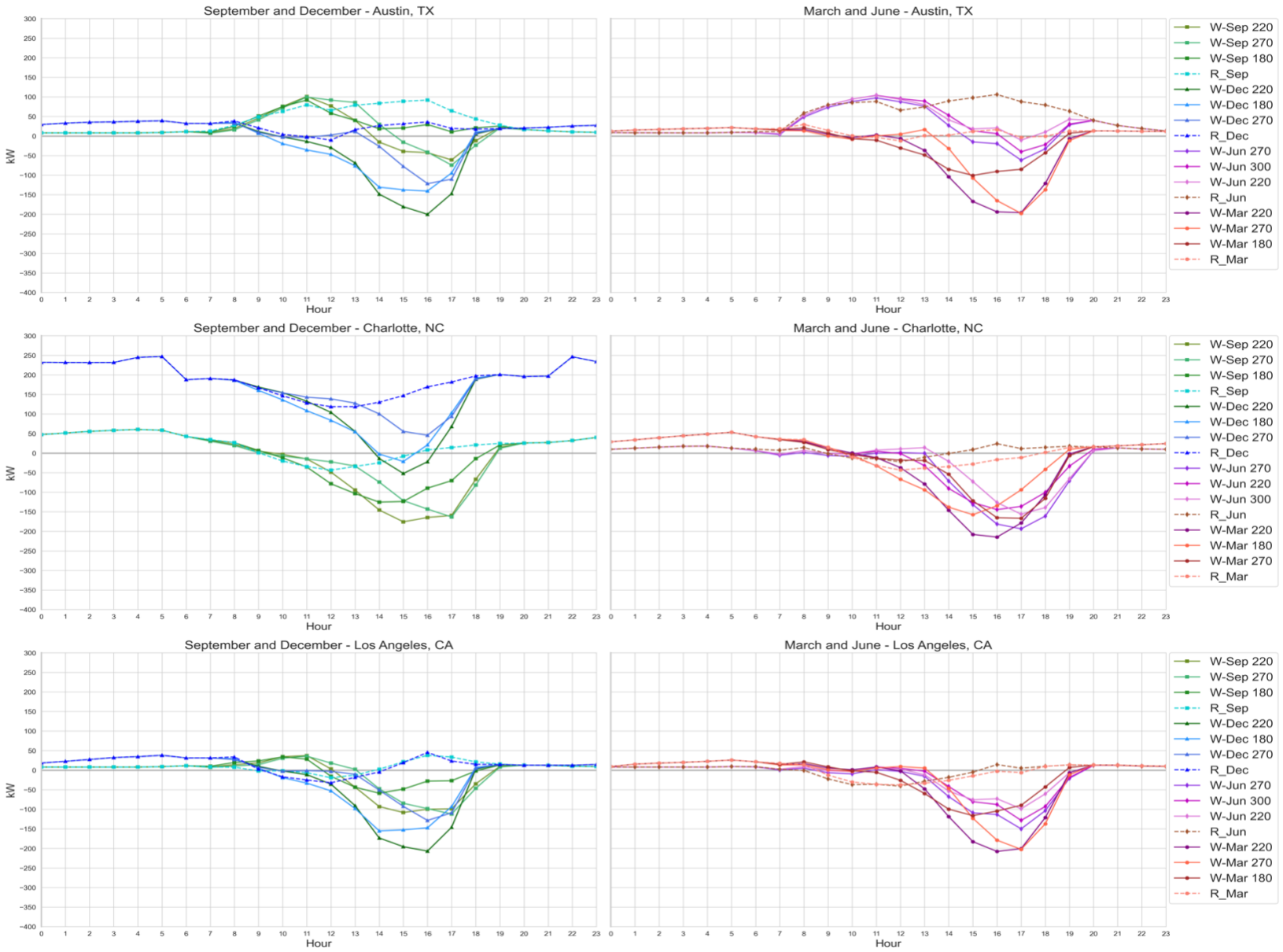
September and December - Austin, TX
March and June - Austin, TX
September and December - Charlotte, NC
March and June - Charlotte, NC
September and December - Los Angeles, CA
March and June - Los Angeles, CA
kW
Hour
W-Sep 220
W-Sep 270
W-Sep 180
R_Sep
W-Dec 220
W-Dec 180
W-Dec 270
R_Dec
W-Jun 270
W-Jun 300
W-Jun 220
R_Jun
W-Mar 220
W-Mar 270
W-Mar 180
R_Mar

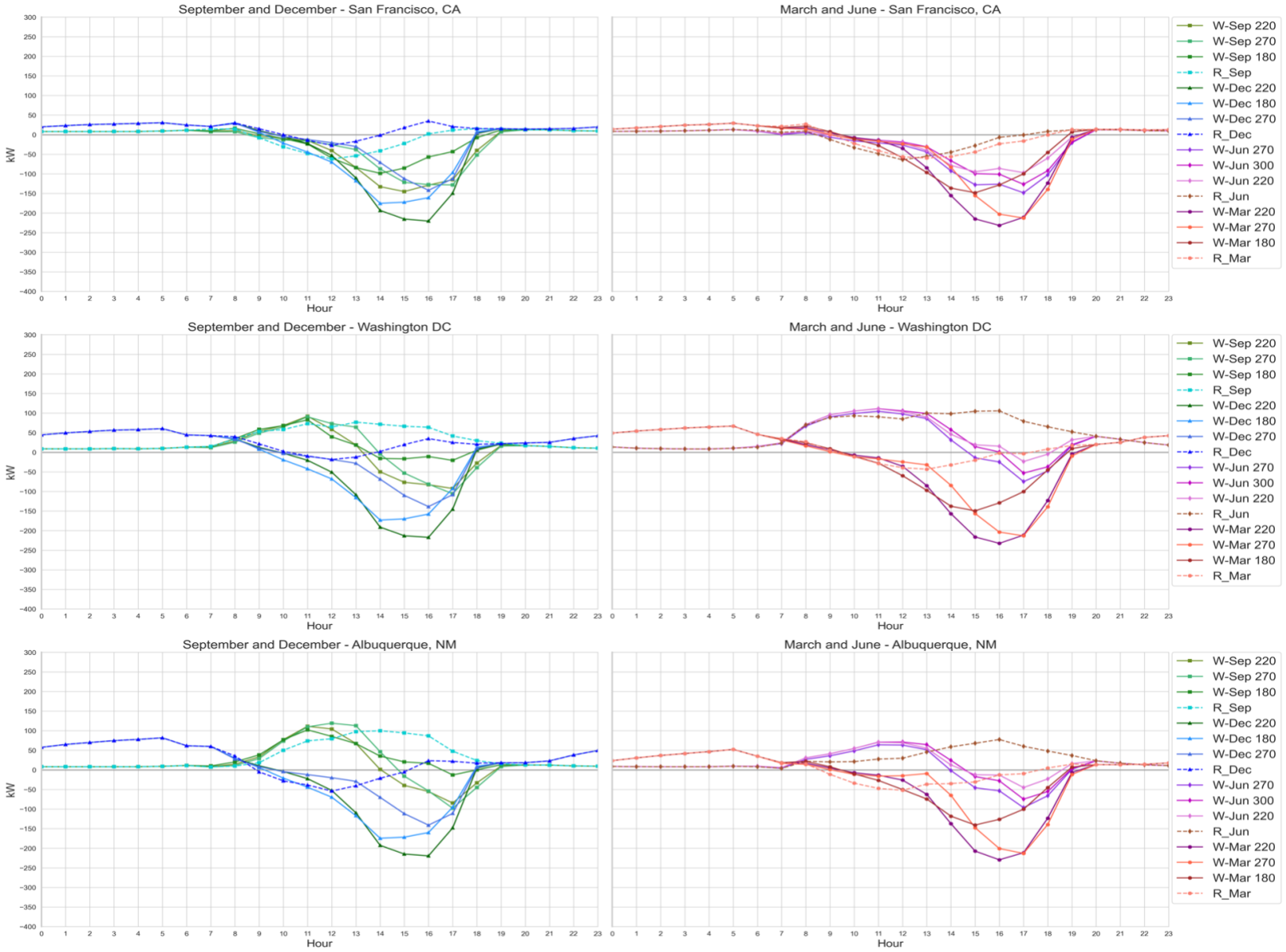
September and December - San Francisco, CA
March and June - San Francisco, CA
September and December - Washington DC
March and June - Washington DC
September and December - Albuquerque, NM
March and June - Albuquerque, NM
kW
Hour
W-Sep 220
W-Sep 270
W-Sep 180
R_Sep
W-Dec 220
W-Dec 180
W-Dec 270
R_Dec
W-Jun 270
W-Jun 300
W-Jun 220
R_Jun
W-Mar 220
W-Mar 270
W-Mar 180
R_Mar

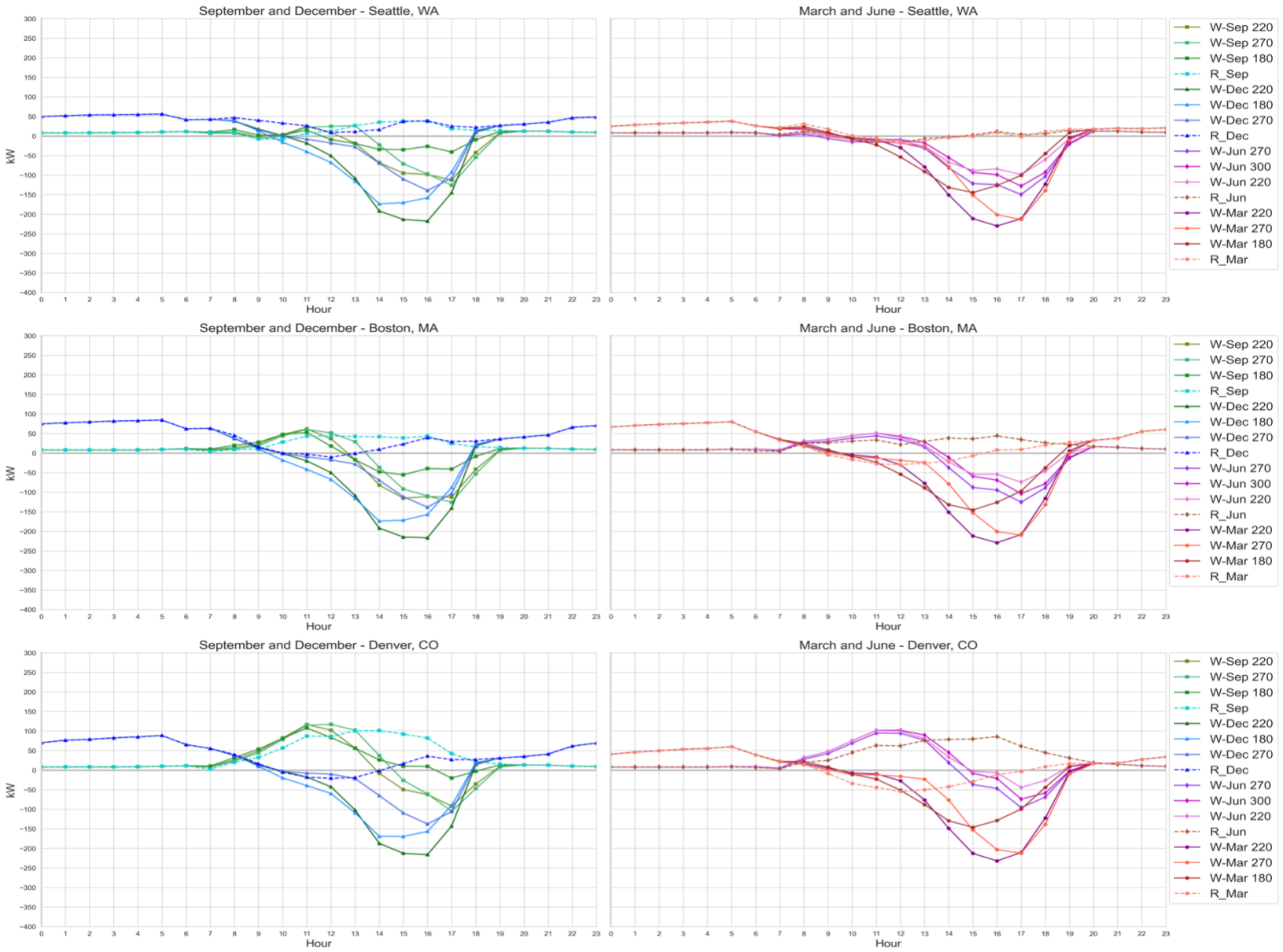
September and December - Seattle, WA
March and June - Seattle, WA
September and December - Boston, MA
March and June - Boston, MA
September and December - Denver, CO
March and June - Denver, CO
kW
Hour
W-Sep 220
W-Sep 270
W-Sep 180
R_Sep
W-Dec 220
W-Dec 180
W-Dec 270
R_Dec
W-Jun 270
W-Jun 300
W-Jun 220
R_Jun
W-Mar 220
W-Mar 270
W-Mar 180
R_Mar

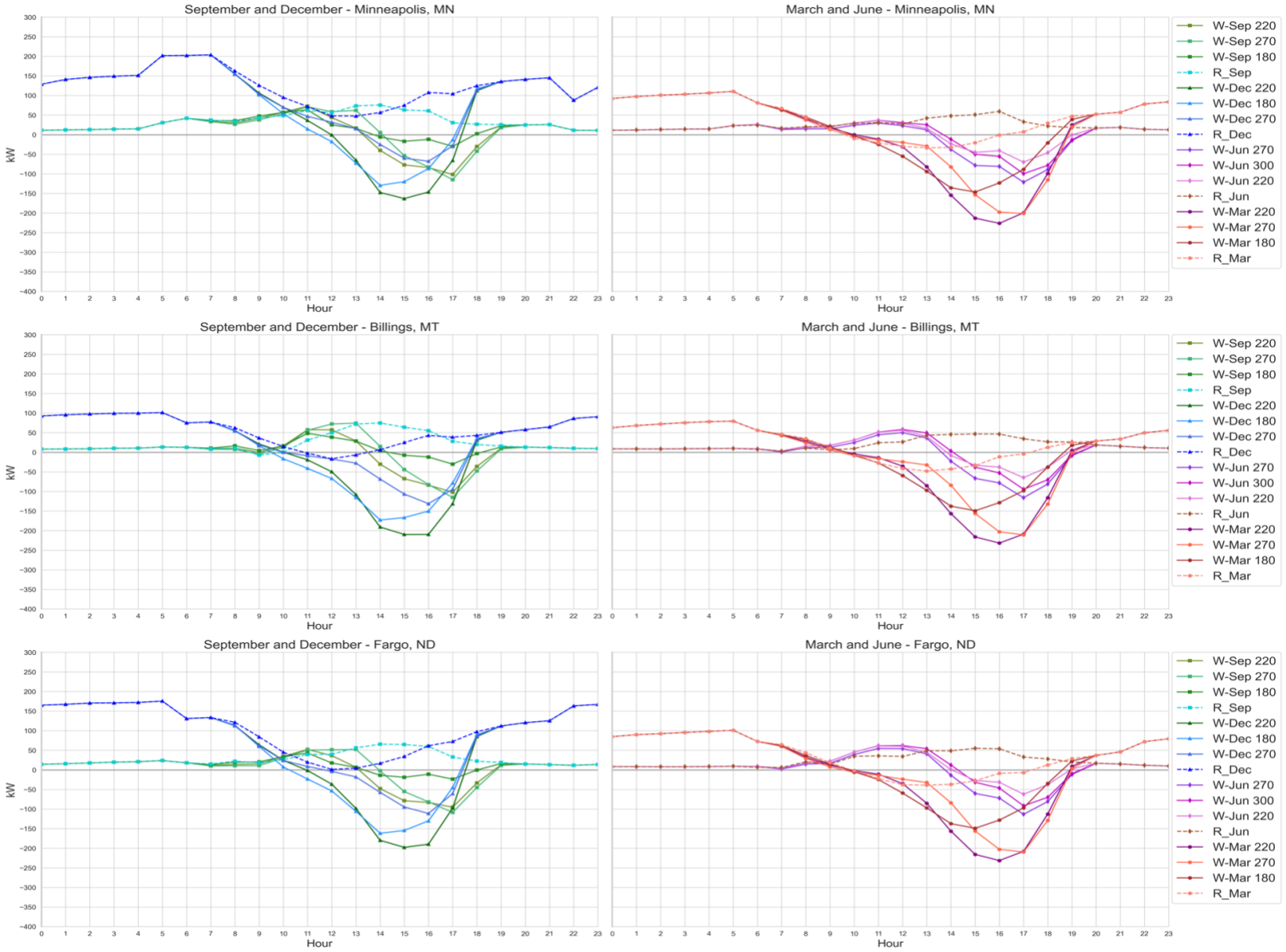
September and December - Minneapolis, MN
March and June - Minneapolis, MN
September and December - Billings, MT
March and June - Billings, MT
September and December - Fargo, ND
March and June - Fargo, ND
kW
Hour
W-Sep 220
W-Sep 270
W-Sep 180
R_Sep
W-Dec 220
W-Dec 180
W-Dec 270
R_Dec
W-Jun 270
W-Jun 300
W-Jun 220
R_Jun
W-Mar 220
W-Mar 270
W-Mar 180
R_Mar

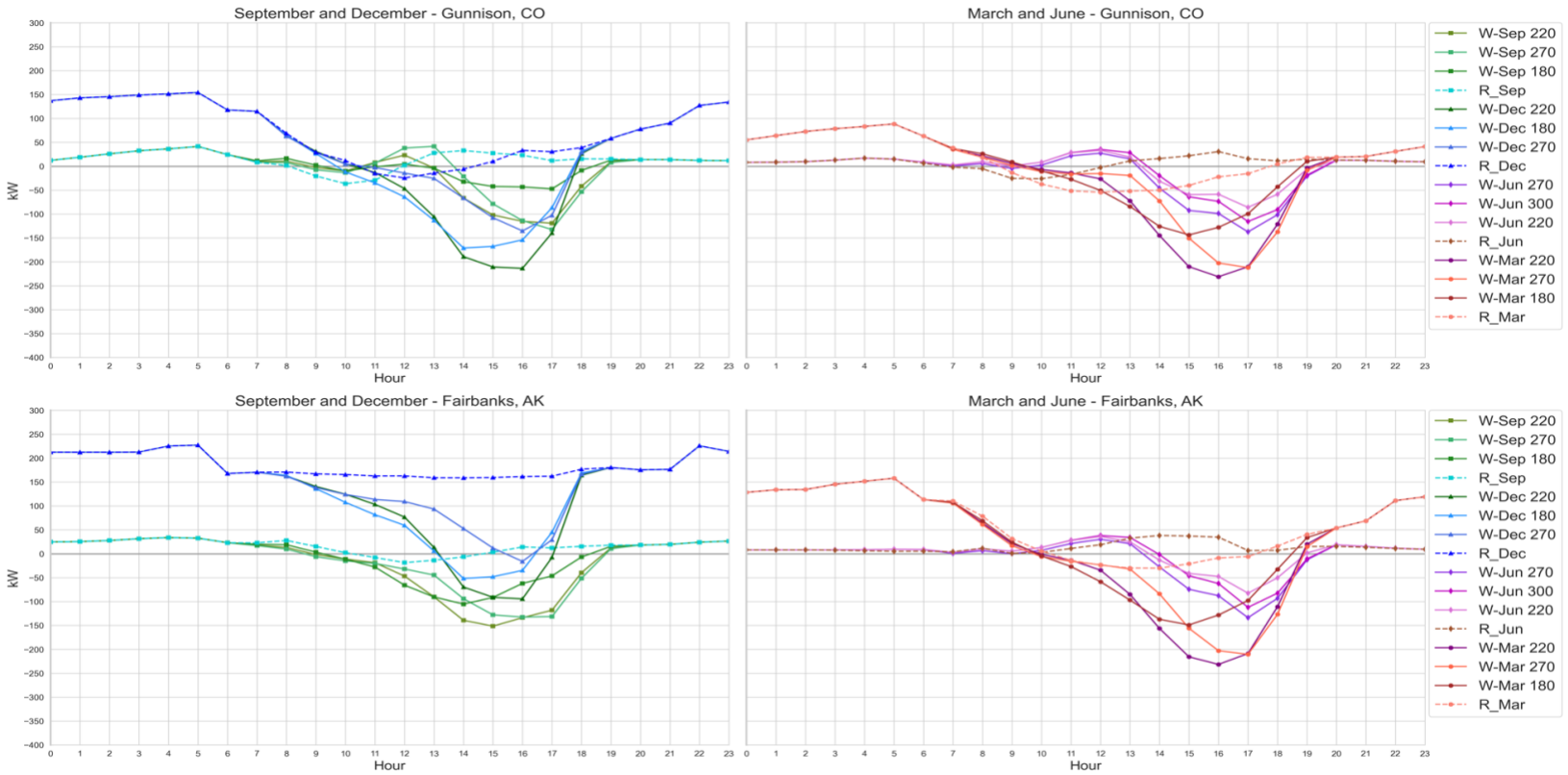

Figure 4.6 Net energy use of the PV-mounted roof and selected PV-west façade typologies in 4 months

Table 4.2 PV-west typologies' scores in mitigating the steep ramp of the duck curve for a fixed system throughout a year.

Azimuth angle / City, State	**180°**	**190°**	**200°**	**210°**	**220°**	**230°**	**240°**	**250°**	**260°**	**270°**	**280°**	**290°**	**300°**	**310°**	**320°**	**330°**	**340°**	**350°**
Miami, FL	0.7	2.8	2.9	5.4	5.2	3.3	3.0	1.7	1.5	2.0	1.4	6.1	2.3	4.7	4.9	1.7	1.3	0.0
Houston, TX	1.6	10.0	1.4	1.8	2.6	19.6	3.6	5.4	6.4	7.0	5.1	6.6	4.0	8.6	4.9	3.4	3.7	0.0
Phoenix, AZ	2.1	14.0	2.1	2.3	0.7	32.2	7.3	4.9	4.8	1.2	2.6	4.0	5.5	4.2	2.6	3.4	5.1	0.0
Austin, TX	1.7	7.7	6.4	4.0	0.9	12.1	7.0	7.5	6.1	4.3	9.7	6.1	3.0	5.7	12.0	10.3	6.7	0.0
Charlotte, NC	0.4	4.1	2.9	13.6	1.4	3.9	1.8	10.4	4.0	1.1	2.4	15.3	1.3	14.6	15.7	5.2	4.2	0.0
Los Angeles, CA	0.1	12.2	7.3	4.9	2.0	1.2	9.2	5.9	3.9	1.7	3.5	3.1	3.0	14.7	2.2	2.8	4.2	0.0
San Francisco, CA	0.3	3.5	12.1	24.4	0.9	2.4	2.5	2.6	2.7	0.5	6.5	14.8	5.0	35.5	21.7	20.2	102.4	0.0
Washington DC	0.0	1.9	1.7	2.5	3.9	3.9	7.4	5.7	6.3	0.7	11.8	9.3	2.0	7.6	30.1	21.1	2.2	0.0
Albuquerque, NM	0.1	2.4	4.2	11.1	2.9	4.0	2.6	3.8	3.5	1.2	10.3	7.8	1.8	15.5	7.3	11.6	2.8	0.0
Seattle, WA	1.8	4.9	5.2	13.6	0.9	9.2	2.8	3.6	3.0	3.3	10.5	11.5	4.7	29.0	4.5	4.7	1.5	0.0
Boston, MA	0.0	0.0	0.1	0.9	3.7	31.4	32.9	33.5	13.0	1.3	22.9	26.4	1.5	27.5	18.2	10.8	5.0	0.0
Denver, CO	0.0	0.0	3.2	27.6	0.5	7.0	1.9	2.6	11.9	2.4	6.7	6.4	4.3	7.9	7.2	10.4	1.2	0.0
Minneapolis, MN	12.0	3.4	4.4	6.7	1.8	3.5	4.9	2.3	2.5	2.8	3.5	4.0	2.0	27.9	24.0	6.7	50.7	0.0
Billings, MT	0.1	6.3	37.4	9.0	1.2	7.6	7.4	9.0	12.6	10.3	15.6	16.6	6.0	7.6	14.3	5.5	2.6	0.0
Fargo, ND	0.3	3.3	5.8	12.0	3.7	5.0	5.7	2.0	2.0	2.7	3.8	6.1	3.9	7.4	10.8	8.5	8.3	0.0
Gunnison, CO	0.1	1.6	30.3	3.1	4.2	4.1	5.0	8.6	10.8	2.1	7.9	2.9	9.9	8.2	2.4	29.8	3.4	0.0
Fairbanks, AK	5.0	7.2	7.4	16.0	34.4	8.1	4.1	5.3	22.7	2.2	44.3	11.1	16.1	34.7	51.4	15.6	16.6	0.0

These scores not only identify the most effective typology for each month but also quantify their efficacy in mitigating the duck curve steep ramp, providing valuable insights for energy planning and management. For instance, in June, the 210° PV-west façade typology in Fargo (ND) achieved a score of 36, while the 340° typology scored 18.6 in the same location and month. Thus, the 210° typology exhibits approximately twice the effectiveness of the 340° typology.

The results of the scores in some of the PV-west façade typologies exceeded 120. This primarily stemmed from the calculation of the equation's derivative. In certain cases, the rate of change of the net energy use (y) with respect to hours (x) was minimal, signifying negligible change in the net energy use curve between consecutive hours. Dividing by this small value resulted in a large number. Consequently, when multiplied by the weighting factors (ω_t) and time factor (t_{max}), the final scores surpassed 120.

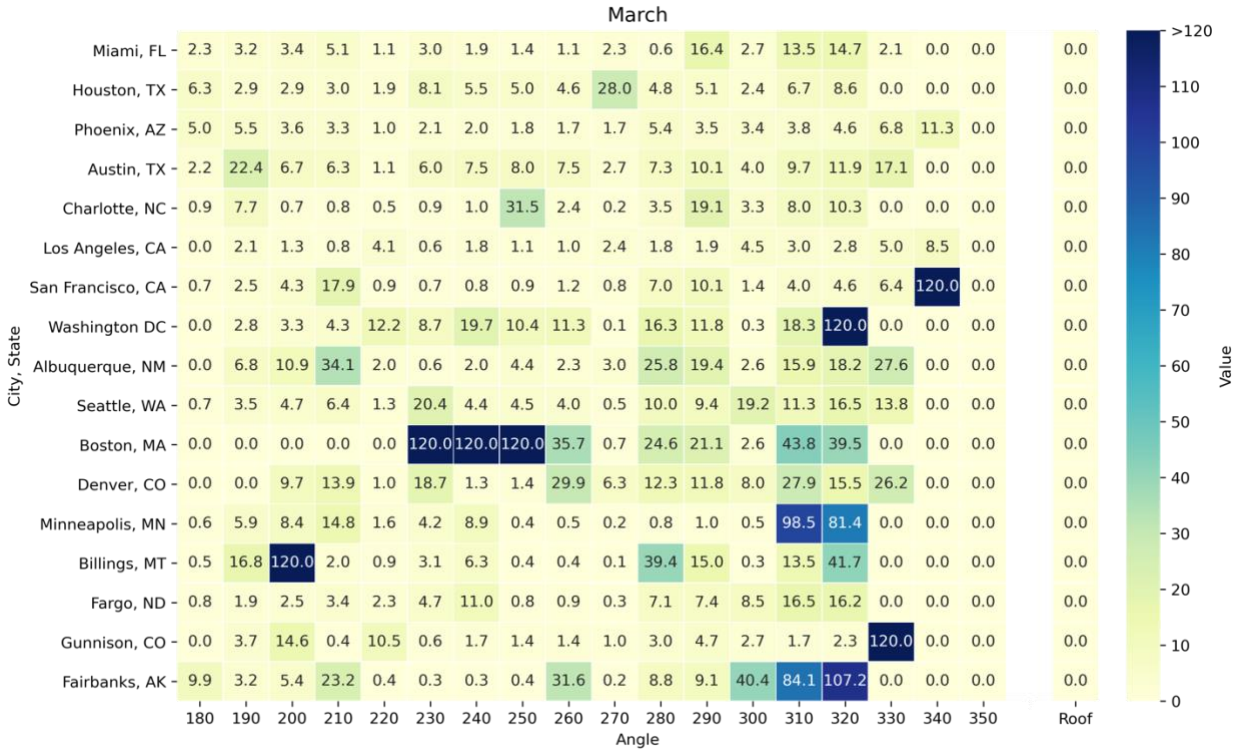

Figure 4.7 PV-west and PV-mounted roof typologies' score in March.

These high scores indicate that the corresponding PV-west typology effectively mitigated the duck curve steep ramp. However, such values significantly exceed scores for other typologies, hindering meaningful comparisons of performance across different typologies or months. Therefore, we opted to limit the scores by replacing exceptionally high values with 120. This threshold value is sufficiently high to represent highly effective scenarios while remaining low enough to prevent skewing the scoring system or hindering subsequent mathematical analysis.

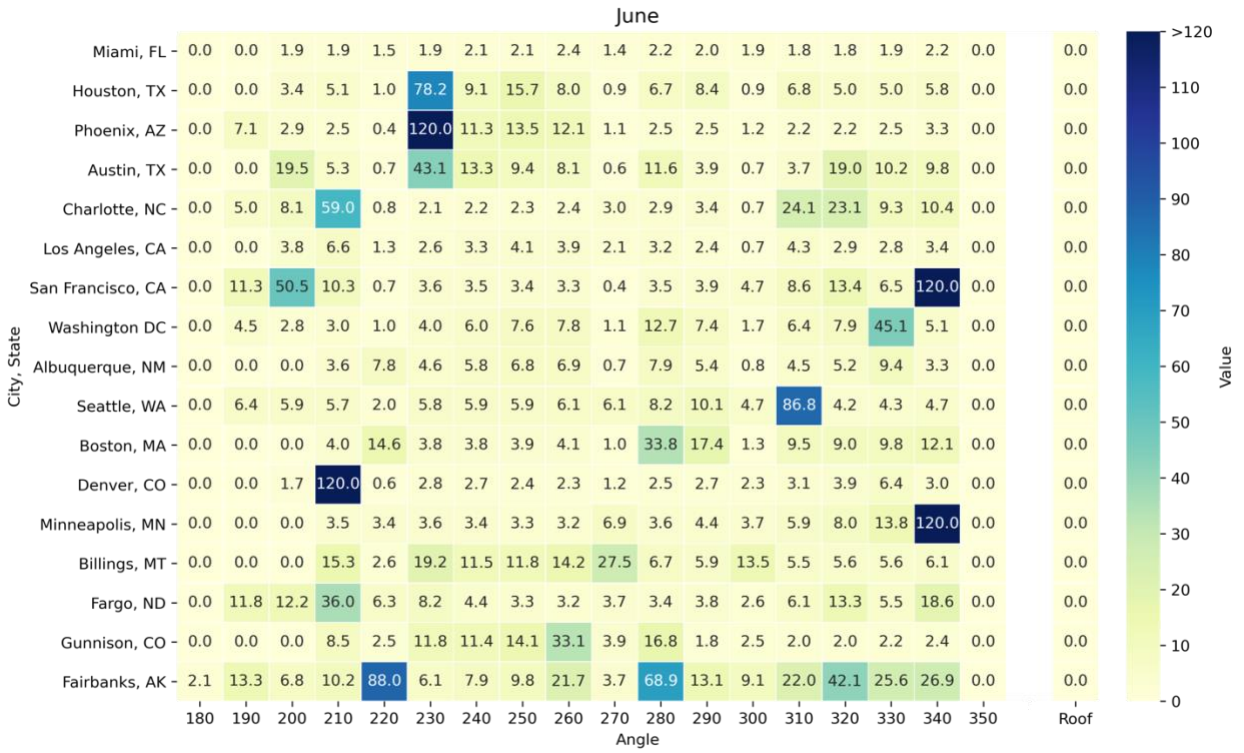

Figure 4.8 PV-west and PV-mounted roof typologies' score in June.

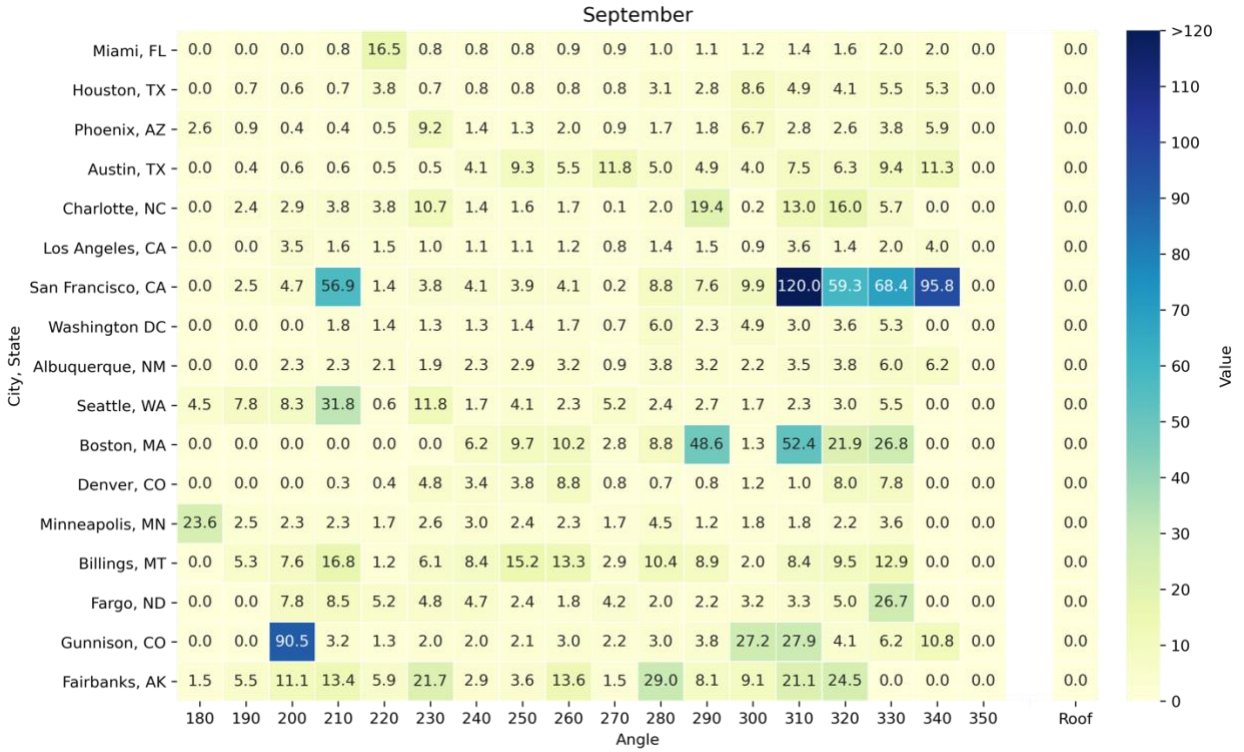

Figure 4.9 PV-west and PV-mounted roof typologies' score in September.

4. Conclusion and discussion

Transitioning to renewable energy sources is a cornerstone of sustainability efforts, as it reduces reliance on fossil fuels and mitigates the environmental impact of energy generation. By addressing the duck curve and optimizing the integration of renewable energy into the grid, cities and societies can accelerate their transition towards a low-carbon future, thereby mitigating climate change and preserving natural resources for future generations.

This study aimed to conduct a comprehensive evaluation of the impact of BIPV systems, such as PV-west façade and PV-mounted roof, on alleviating the steep ramp of the duck curve. Building net energy use was simulated and calculated for 18 PV-west façade and PV-mounted roof typologies across 17 U.S. locations in all ASHRAE climate zones. The findings of this study have

led to the following conclusions regarding the effectiveness of the PV-west façade in alleviating the steep ramp of the duck curve in each ASHRAE climate zone:

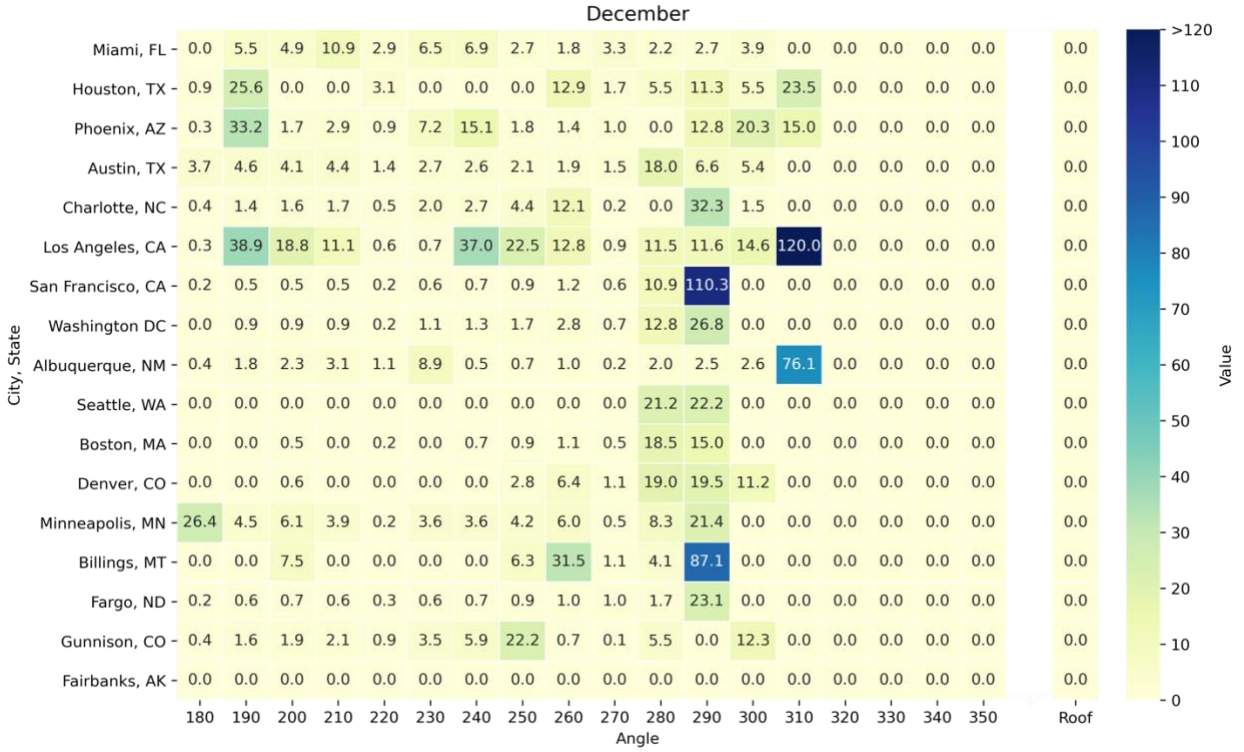

Figure 4.10 PV-west and PV-mounted roof typologies' score in December.

4.1 Very hot and hot climates: These zones receive high solar irradiance and potentially have significant cooling loads. While PV-west facades could be particularly effective to offset the building energy demands, the results for zone 1 suggest limited benefits in mitigating the duck curve steep ramp as the scores ranged between 0 to 17 across all months. For climate zone 2, the overall impact of west-oriented PV-west facade typologies on mitigating the steep ramp of the duck curve varied depending on the time of the year, as they obtained higher scores in June.

4.2. Warm, mixed and cool climates: The effectiveness of PV-west facades significantly depended on sub climate specifics. higher scores observed in June and December in climate zone

3 and March in climate zone 4. However, Zone 5 showed relatively high scores across all months, suggesting significant potential for mitigating the duck curve in these temperate regions.

4.3. Cold, very cold and Arctic climates: The effectiveness of PV-west facades was higher during warmer months compared to colder months. In Zone 6, higher scores were observed in March. Scores for Zone 7 suggest more prominent results for PV-west facades in sub-climate zone B. Zone 8 highlights the potential benefits during warmer months.

Monthly scores helped quantify the effectiveness of each PV-west typology in alleviating the steep ramp of the duck curve for months of March, June, September and December. Since the outperforming typology varied by month, a kinetic BIPV system could potentially maximize benefits by adjusting its west-facing angle quarterly based on the top-performing typology for each month. Nevertheless, weighted average of all PV-west angles based on the SRR in corresponding azimuth orientation resulted in identifying one PV-west typology that outperforms throughout the year for a fixed BIPV system. It becomes evident that certain angles consistently yield high scores across different locations and months, indicating their robustness in mitigating the duck curve. For example, angles such as 280°, 310°, and 320° frequently receive high scores across several locations, proving PV-west facade efficacy in managing energy fluctuations and contributing to a smoother energy consumption profile. Conversely, some angles including 350°, 180° and 270° exhibit lower scores, indicating their limited impact on mitigating the steep ramp. By identifying these high-scoring angles, policymakers and energy planners can make informed decisions regarding the optimal orientation of PV-west facades to better manage electricity demand and promote grid stability.

While the findings of this study demonstrated that the PV-west façade offers advantages for power plants in balancing high levels of electricity demand during late hours of the day, it is

noteworthy that building owners and consumers may not derive direct benefits unless they are enrolled in time-of-day electrical rate programs. This is particularly relevant for smaller-scale and residential buildings. However, it's important to acknowledge that residential buildings were outside the scope of this paper.

5. limitations

A limitation of this study is the unavailability of precise real-world data regarding the timing of peak electricity demand for the commercial building sector or office buildings. This data is critical for accurately assessing the potential impact of integrating PV panels on the west façade to alleviate the duck curve's steep ramp in the afternoon hours. However, to address this limitation, we utilized detailed simulations replicating realistic building operation conditions. These simulations were designed to capture potential trends and identify real-world implications as accurately as possible. The findings from these simulations provide valuable insights, and future studies that can incorporate real-world data as it becomes available will further strengthen these conclusions.

6. Acknowledgement

This study was funded by the U.S. National Science Foundation (NSF). Award number: 2122014.

7. References

1. Akubude, V., K. Nwaigwe, and E. Dintwa, *Production of biodiesel from microalgae via nanocatalyzed transesterification process: A review.* Materials Science for Energy Technologies, 2019. **2**(2): p. 216-225.
2. Olczak, P., et al., *Analyses of duck curve phenomena potential in polish PV prosumer households' installations.* Energy Reports, 2021. **7**: p. 4609-4622.
3. Richard Bowers, E.F., Katherine Antonio. *As solar capacity grows, duck curves are getting deeper in California*. 2023 [cited 2024; Available from: https://www.eia.gov/todayinenergy/detail.php?id=56880.
4. ISO-NE. *Solar Power in New England: Concentration and Impact*. 2018 [cited 2022; Available from: https://www.iso-ne.com/about/what-we-do/in-depth/solar-power-in-new-england-locations-and-impact.
5. AEMO, *AEMO observations: Operational and market challenges to reliability and security in the NEM*. 2018.
6. Balasubramanian, K. *Germany's duck curve – Integrating renewables into smart grids*. 2023 [cited 2024; Available from: https://www.gridx.ai/blog/germanys-duck-curve-integrating-renewables-into-smart-grids.
7. Lefteris Karagiannopoulos. *To meet its 2050 net-zero target, the US needs to cover land 50 times the size of Austin with solar PV*. 2021 [cited 2022; Available from: https://www.rystadenergy.com/newsevents/news/press-releases/to-meet-its-2050-net-zero-target-the-us-needs-to-cover-land-50-times-the-size-of-austin-with-solar-pv/.
8. NREL, *Solar Future Study*. 2021.
9. Library, S. *DOES WEATHER AFFECT SOLAR ENERGY PRODUCTION?* 2023 [cited 2024; Available from: https://solarliberty.com/blog/how-weather-affects-solar-production/#:~:text=Solar%20panel%20electrons%20move%20as,the%20density%20of%20the%20clouds.
10. Eric O'Shaughnessy, J.C., Kaifeng Xu, *Solar PV Curtailment in Changing Grid and Technological Contexts*. 2019.

11. Nwaigwe, K., P. Mutabilwa, and E. Dintwa, *An overview of solar power (PV systems) integration into electricity grids.* Materials Science for Energy Technologies, 2019. **2**(3): p. 629-633.
12. Sioshansi, F., *California's 'Duck Curve'arrives well ahead of schedule.* The Electricity Journal, 2016. **29**(6): p. 71-72.
13. Palmintier, B., et al., *Emerging Issues and Challenges in Integrating Solar with the Distribution System.* Office of Energy Efficiency & Renewable Energy, Washington DC, 2016.
14. Sheha, M., K. Mohammadi, and K. Powell, *Solving the duck curve in a smart grid environment using a non-cooperative game theory and dynamic pricing profiles.* Energy Conversion and Management, 2020. **220**.
15. Cole, W., A.W. Frazier, and C. Augustine, *Cost projections for utility-scale battery storage: 2021 update*. 2021, National Renewable Energy Lab.(NREL), Golden, CO (United States).
16. Rouholamini, M., L. Chen, and C. Wang, *Modeling, Configuration, and Grid Integration Analysis of Bifacial PV Arrays.* IEEE Transactions on Sustainable Energy, 2021. **12**(2): p. 1242-1255.
17. Shigenobu, R., M. Ito, and H. Taoka, *Optimal design of bifacial PV system to mitigate duck-curve problem of power system with the UC problem.* Energy Reports, 2021. **7**: p. 7004-7014.
18. EIA. *Solar photovoltaic output depends on orientation, tilt, and tracking*. 2014 [cited 2022; Available from: https://www.eia.gov/todayinenergy/detail.php?id=18871.
19. Hassan, M.M., et al., *Energy saving potential of photovoltaic windows: Impact of shading, geography and climate.* Solar Energy, 2022. **240**: p. 342-353.
20. Alrashidi, H., et al., *Thermal performance evaluation and energy saving potential of semi-transparent CdTe in Façade BIPV.* Solar Energy, 2022. **232**: p. 84-91.
21. DOE, *Customer Acceptance, Retention, and Response to Time-Based Rates from the Consumer Behavior Studies*, in *Smart Grid Investment*. 2016.
22. Maticka, M.J., *The SWIS DUCK–Value pricing analysis of commercial scale photovoltaic generation in the South West Interconnected System.* The Electricity Journal, 2019. **32**(6): p. 57-65.

23. Roger E. Collanton, A.I., Anna McKenna, Jordan Pinjuv, *CAISO time-of-use periods analysis*. 2016.
24. Elesia Fasching, K.A. *Record U.S. small-scale solar capacity was added in 2022*. 2023 [cited 2024; Available from: https://www.eia.gov/todayinenergy/detail.php?id=60341#:~:text=Small%2Dscale%20solar%E2%80%94also%20called,capacity%20in%20the%20United%20States.
25. Zack Marohl, J.T., Chrishelle Lawrence. *Commercial buildings have gotten larger in the United States, with implications for energy*. 2020 [cited 2022; Available from: https://www.eia.gov/todayinenergy/detail.php?id=46118#:~:text=CBECS%20estimates%20that%205.9%20million,was%20last%20conducted%20in%202012.
26. Shoemaker, S. *How much energy is consumed in U.S. buildings?* 2023 [cited 2023; Available from: https://www.eia.gov/tools/faqs/faq.php?id=86&t=1.
27. Hossei, H. and K.-H. Kim. *Circuit Connection Reconfiguration of Partially Shaded BIPV Systems, a Solution for Power Loss Reduction*. in *ACSA Annual Meeting In Common*. 2023.
28. Hossei, H. and K.-H. Kim, *Comprehensive analysis of energy and visual performance of building-integrated photovoltaics in various climate zones.* Energy and Buildings, under review.
29. Chris Machey. *LADYBUG TOOLS* 2022; Available from: https://www.food4rhino.com/en/app/ladybug-tools.
30. Energy, U.S.D.o., *EnergyPlus™ Version 22.1.0 Documentation*. Engineering Reference. 2022.
31. NREL, A., LBNL, ORNL, and PNNL. *OpenStudio*. 2023 2024]; Available from: https://openstudio.net/.
32. DOE. *Weather Data*. 2024; Available from: https://energyplus.net/weather.
33. Associates, R.M. *Rhino 8*. 2024 [cited 2024; Available from: https://www.rhino3d.com/.
34. ASHRAE. *ASHRAE Climate Zones*. 2011 [cited 2024; Available from: https://openei.org/wiki/ASHRAE_Climate_Zones.
35. Jacobson, M.Z. and V. Jadhav, *World estimates of PV optimal tilt angles and ratios of sunlight incident upon tilted and tracked PV panels relative to horizontal panels.* Solar Energy, 2018. **169**: p. 55-66.

36. Alami, A.H., et al., *Management of potential challenges of PV technology proliferation.* Sustainable Energy Technologies and Assessments, 2022. **51**: p. 101942.
37. Dobos, A.P., *PVWatts version 5 manual*. 2014, National Renewable Energy Lab.(NREL), Golden, CO (United States).
38. Comstock, O. *U.S. natural gas consumption has both winter and summer peaks*. 2020 [cited 2023; Available from: https://www.eia.gov/todayinenergy/detail.php?id=42815#:~:text=During%20winter%2C%20homes%20and%20businesses,gas%20in%20the%20winter%20months.
39. EIA. *Hourly electricity consumption varies throughout the day and across seasons*. 2020 [cited 2024; Available from: https://www.eia.gov/todayinenergy/detail.php?id=42915.

CHAPTER 5 (PAPER 4)

CIRCUIT CONNECTION RECONFIGURATION OF PARTIALLY SHADED BIPV SYSTEMS, A SOLUTION FOR POWER LOSS REDUCTION

Hamideh Hossei,University of North Carolina at Charlotte

Kyoung Hee Kim,University of North Carolina at Charlotte

Abstract

Integrating PV panels as a source of clean energy has been a widely established method to achieve net-zero energy (NZE) buildings. The exterior envelope of high-rise buildings can serve as the best place to integrate PV panels for utilizing solar energy. The taller the building, the higher the potential to utilize solar energy by PV panels. However, shadows casting on the BIPV façade systems are unavoidable as they are often subject to partial shades from panels self-shading as well as building walls. Partial shading or ununiform solar radiation on the PV surface causes a dramatic decrease in the current output of the circuit. For that reason, in BIPV facades the default circuit connection of manufactured PV panels does not output maximum power under partial shading conditions. This paper investigates the different circuit connections in the BIPV façade system to achieve higher energy yields while addressing design requirements. To this end, PV panel's power production in different circuit connection reconfiguration scenarios was explored both by simulation and experimentation in two levels of building integrated photovoltaics (BIPV) components: 1) PV cells, and 2) strings of PV cells. The results of simulations demonstrated that the maximum power generation occurred when the circuit connection between cells within a string is series, and the circuit connection between the strings within a PV panel is parallel. Comparing

the results of Ladybug (LB) energy simulations with the proposed Grasshopper (GH) analysis recipe showed that the developed GH definition will increase the BIPVs energy simulation by 90%. To validate the simulation results, experimental tests were conducted. The measured power output indicated that the series-parallel circuit connection increased the energy yields of the BIPV facades 71 times in real-world applications compared to the manufactured series-series PV panels.

Keywords: BIPV façade systems, circuit connection reconfiguration, partial shadows, power performance.

1.Introduction

In 2021, the U.S. set a greenhouse gas reduction goal of 40% by 2030 [1] and 80% by 2050[2]. The built environment is the dominant energy consumer in the U.S. using more than 38% of the total energy and 76% of the electricity [3], which accounts for 40% of the total greenhouse gas (GHG) emissions in the country [4]. In 2021, U.S. commercial buildings consumed 17,410 trillion Btu of energy [5]. Therefore, decreasing building energy consumption while generating on-site electricity will be a highly effective solution to reduce GHG emissions. Currently, PV installed on rooftops is the most common approach for generating on-site solar energy *[6]*. However, many buildings will not have sufficient rooftop area that is exposed to sunlight to install PV panels due to the overshadowing of block structures, electrical boxes, elevator bulkheads, etc. (Roberts, Simon 2009). Figure 1 depicts shadows cast on the rooftop of a tall building in the city of Charlotte in the month of February at 9 am, 12 pm, and 3 pm. This example highlights the efficacy of the façade surface to mitigate GHG emissions. With more than 6 million commercial buildings in the U.S. [7], the total area of the exterior envelopes of those buildings has a great potential to integrate solar panels to offset electricity usage of the buildings' energy load demand.

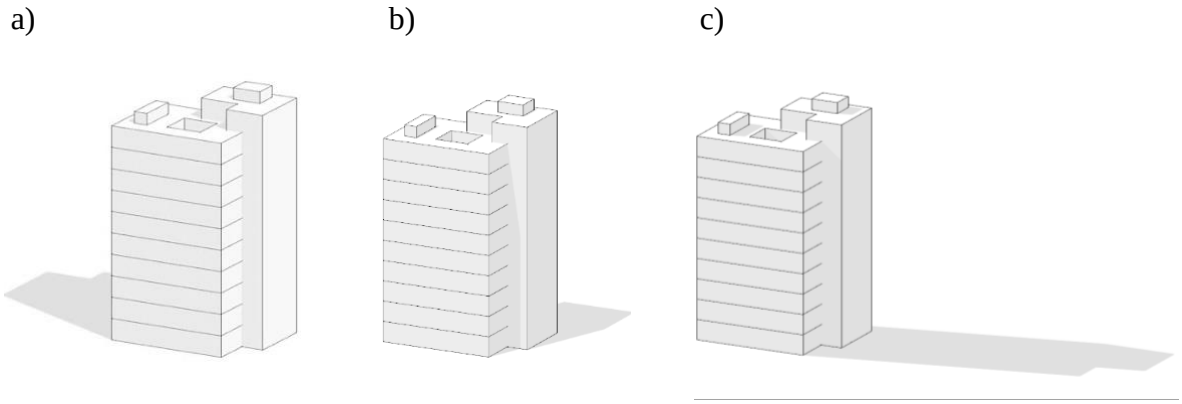

Figure 5.1 Sun path and shadow analysis of a building in Charlotte on August a) 10 am, b) 1 pm, c) 4 pm.

This paper proposed the optimum BIPV façade systems' circuit connection for louvered PV panels that are integrated into the south façade, based on a robust analysis recipe to evaluate irradiance nonuniformity on the PV panel surface. The power output of partially shaded PV panels with different circuit connections between PV cells and strings of PV cells was calculated. The simulation and calculated results were validated by experiment tests. The remaining part of the paper proceeds as follows: Literature review and precedent case study, methodology, experiment, architecture design, results, conclusion and discussion.

2. Literature review

Compared with ground-mounted PV panels, addressing partial shadows in a BIPV façade system is highly difficult. Currently, the tools and methods suggested by researchers to tackle partial shading problems are not applicable to BIPV façade systems as they are designed to be integrated into large-scale PV systems. The reason is that the radiation non-uniformity due to partial shadows in the BIPV façade systems happens on the scale of solar cells, which causes

several limitations that make the BIPV façade systems improper to incorporate those tools or methods.

Ishaque et al. studied maximum power point (MPPT) tracking techniques for PV power systems considering the partial shading conditions [8]. However, in smaller-scale PV systems like BIPV façade systems, partial shading on the PV panel surface causes multiple local maximum power points (LMPP), and integrating traditional MPPT techniques into the system leads to a significant power loss in a BIPV façade system [9].

Another method, proposed by Hasyim et al., is installing several bypass diodes in one PV panel to avoid the current drop in PV cells' electric circuit[10]; however, to this date, it did not meet the solar PV manufacturers' specifications standards due to unavoidable major costs [11]. Apart from high costs, the bypass diodes cannot be applied on the scale of PV cells because of the cells' low output voltage[12]. For the same reason, microinverters are not suitable for BIPV façade systems due to their minimum voltage input threshold of 30 V to 40 V [13]. Many of the BIPV and building applied PV panels (BAPVs) performance studies simulated either the PV systems' power output without considering the adverse effects of the shadows. [14]Researchers studied partial shadows on BIPV performance however they did not propose a solution to effectively address this challenge. A number of studies investigated the effect of partial shadows on ground-mounted solar panels[15].Since there is not a well-developed method to address the partial shadows on the PV panels in BIPV application, the results of real-world application of the same designed system will have a big shift compared with the simulated model. Based on a study conducted by Lee et al., shadows cast on a-Si thin-film solar cells on a south-facing double-glazed window reduced the annual energy performance to 1.52 h/day. However, this performance yield was about 2.15 h/day without considering the shading [16]. Depending on the PV panel surface area, this shift can be

escalated several times in larger-scale projects. Cannavale et al. investigated a BIPV case study in southern Italy. The results indicate that the energy performance was significantly diminished by 50% due to neighboring buildings casting shadows on the façade [17].

Yadav et al. considered the shadow effect of the variables such as width, height, and horizontal distance of the adjacent buildings in the evaluation of the optimum tilt angle, insolation, and performance of the BIPV systems [18]. Bana and Saini investigated different uniform and nonuniform shading scenarios on the energy production of the PV modules in various interconnections. The result of their experimental tests demonstrated that uniform shading on 50% of the PV array decreased the energy yields by 60%. They concluded that while the power outcome reduction can be caused by several shaded modules or shaded areas and the position of the shaded modules in the whole PV array, higher energy yields can be achieved through reconfiguration methods that connect similar shaded areas together [19] [12]. Power output reduction of the PV array that is partially shaded is proportional to the area that receives the least amount of radiation [15].

Since the PV cells in manufactured PV panels are connected in series, an electric current drop of one cell will reduce the current output of the entire panel. Radiation on the PV panels' surface is the main source of current flow, therefore, partial shadows dramatically reduce the electrical current through the entire panel. Roberts and Simon introduced panels self-shading as the main issue of the BIPV façade systems (Roberts, Simon 2009). One solution to tackle this problem is to use a circuit connection between PVs in the BIPV façade components that are customized based on the shadow patterns to connect the PV area that receives similar irradiance, and as a result, prevent power loss [15].

This method also extends the lifetime of the PV system since it reduces the possibility of mismatch losses[20] and prevents unnecessary investment due to errors of system oversizing and downsizing. The Z3 building of Ed. Züblin AG in Stuttgart, Germany is an example of connecting PV cells based on solar intensity and shadow patterns. In the Z3 building, wooden lamellas on the façade surface cast shadows near the edges of PV modules. By dividing each vertical module into three separate zones based on shadow patterns and connecting the vertical divisions in a separate circuit, the negative impact of partial shadows on energy yield is reduced [21].

3. Methodology

3.1 Geometry: A typical office building, with PV panels installed on the south façade, was modeled in Rhino for the simulations' geometry. It is widely accepted that the south-oriented façade's PV panels should install horizontally on the façade surface with a tilting angle equal to the latitude of the site location [22]. Thus, the solar panels also perform as shading louvers while generating electricity during sun hours of the day and year. The geographical location was set to the city of Charlotte in the state of North Carolina, U.S.

3.2. Power output calculation: To define the optimum circuit connection of the BIPV façade system in scenarios where the PV surface receives nonuniform irradiance, the irradiance levels were simulated using GH and other plugins such as LB and ClimateStudio (CS), the PVLightHouse website [23], and Excel (Figure 5.2).

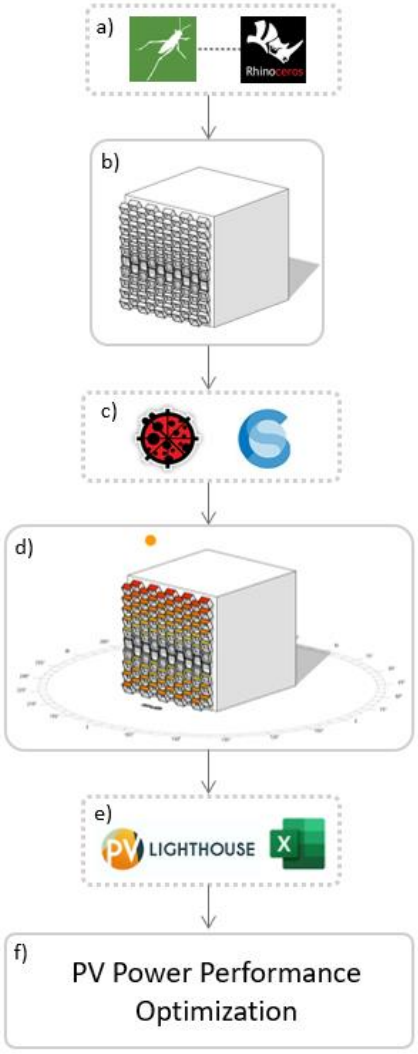

Figure 5.2 Workflow graphics: a) 3D modeling: Rhino and its plugin GH, b) Building geometry: integrating PV panels on the south façade, c) Shadows and solar analysis: Ladybug and ClimateStudio, d) Power output evaluation, e) Maximum electricity output: by calculation.

Setting the grid size of the LB incident radiation component equal to 0.05 m made the solar irradiance analysis grid the same size as each PV cell that was used in the experimental tests. LB outputs the results based on kWh/m^2. Since the PV panel area was 1 m^2, the output units of hourly irradiance simulation on the PV surface will be kW. Therefore, after multiplying the PV cells' efficiency by those values, the output will be panel power generation.

3.3. Calculating Imp and Vmp: It is obvious that the top PV panel of the array in a louvered BIPV façade will always receive the highest amount of solar radiation. Studying the simulated shadow patterns on the PV surface of the louvered PVs–excluding the first panel–installed on the south façade showed that the string of PV cells that is closer to the building exterior surface received less irradiance. However, the strings of the PV cells that are located closer to the exterior edge of the PV panel received a higher irradiance level. Thus, to connect cells that receive the same range of irradiance on their surfaces, the cells in the analysis grid rows should be connected in one circuit and then each row should be connected together. To reduce the time of simulations, a single PV panel located in the middle of the array was selected to simulate the incident radiation and calculate the power output of the cells in different circuit connections. Maximum current power (I_{mp}) and maximum voltage power (V_{mp}) output of a 1 cm^2 PV cell in different irradiance levels were extracted from the PVLighthouse website (PVLightHouse, 2022). Using the PVLighthouse website data, a GH definition was developed to calculate the hourly power output of one partially shaded PV panel based on the I_{mp} and V_{mp} of the irradiance received on each analysis grid cell during the sun hours of the entire year. Different circuit connections include the following: 1) series connection between cells and series connection between strings, 2) series connection between cells and parallel connection between strings, and 3) parallel connection between cells and parallel connection between strings. In this paper, series-series, series-parallel, and parallel-parallel circuit connections refer to the mentioned circuit configurations, respectively.

The GH definition determined the I_{mp} and V_{mp} of the grid cells based on the kW irradiance range that each analysis grid received. Afterward, by having I_{mp} and V_{mp} associated with each cell, the power output (P) of the circuit connections can be calculated using the formulas below.

For parallel connection,

$$P = (I_1 + I_2 + \cdots + I_n) \times V_{min}$$

and for series connection,

$$P = I_{min} \times (V_1 + V_2 + \cdots + V_n)$$

where n is the number of cells in the electrical circuit.

4. Experiment

Experimental tests were conducted to validate the simulation results. To determine the PV cells' efficiencies, I and V of a string consisting of 9 mini monocrystalline PV cells connected in series circuit connections were measured outdoors in 1000 w/m^2 irradiance condition. Comparing the I and V output with the I and V provided in the PV cells data sheet, the calculated efficiency of the cells was 12%. Two panels, each consisting of 36 PV cells, were made by installing the cells on a rectangular acrylic board. In one panel the PV cells were connected in series-series, demonstrating the conventional PV panels that are currently being used in the industry and BIPV construction (Figure 5.3-a). The PV cells in the other panel were connected in a series-parallel electric circuit (Figure 5.3-b). The tilting angle of the panels was 35.22°, which is equal to the latitude of the city of Charlotte. To make the experimental setup similar to the south façade, the panels were located toward the south geographic direction (Figure 5.3-c). While the panel in the front cast shadows on half of the panel in the back, a piece of cardboard was used to cast shadows on the same area of the front PV panel. The distance between PV panels was the same as the simulation's geometry. The irradiance levels on the PV panels' surface were measured using the day star meter sensor. I and V output of the panels were measured by multimeters. All of the measured data were recorded every 15 minutes from 11:30 am to 12:30 pm for five days from

October 5th to October 9th. The irradiance levels during the five days of the experiment were between 210 W/m^2 to 1020 W/m^2. The measured output of the panel with series-series circuit connection, which was representing the industry-manufactured panels, ranged from 7.8 mA to 13.7 mA and 77.8 v to 83.0 v for current and voltage, respectively. However, the PV panel with a series-parallel circuit connection generated 1.07 A to 3.3 A and 19.6 v to 21.5 v of current and voltage, respectively.

a)

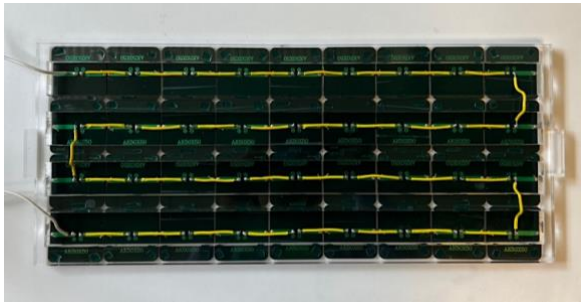

b)

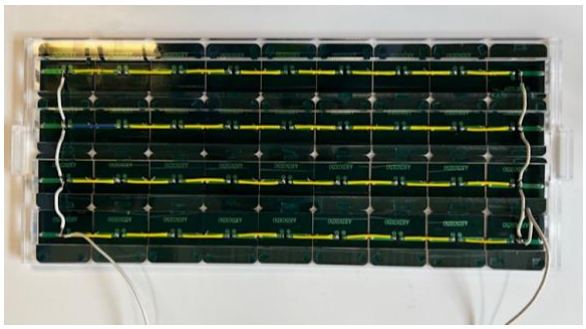

c)

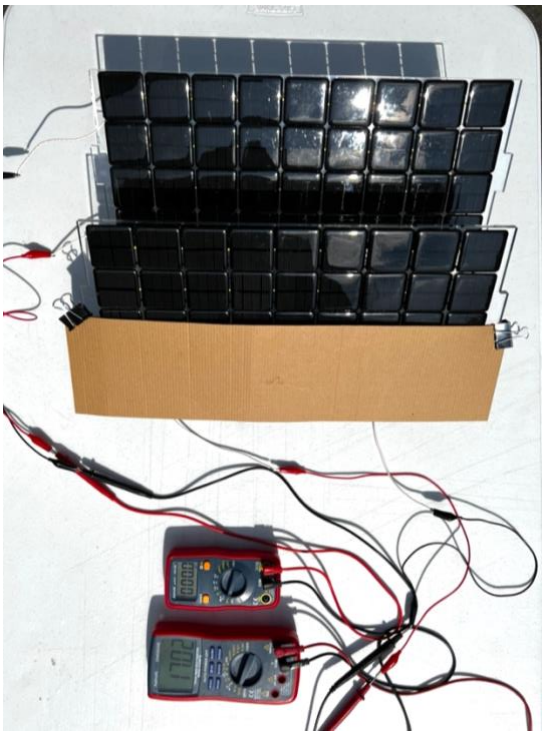

Figure 5.3 Experimental setup: a) series-series connection, b) series-parallel circuit connection, measuring the I, V, irradiance levels.

5. Architecture design

The louvered PV panels integrated into the façade will also perform as a shading device to reduce cooling loads, carbon emissions, and glare problems while offering view-out, on-site clean energy. Figure 5.4 illustrates one typology of the BIPV façade systems and their simulated performance.

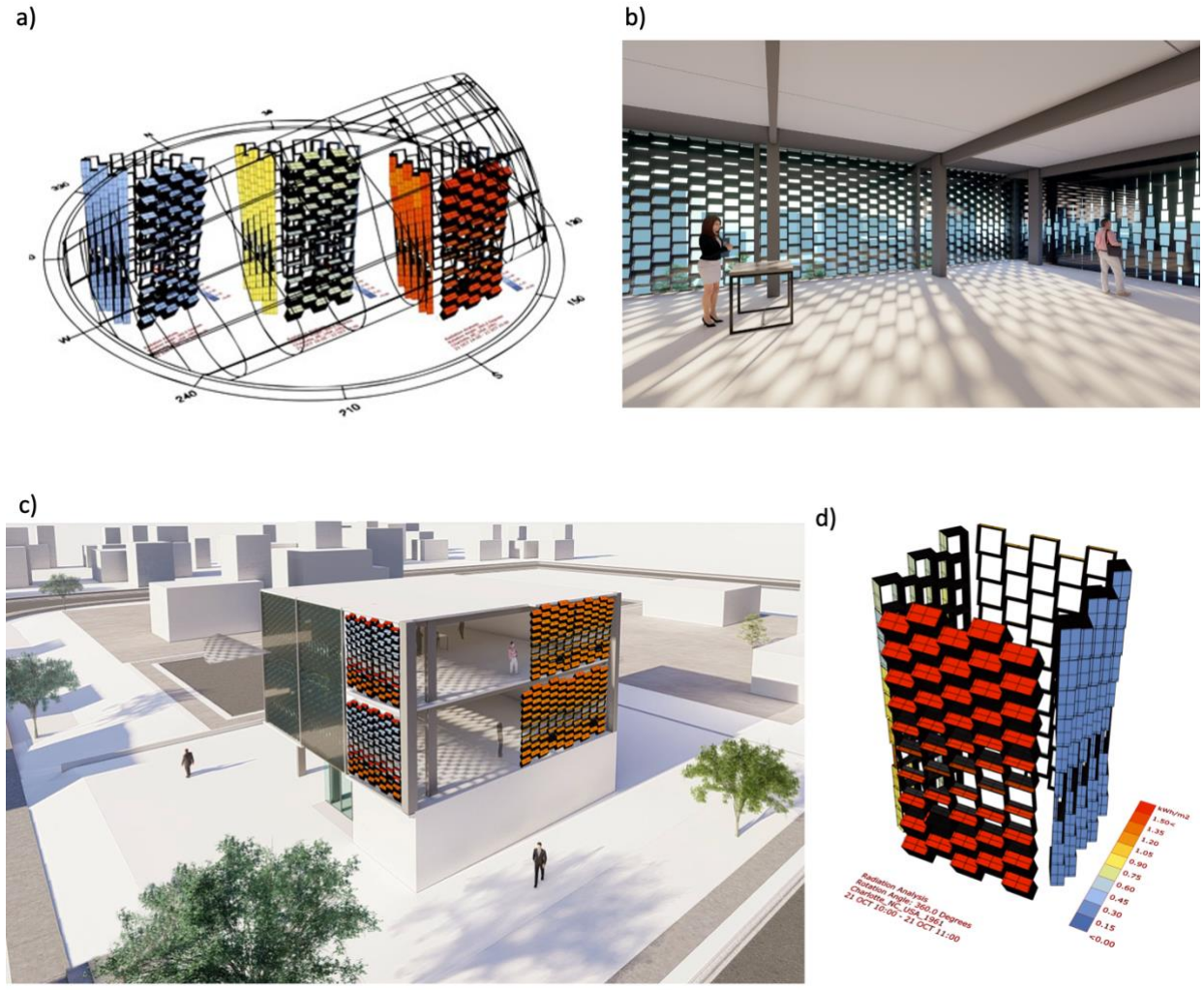

Figure 5.4 The proposed BIPV façade system architecture design: a) incident radiation on PV surface simulations on Oct 21st at 8 pm, 5 pm, and 2 pm from left to right respectively, b) interior view, c) bird eye view, d) incident radiation on PV surface simulations.

6. Results

This paper investigated the optimum circuit connection for BIPV façade systems through simulation and experimental tests. After an in-depth shadow analysis, the simulations were conducted using two methods, including 1) using LB incident radiation component and applying PV material efficiency to calculate the power output and 2) developing a GH script to define the current and voltage output and calculate the power output of the panel of different circuit connections including series-parallel and parallel-parallel. Since the PV cells in PV panels are connected in series in today's manufacturing industry, the results of the LB simulations can be considered for series-series circuit connection. Figure 5.5 visualizes the annual power generation of LB and GH script for two circuit connections of series-parallel and parallel-parallel. Although the power output of the parallel-parallel circuit connection is higher than the series-series and series-parallel connection, it will be inapplicable for the BIPV systems due to the significantly low voltage output that will not meet the minimum required voltage input of the microinverter.

The results of the experimental tests were compared with the simulated circuit connections' power output on the corresponding day of the year. The LB incident radiation simulation results on Oct 8th at noon were 61 W. After applying the efficiency of the cells, the simulated power output will be 7.32 W. However, in the experimental tests, the measured I and V of the partially shaded panel with series-series connection were 0.011 A and 83 v respectively. Therefore, the power output of that PV panel in real-world applications will be about 1 W. To make sure that the comparison between the LB incident radiation output and the experimentation results is accurate, the least value of the simulated incident radiation list, which is related to the grid cell of the analysis grid that receives minimum amounts of incident radiation on October 8th was extracted. After applying the PV cells' efficiency, the power output of that specific cell was calculated. The

calculation result was 2.8 W, which is close to what was measured in the experiment. The power output result of the series-parallel circuit connection that the GH script calculated was 78 W. The measured I and V of the PV panel with the series-parallel circuit connection were 3.3 A and 21.5 v respectively. Therefore, the generated power was about 71 W.

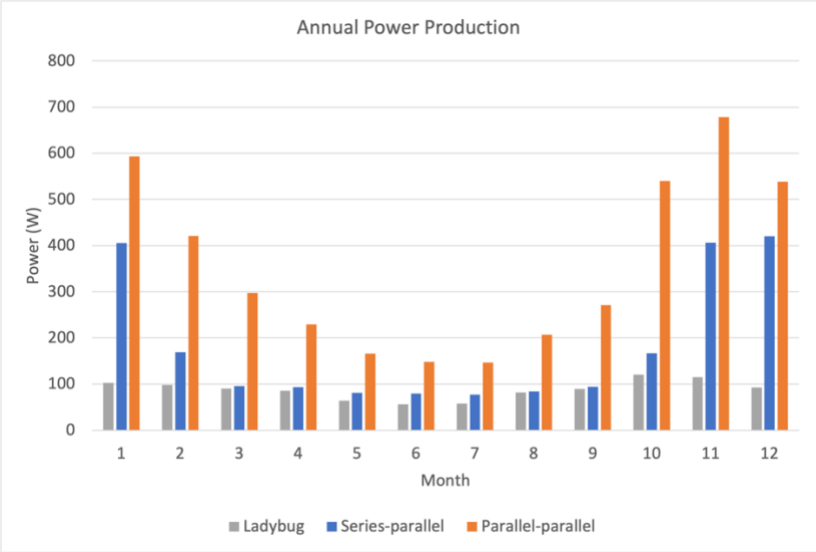

Figure 5.5 the annual power production of different simulation methods.

Results of the experimental tests show that the series-parallel circuit connection increases the energy yields of the BIPV façades 71 times in real-world applications. Additionally, the GH analysis recipe that this paper presented for the circuit connection reconfiguration will increase the BIPV façades energy yield by 10.6 times, which will not only help architects and designers make better decisions in the early stages of the design but also prevent wasting resources to scale up the PV system size to meet the building energy requirements.

7. Conclusion and discussion

Despite the building façade accounting for up to 80% of the building surface area, the current architectural integration of solar energy is largely focused on roofs. The façade of a

building is a great place to harness solar energy and enhance the building's overall energy performance. However, the BIPV façade systems are often subject to partial shadows from panels' self-shading and building walls. Therefore, traditional default circuit connections do not output maximum power for BIPV applications. This study focused on maximizing the energy yield of the BIPV façade systems while minimizing discrepancies between simulation results and real-world application performance. In this paper, simulation and experimental power output of the partially shaded PV panels in different circuits and connections were investigated. Comparison analysis of the results of the LB incident radiation simulations and the measured data in the experiment setup showed that there is a great difference between simulation results and the real-world performance of the partially shaded solar panels. LB does not consider the current drop due to the nonuniform irradiance levels on the PV surface under partially shaded conditions. Therefore, architects and designers need to consider the impact of the current drop in the electric circuit caused by partial shadows in a BIPV system so the designed BIPVs perform in the real-world application as they were intended during the design stage of the project.

The investigation of the BIPV facades and circuit connections in this paper is an important step toward implementing net zero energy architecture practices. The findings of this research are expected to provide design guidance to both researchers and professionals about how photovoltaic systems perform with different design options and surrounding contexts, especially under partial shading conditions. This would also help BIPV designers in the decision-making process to find optimum solutions while focusing on creative aspects of BIPV design. By using correct circuit connections, BIPV facades maximize renewable energy production while also ensuring the safety and longevity of the system.

8. References

1. USDepartmentofState, <*The-Long-Term-Strategy-of-the-United-States*>. 2021.

2. Lefteris Karagiannopoulos. *To meet its 2050 net-zero target, the US needs to cover land 50 times the size of Austin with solar PV*. 2021 [cited 2022; Available from: https://www.rystadenergy.com/newsevents/news/press-releases/to-meet-its-2050-net-zero-target-the-us-needs-to-cover-land-50-times-the-size-of-austin-with-solar-pv/.

3. EIA, *AN ASSESSMENT OF ENERGY TECHNOLOGIES AND RESEARCH OPPORTUNITIES*, in *Chapter 5: Increasing Efficiency of Building Systems and Technologies*. 2015.

4. EIA, *2019 Global Status Report for Buildings and Constructi on*. 2019.

5. EIA. *Energy consumption estimates by sector*. 2022 [cited 2022; Available from: https://www.eia.gov/consumption/.

6. Isa Zanetti, P.B., Francesco Frontini, Erika Saretta, <*Building-integrated-Photovoltaics:Product-overview-for-solar-building-skins*>. 2017, University of Applied Sciences and Arts of Southern Switzerland.

7. EIA. *Solar photovoltaic output depends on orientation, tilt, and tracking*. 2014 [cited 2022; Available from: https://www.eia.gov/todayinenergy/detail.php?id=18871.

8. Ishaque, K. and Z. Salam, *A review of maximum power point tracking techniques of PV system for uniform insolation and partial shading condition.* Renewable and Sustainable Energy Reviews, 2013. **19**: p. 475-488.

9. Satpathy, P.R., S. Jena, and R. Sharma, *Power enhancement from partially shaded modules of solar PV arrays through various interconnections among modules.* Energy, 2018. **144**: p. 839-850.

10. Hasyim, E.S., S. Wenham, and M. Green, *Shadow tolerance of modules incorporating integral bypass diode solar cells.* Solar cells, 1986. **19**(2): p. 109-122.

11. Dhimish, M., et al., *PV output power enhancement using two mitigation techniques for hot spots and partially shaded solar cells.* Electric Power Systems Research, 2018. **158**: p. 15-25.

12. Pareek, S. and R. Dahiya, *Enhanced power generation of partial shaded photovoltaic fields by forecasting the interconnection of modules.* Energy, 2016. **95**: p. 561-572.

13. *<GaN_based_transformer-less_microinverter_with_coupled_inductor_interleaved_boost_and_half_bridge_voltage_swing_inverter.pdf>*.

14. Taveres-Cachat, E., et al., *A methodology to improve the performance of PV integrated shading devices using multi-objective optimization.* Applied energy, 2019. **247**: p. 731-744.

15. Matam, M. and V.R. Barry, *Improved performance of Dynamic Photovoltaic Array under repeating shade conditions.* Energy Conversion and Management, 2018. **168**: p. 639-650.

16. Lee, H.M., et al., *Operational power performance of south-facing vertical BIPV window system applied in office building.* Solar Energy, 2017. **145**: p. 66-77.

17. Cannavale, A., et al., *Improving energy and visual performance in offices using building integrated perovskite-based solar cells: A case study in Southern Italy.* Applied Energy, 2017. **205**: p. 834-846.

18. Yadav, S., S. Panda, and M. Tripathy, *Performance of building integrated photovoltaic thermal system with PV module installed at optimum tilt angle and influenced by shadow.* Renewable Energy, 2018. **127**: p. 11-23.

19. Bana, S. and R.P. Saini, *Experimental investigation on power output of different photovoltaic array configurations under uniform and partial shading scenarios.* Energy, 2017. **127**: p. 438-453.

20. Zomer, C. and R. Rüther, *Simplified method for shading-loss analysis in BIPV systems. Part 2: Application in case studies.* Energy and Buildings, 2017. **141**: p. 83-95.

21. Kuhn, T.E., et al., *Review of technological design options for building integrated photovoltaics (BIPV).* Energy and Buildings, 2021. **231**.

22. Duffie, J.A. and W.A. Beckman, *Solar engineering of thermal processes*. 2013: John Wiley & Sons.

23. Keith McIntosh, M.A., Ben Sudbury, . *Equivalent circuit calculator*. 2022 [cited 2022; Available from: https://pvlighthouse.com.au/.

CHAPTER 6. CONCLUSION

In this comprehensive conclusion, the findings from four papers are synthesized, providing a thorough analysis of the impact of BIPV systems on building energy and PV power production performances while addressing the challenges associated with duck curve.

The first paper entitled "*Comprehensive analysis of energy and visual performance of building-integrated photovoltaics in all ASHRAE climate zones*" provided a comprehensive evaluation of south-facing PV-integrated louvers across all ASHRAE climate zones, assessing their impact on potential PV power production, building energy performance, and visual comfort. It was found that PV-louver typologies can effectively reduce building energy consumption, especially in climate zones 1 to 3 (very hot, hot, and warm thermal climate zones). Wider south-PV louvers with longer spacing were particularly effective in climate zone 4 (mixed) where moderate cooling needs required. More investigations in climate zone 5 (cool) needed to draw a solid conclusion about outperforming BIPV typology.

In climate zones 6 to 8 (cold, very cold, and artic thermal climate zones), façade typologies may have an adverse effect on building energy consumption. The findings of the study emphasized on the necessity of considering climate-specific data and sub-climate variations when designing BIPV louver systems to balance out trade-offs between building energy consumption and PV system power production. Although south-PV louvers slightly increased the lighting loads, they successfully met occupants' visual comfort by providing desired illuminance levels and preventing glare on the office working surface across a large portion of the floor. Conversely, in PV-mounted roof typologies, lighting loads were lower, but they failed to control the amount of sunlight

penetration into the building, causing excessive illuminance levels on the office working surface and consequently disturbing glare across a large portion of the floor.

The second paper entitled *"Assessing the PV-integrated south facade in mitigating the BIPV system oversupply"* addressed the issue of PV power oversupply or curtailment at mid-day hours. The results of this paper revealed that in very hot, hot, and warm climates, south PV-louver typologies consistently outperformed roof-mounted PV systems throughout the year in mitigating the PV oversupply. Conversely, roof typologies were mainly more effective in mixed climate zone. Overall, the study demonstrates the potential of south facade PV-louvers for curtailment mitigation, but optimal performance depends on specific location, time of the year, climate zone, and sub-climate factors.

The third paper entitled "*Assessing the impact of PV-integrated west facade in alleviating the duck curve steep ramp in all ASHRAE climate zones*" focused on the impact of PV-west facades and PV-mounted roofs on alleviating the steep ramp of the duck curve across all ASHRAE climate zones. The results indicated that while PV-west facades can be particularly effective in very hot, hot and warm regions, their performance varies significantly with sub-climate specifics and time of year. In very hot and cold climates, the effectiveness of PV-west facades is more pronounced during warmer months. The study also revealed that certain azimuth angles consistently yield high scores across different locations, indicating their robustness in mitigating the duck curve. Identifying these optimal angles can aid policymakers and energy planners in making informed decisions to enhance grid stability.

Although building facades account for the majority of the surface area and offer significant potential for solar energy production, current integration of PV systems primarily focuses on roofs. The forth paper entitled *"Circuit connection reconfiguration of partially shaded BIPV systems, a*

solution for power loss reduction" highlighted that while BIPV façade systems have great potential for harnessing solar energy, they are often subject to partial shadows, resulting in suboptimal power output. Through simulation and pilot experiment tests, it was demonstrated that hybrid circuit connections significantly outperform traditional circuit connection that is being used in manufacturing the PV modules. Hybrid circuit connection resulted in mitigating power drops due to self-shading, thereby maximizing energy yield.

In conclusion, these studies highlight the importance of a comprehensive approach to designing BIPV systems. Integrating advanced circuit connections, optimizing PV-louver depth, and strategically orienting PV façades can significantly enhance energy performance, reduce power curtailment, and support grid stability across different climatic conditions.

6.1 Contributions

The research presented in this dissertation is valuable to the scientific community, the architecture, engineering, and construction industries, and policymakers for advancing the implementation of BIPV systems. This research provides key insights into how south-facing PV louvers and west-facing PV facades can be strategically integrated into buildings toward more sustainable built environments. Architects and engineers can use these findings to select BIPV configurations tailored to specific climate zones, building characteristics, and energy objectives.

The construction industry benefits from identifying promising BIPV solutions that improve energy efficiency, reduce energy costs, and incorporate new energy technologies and sustainable building systems into the built environment. Policymakers gain essential data to inform building codes and incentive programs that promote the wider adoption of BIPV technologies. Ultimately, this research advances BIPV technology and its integration into the built environment, leading to

reduced energy consumption, minimized power curtailment, and a more stable and resilient electricity grid for the future.

6.2 Research Limitations

One of the main limitations of this research is its focus on office building programs. While BIPV systems effectively offset energy consumption and contribute to sustainable cities, evaluating their performance across diverse occupancy profiles is challenging. For instance, residential buildings exhibit significant variations in occupant behavior and energy consumption patterns. Most importantly, validating simulations for these varied building types to closely match real-world conditions is complex. These factors complicate accurate simulation of BIPV systems in non-office settings. In contrast, office buildings typically maintain predictable occupancy schedules and energy consumption patterns, facilitating reliable energy models and generating accurate, meaningful data on BIPV performance. Therefore, by focusing on office buildings, this research prioritizes the generation of reliable results that can inform future BIPV applications across various building typologies.

Another limitation of this study was unavailability of precise real-world data on the timing of peak electricity demand for office buildings. This data is critical for accurately assessing the potential impact of BIPV facades in alleviating the duck curve steep ramp and mid-day valley. However, to overcome this limitation, we employed detailed simulations that replicate realistic building operation conditions. These simulations were designed to capture potential trends and identify real-world conditions as accurately as possible. The findings from these simulations provide valuable insights, and future studies that can incorporate real-world data as it becomes available, will further refine the conclusions.

Lastly, in this research, the BIPV systems were modeled using a combination of software tools, primarily utilizing the EnergyPlus code within the Ladybug, an energy simulation tool running on Rhino 3D modeling software. The modeling approach involved defining parameters such as irradiance levels, panel efficiency and loss factors. However, the simulation framework has limitations, particularly in calculating temperature effects of operating PV systems in real-world conditions. Due to the constraints of the software used, the focus was on key factors that could provide meaningful insights into the performance of the PV system within the study's scope. While acknowledging these limitations, the study aimed to contribute novel findings regarding the overall energy behavior and potential BIPV system power performance.

6.3 Future Research Directions

The findings from this dissertation offer several opportunities for future research. Investigating more locations within each sub-climate zone will provide more refined results, strengthening and making the outcomes of this study more robust. Additionally, employing advanced modeling techniques or alternative software tools capable of addressing the temperature effects of PV modules in different façade integrations, such as double skin façades and closed cavity façades, will enhance the accuracy and comprehensiveness of the BIPV systems presented in the simulation results.

The proposed hybrid circuit connection of BIPV systems in Chapter 2 on a larger scale and over a longer period is important future research because the data collected will yield more robust results, helping to expand the existing findings.

A holistic method evaluating energetic and economic benefits of PV-south louvers in chapter 3 versus PV-west fins and/or PV-mounted rooftop scenarios in chapter 4 is another

promising future direction to help decision-makers in selecting sustainable BIPV design and evaluating duck curve alleviations and. Finally, incorporating electricity tariffs, time-of-use price rates, levelized cost of energy (LCOE), policies, and incentives would also be helpful in improving the decision-making process that considers the economic feasibility and building program feasibility.

6.4 References

1. USDepartmentofState, <*The-Long-Term-Strategy-of-the-United-States*>. 2021.
2. Lefteris Karagiannopoulos. *To meet its 2050 net-zero target, the US needs to cover land 50 times the size of Austin with solar PV*. 2021 [cited 2022; Available from: https://www.rystadenergy.com/newsevents/news/press-releases/to-meet-its-2050-net-zero-target-the-us-needs-to-cover-land-50-times-the-size-of-austin-with-solar-pv/.
3. DOE. *DOE Releases Solar Futures Study Providing the Blueprint for a Zero-Carbon Grid*. 2021 [cited 2022; Available from: https://www.energy.gov/articles/doe-releases-solar-futures-study-providing-blueprint-zero-carbon-grid#:~:text=A%20clean%20grid%20requires%20massive,per%20year%20from%202025%2D2030.
4. Jeannette Brinch, K.W., David Hurlbut, Joe Gracia, Stan Hadley, Vladimir Koritarov, Jim Kuiper, Andy Ayers, Andy Orr, Pam Richmond, Katie Rollins. *Energy Zone Mapping Tool*. 2020; Available from: https://ezmt.anl.gov/.
5. Palmintier, B., et al., *Emerging Issues and Challenges in Integrating Solar with the Distribution System.* Office of Energy Efficiency & Renewable Energy, Washington DC, 2016.
6. CASIO, *Fast Facts*. 2016.
7. Sun, Y., et al., *2018 renewable energy grid integration data book*. 2020, National Renewable Energy Lab.(NREL), Golden, CO (United States).
8. DOE. *Guide to Determining Climate Regions by County*. 2015 [cited 2022; Available from: https://www.energy.gov/sites/prod/files/2015/10/f27/ba_climate_region_guide_7.3.pdf.
9. ISO-NE. *Solar Power in New England: Concentration and Impact*. 2018 [cited 2022; Available from: https://www.iso-ne.com/about/what-we-do/in-depth/solar-power-in-new-england-locations-and-impact.
10. Paul Denholm, M.O.C., Gregory Brinkman, and Jennie Jorgenson, *Overgeneration from Solar Energy in California: A Field Guide to the Duck Chart*. 2015, NREL.
11. EERE. *Solar Futures Study*. 2021 [cited 2022; Available from: https://www.energy.gov/eere/solar/solar-futures-study.

12. Shirinbakhsh, M. and L.D. Harvey, *Feasibility of achieving net-zero energy performance in high-rise buildings using solar energy.* Energy and Built Environment, 2023.
13. Hossei, H. and K.-H. Kim. *Circuit Connection Reconfiguration of Partially Shaded BIPV Systems, a Solution for Power Loss Reduction*. in *ACSA Annual Meeting In Common*. 2023.
14. EIA. *Solar photovoltaic output depends on orientation, tilt, and tracking*. 2014 [cited 2022; Available from: https://www.eia.gov/todayinenergy/detail.php?id=18871.